



## Appendix E

### Subsidence Assessment





ABN: 19 113 083 060

9 Reid Drive  
CHATSWOOD WEST 2067  
NSW AUSTRALIA

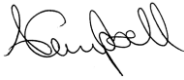
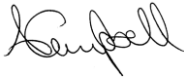
Telephone: +61 405 046 117  
[www.beck.engineering](http://www.beck.engineering)

# **GEOTECHNICAL ASSESSMENT OF SURFACE IMPACTS FOR PROPOSED UNDERGROUND MINING AT LAKE COWAL**

**PREPARED FOR**

**EMM and EVOLUTION**

## DOCUMENT CONTROL

Date	Version	Comments	Signed
2020JUN16	DRAFT	Modelling forecasts for the updated underground mine design, including the surface box cut and portal	
2020JUL06	FINAL	Additional commentary and feedback following feedback from EMM and Evolution	

**COPYRIGHT NOTICE**

Copyright of this document is retained by Beck Engineering Pty Ltd. Copyright is enforced to protect client interests.

## **EXECUTIVE SUMMARY**

Beck Engineering Pty Ltd (BE) has conducted a life-of-mine (LOM) assessment of surface subsidence at the Lake Cowal mine. The main aims of this project were to:

1. Simulate open pit and planned underground mining using a 3D finite element model.
2. Forecast surface subsidence during planned underground mining up to the end of mine life.

Our assessment method is based on three-dimensional numerical modelling using finite element methods, including calibration. The calibration is qualitative, and in our view, the model can be used to forecast conditions over the mine life with moderate reliability.

### **Main findings**

This report details the findings from model iteration R07. This simulation includes the most recent mine underground mine design, including a box cut, portal and additional decline. A review of the mine design provided identified 19 stopes that were located in close proximity to the weathered cover sequence geology, or within the cover sequence layers. These stopes have a significantly elevated risk of chimneying to surface due to the close proximity of the weak cover layers. Prior to building the numerical model, it was recommended that a minimum crown pillar thickness between the top of any planned stope and the top of the fresh rock surface be used to update the current design. A minimum stope width to crown pillar thickness of 1:2 was recommended. This corresponds to a minimum crown pillar thickness of ~20m to 30m for the 10 to 15m wide stopes. The mine design as subsequently updated by Evolution and the 19 stopes removed from the mine plan used for the R07 numerical model.

Our main findings for the latest model iteration (R07) are:

1. Vertical displacement forecasts on the surface above the proposed underground mine are generally less than 15mm and considered negligible. This amount of displacement is well within the limits and precision of current geological understanding, material properties and capabilities of a mine-scale model.
2. Forecast surface movement is slightly upwards (upsidence, not subsidence). This is due to displacement along the Glenfiddich fault, which becomes slightly mobilised due to nearby underground mining. There is also minor uplift in proximity to the pit due to continued mining of the pit and removal of 'dead-weight' (or overburden pressure).
3. Unlike caving methods or mining methods used for underground coal mining, such as longwall mining, surface subsidence is generally minimal, and often negligible for most stoping operations, particularly stoping operations targeting near vertical and relatively thin gold orebodies such as Lake Cowal underground.
4. The updated underground mine design and layout is appropriate for minimising (potential) surface subsidence. This is because of the planned sequence, relatively small stope dimensions with planned paste backfill, 20-30m crown pillar thickness in fresh rock and planned cablebolt ground support for the stope crowns. Of course, these controls do not completely eliminate the potential for any impact to surface as there are potentially unknown geological conditions present. The proposed underground mine design is considered feasible for minimising any impacts to surface and is forecast to have negligible impact to the surface topology provided stopes/crown pillars do not fail. It is noted that some geological conditions cannot be completely characterised and understood until development in planned mining blocks, particularly the upper stoping blocks, has been completed. Additional monitoring, measurement and risk mitigation measures addressing stope

stability are addressed in the recommendations section. Failure of stope crown pillars is a key hazard that must be managed by the mine.

5. A potential hazard for the underground mine is stope failure or chimney failure of the upper stopes in the mine. The model does not forecast significant rockmass damage or major instability above these stopes. However, local geological conditions encountered in this domain may be different from the current understanding. Chimney failure and stope instability is a potential hazard in all stoping mines and must be managed appropriately. Chimney failure of a stope to surface at Lake Cowal would likely result in any surface water in the lake to report to the underground workings. The mine will need to carefully manage this hazard through mine design, sequence, timely paste fill and (possibly) cablebolt stope walls and crowns. We have provided recommendations to mitigate this hazard.
6. Some stope hangingwalls are in close proximity to the Glenfiddich fault, which is in proximity to much of the mineralised zone on the hangingwall side. There is increased potential for hangingwall overbreak and stope failure / chimneying along the Glenfiddich fault, and other faults in proximity to mining that intersect with the weak oxide and transported material, such as the Galways splays.
7. There is potential for (increased) water inflow into underground workings along faults (i.e. Glenfiddich and Galway splay faults) that are slightly mobilised in proximity to the underground workings. Water inflow to the underground will depend on degree of saturation of overlying cover sediments in proximity to these faults, and the hydraulic conductivity of the individual faults.
8. There is minimal interaction between the underground and open pit mine. The interaction for stress, strain and displacement are considered negligible. This is due to the small footprint of the underground mine in proximity to the pit.

### Recommendations

Our recommendations arising from this project are outlined below. BE would be pleased to assist EMM and Evolution with implementing the recommendations if required.

1. Stopes within the oxide and transported layers are not likely to be stable and should not be planned at this stage of the project. Current geological interpretation demonstrates the depth and thickness of the transported and oxide layers is variable. The mine should continue to update the interpretation of these boundaries with information from ongoing drilling programmes. The location of the top of fresh rock is most important for the underground mine design.
2. Geotechnical characterisation and development of a detailed geotechnical domains model and structural model, particularly in the upper mining areas of the underground mine. The geotechnical and structural models will require on-going refinement over the mine life which is the normal practice in any mine.
3. The mine should review the planned mining sequence and consider delaying the mining of the upper most row of stopes in the upper most stoping blocks. Mining these stopes first, or very early in the mine life is when the mine has the least geological knowledge and understanding of stope performance (relative to other stages of underground mining). This includes the understanding of the hydraulic properties of the faults and (potential) water inflows to the underground mine.
4. Other recommendations and control measures to minimise the potential for stope overbreak or chimney failure that may impact the surface are listed below. Depending on local geological conditions encountered, the mine should review the list below, and select the controls appropriate to the conditions encountered. We understand some of these controls are currently being planned. Additional controls, if required would normally be identified and planned as part of the risk assessment and detailed design process.

- a. A detailed crown pillar stability assessment must be conducted for each stope on the upper mining levels. We recommend the use of empirical methods as a minimum, or a combination of empirical and numerical methods. The mine must ensure the risk of crown pillar failure is suitably controlled.
  - b. Mine single lift stopes in the upper stoping block. Smaller stopes are more stable than large stopes. A smaller stope void increases the potential for stope overbreak and failure material to fill the void due to the swell of the broken material, prior to extensive failure or chimneying to surface.
  - c. Stope sequencing to minimise risk of failure and unravelling along faults, particularly where stopes are bounded by multiple faults. Multiple stopes in close proximity should not be mined at the same time.
  - d. Top down drilling of the upper stopes will provide access to the top of the stope (the overcut drive) which enables cablebolting of the stope crown and hangingwall and access for rapid tight filling with paste.
  - e. Tight fill stopes, as far as practical.
  - f. Backfilling stopes in a timely manner.
  - g. Developing the overcut drive with a downwards grade from the access. This will enable the stopes to be tight filled to the backs with paste.
  - h. Ensuring paste lines and other backfill infrastructure is in place prior to firing stopes with potential for instability or in proximity to major faults.
  - i. Reducing the strike length and width of stopes to reduce potential instability. A review of the stope dimensions should be conducted following stope development and structural mapping of the area.
  - j. Cablebolting of stope crowns, when appropriate.
  - k. Review of a stand-off between stope walls and major faults, such as the Glenfiddich fault is appropriate based on local conditions
  - l. Employing a continuous mining sequence. Secondary stopes have a higher risk of instability (generally).
  - m. Avoid mining stopes where major faults confluence in proximity to the stope, particularly near sub-vertical faults such as the Glenfiddich fault and Galway splays.
  - n. Mine stopes on the upper levels when Lake Cowal is dry.
5. Detailed stope stability assessments using geotechnical information from future drilling programmes, laboratory testing and rock mass characterisation from underground exposures.
  6. Stability monitoring of stopes and TARP to backfill stopes that show early signs of large scale instability.
  7. The mine should develop a TARP and undertake a detailed risk assessment for potential stope instability in areas deemed to have elevated risk or potential for surface break through.
  8. Subsidence monitoring above the underground mining precinct.
  9. In situ stress measurement.
  10. Additional laboratory strength testing of each rock type.

11. Characterisation of the major faults, including strength properties and hydraulic conductivity/water inflow rates.
12. Ground water characterisation, including an assessment of the impact of the mechanical rockmass response on ground water flow paths and hydraulic conductivity.

## **Limitations**

In addition to the normal resolution limitations associated with the current mine-scale finite element model, the main limitations of this project are:

1. The structural model provided is of “low” resolution. We understand there are a large number of mapped faults within the open pit that were not provided for the assessment of the underground mine. A detailed pit stability assessment has not been completed as part of this assessment.
2. The early stage of underground mining at Lake Cowal precludes detailed calibration, which limits the reliability of the forecasts at this stage. This is normal for a mine at this early stage of pre-production development. Despite the lack of calibration, the results are generally consistent with our expectations based on the current interpretation of the conditions.
3. Sensitivity analyses have not been performed to bracket the range of likely outcomes for the surface impacts to mining.
4. Stope crown pillar stability assessment has not been conducted as sufficiently detailed information at present and is outside the scope of the subsidence assessment. Preliminary recommendations for crown pillar thickness have been integrated into the revised underground mine design.
5. The in-situ stress regime has been assumed using data from a nearby mine as there has been no insitu stress testing to date at Lake Cowal. Local conditions may have a different insitu stress orientation and/or gradient.
6. The impact of ground water inflow to the underground mine has not been included in the model. The model does not include:
  - a. Stress increase from porewater pressure
  - b. Overburden pressure from seasonal surface water (although this effect would be small)
  - c. An assessment of changes to ground water flow or surface water percolation due to rock mass damage, including damage within the major faults, caused by underground mining. We note that small amounts of strain above planned stoping or on structures will increase the hydraulic conductivity of the rock mass and may lead to (increased) water inflow to the underground mine.

It is essential to note that the current forecasts of LOM behaviour are still subject to considerable uncertainty due to the limited quantitative data available for model calibration at this early stage of the underground. This is the normal situation for mines in the early stages of underground mining. On-going data collection and further direct experience with stoping at Lake Cowal and improved calibration will help reduce uncertainty.

## **Enquiries**

Please direct further enquiries to the undersigned.

Sincerely,



**Alex Campbell**

PhD, MEngSc (Mining Geomechanics), BE (Civil), BE (Mining Hons I) MAusIMM (CP), RPEQ  
Principal Engineer, Mining & Rock Mechanics



## **TABLE OF CONTENTS**

1	INTRODUCTION .....	12
2	PROJECT WORKFLOW, BACKGROUND DATA & MODEL COMPOSITION .....	14
2.1	Project workflow & modelling framework .....	14
2.2	Geological setting .....	15
2.3	Structures.....	16
2.4	Estimated material properties for modelling .....	18
2.5	Stress field.....	22
2.6	Hydrogeological conditions.....	23
2.7	Stope filling methodology and fill properties.....	24
2.8	Mining geometry and sequence .....	24
2.9	Rockmass damage scale.....	27
3	FORECASTS, INTERPRETATION & DISCUSSION.....	28
3.1	Surface impacts.....	28
3.2	Open pit and underground interaction.....	44
3.3	Stope overbreak and chimney failure potential.....	53
4	CONCLUSIONS, RECOMMENDATIONS & LIMITATIONS.....	63
5	REFERENCES.....	67
6	APPENDIX – LR2 FRAMEWORK.....	68
A.1.	CONSTITUTIVE MODEL AND PHYSICAL COMPOSITION.....	68
A.1.1.	The LR2 constitutive framework.....	68
A.1.2.	Constitutive model for the continuum parts.....	69
A.1.3.	Representation of explicit structure.....	72
A.1.4.	Extension for the case of transversal isotropy .....	73
A.1.5.	Model parameter to determine rock strength.....	75
A.1.6.	Modelling softening behaviour .....	76
A.1.7.	The common damage scale .....	77
A.1.8.	Assessing seismic potential with RER.....	77
A.1.9.	Mechanical response in the presence of pore-water pressure.....	78
A.1.10.	References.....	78

## LIST OF FIGURES

Figure 1-1: Perspective view showing LOM geometry.....	12
Figure 1-2: Perspective view showing the model geometry.....	13
Figure 2-1: Cross section through the open pit showing geological domains at Lake Cowal.....	15
Figure 2-2: Cross section through the numerical model showing lithology domains in the underground mining precinct.....	16
Figure 2-3: Fault details provided by Evolution Mining.....	16
Figure 2-4: Perspective views showing structures built in FE mesh together with meshed LOM geometry. 17	17
Figure 2-5: Material properties used by Itasca (and AMC) for numerical modelling undertaken in 2015/1619	
Figure 2-6: Indicative rockmass softening curve demonstrating the plastic strain transition points $\epsilon_1$ and $\epsilon_2$ . 19	19
Figure 2-7: In situ stress applied in the FE model.....	22
Figure 2-8: Stress provinces in the Australian continent (after Lee et al. 2010).....	23
Figure 2-9: Stopes in proximity and intersecting the weathered layers in the latest underground mine design .....	26
Figure 2-10: Upper levels of stoping intersecting the top of fresh rock boundary.....	26
Figure 2-11: Stopes shown in green were recommended not to be included in the underground mine design due to chimneying potential.....	27
Figure 2-12: Rockmass damage scale.....	27
Figure 3-1: Cross section through the proposed underground mine showing indicative thickness of the cover units relative to the underground mine. ....	29
Figure 3-2: Cross section through the proposed underground mine showing indicative thickness of the transported material and soft oxide cover units relative to the underground mine.....	30
Figure 3-3: Aerial photo of the pit and Lake Cowal, with respect to the planned underground mine footprint .....	31
Figure 3-4: Subsidence classes and criteria.....	32
Figure 3-5: Damage limits and classification for surface infrastructure (after Harrison).....	32
Figure 3-6: Forecasts vertical displacement from the end of 2019 to the end of mine life above the proposed underground mine (horizontal and vertical cross sections through the model) .....	33
Figure 3-7: Forecasts vertical displacement from the end of 2019 to the end of mine life above the proposed underground mine (horizontal and vertical cross sections through the model) .....	34
Figure 3-8: Forecasts vertical displacement from the end of 2019 to the end of mine life above the proposed underground mine (vertical cross section through the model). Arrows indicate the direction of movement.....	35
Figure 3-9: Forecasts vertical displacement from the end of 2019 to the end of mine life above the proposed underground mine (plan view on surface) .....	36
Figure 3-10: Vertical movement forecast from the end of 2019 to the end of mine life. Movement is between the Galway splays and Glenfiddich fault which bound the proposed underground stope production. .....	37

Figure 3-11: Cross section through the model showing forecast total displacement from the end of 2019 to the end of mine life for the proposed underground mine ..... 38

Figure 3-12: Detailed report for movement and damage over time above the planned underground mine ..... 39

Figure 3-13: Detailed report for movement and damage over time above the planned underground mine ..... 40

Figure 3-14: Detailed report for movement and damage over time on the dam wall to the north of the open pit ..... 41

Figure 3-15: Detailed report for movement and damage over time on the dam wall ..... 42

Figure 3-16: Detailed report for movement and damage over time on the dam wall to the east of the open pit ..... 43

Figure 3-17: Cross section of total displacement through the underground mine (displacement shown is from end of 2019 to end of mine life) ..... 45

Figure 3-18: Cross section of total displacement through the underground mine (displacement shown is from end of 2019 to end of mine life) ..... 46

Figure 3-19: Cross section of total displacement through the underground mine (displacement shown is from end of 2019 to end of mine life) ..... 47

Figure 3-20: Cross section of rockmass damage forecast in the underground mine precinct. Note the most significant damage is in the transported and soft oxide layers in proximity to the open pit ..... 48

Figure 3-21: Rockmass damage forecast in the underground mine precinct. .... 49

Figure 3-22: Rockmass damage forecast in the underground mine precinct. .... 50

Figure 3-23: Cross section showing major principal stress. .... 51

Figure 3-24: Cross section showing major principal stress. .... 52

Figure 3-41: A stope that has chimneyed approximately 200m vertically through to surface at an underground mine in QLD. The surface breakthrough was approximately 10m x 20m across ..... 55

Figure 3-45: Cross section through the proposed underground mine showing indicative thickness of the cover units relative to the underground mine. .... 56

Figure 3-46: Forecast rock mass damage in the vicinity of the upper stoping blocks (showing the Galway and Glenfiddich faults) ..... 57

Figure 3-47: Example of crown pillar failure mechanism in steeply dipping rockmass (After Carter) ..... 58

Figure 3-48: Principal surface crown pillar failure mechanisms (after Carter) ..... 59

Figure 3-49: Schematic of groundwater distribution at Lake Cowal, showing potential effects of underground mining and water flow along faults intersecting the water bearing cover units and the underground workings. .... 60

Figure 3-50: Schematic of crown pillar with nomenclature ..... 61

Figure A.1-1 Three dimensional representation of the Menetrey/Willam failure surface in the principal stress space ..... 70

## **LIST OF TABLES**

Table 2-1: Rock mass properties used in the FE model.....	20
Table 2-2: Summary of model sequence Q01 with corresponding calendar dates.....	24
Table 3-1. Acceptable risk exposure guidelines (after Carter et al, 2008).....	62
Table A.1-1 Material properties for traction-separation cohesive sections.....	73
Table A.1-2 Material properties for continuum LR2 material.....	75

## **1 INTRODUCTION**

Beck Engineering Pty Ltd (BE) has conducted a life-of-mine (LOM) assessment of surface subsidence at Cowal Gold Operations (CGO) as part of the EIS process for the proposed Underground Mine. The main aims of this project were to:

1. Simulate open pit and planned underground mining using a 3D finite element model.
2. Forecast surface subsidence during planned underground mining up to the end of mine life.

Our assessment method is based on three-dimensional numerical modelling using finite element methods, including calibration. The underground and open pit mine geometry for this project is shown in Figure 1-1. This report documents our findings and our recommendations for EMM and Evolution Mining’s consideration.

The subsidence assessment at Lake Cowal has undergone several iterations. These assessments include:

- July 2019 – Subsidence assessment of the original underground mine design and rock mass properties provided by Evolution
- October 2019 - Subsidence assessment of the original underground mine design using revised rock mass properties provided by Evolution
- November 2019 – Same model inputs as the October 2019 assessment but with an alternate fresh air in-take design
- May/June 2020 – Assessment of the revised underground mine design. A review of the mine design prior to model simulation identified 19 stopes on the upper levels within the weak oxide layers. These stopes were removed from the mine design by Evolution and not included in the model simulation.

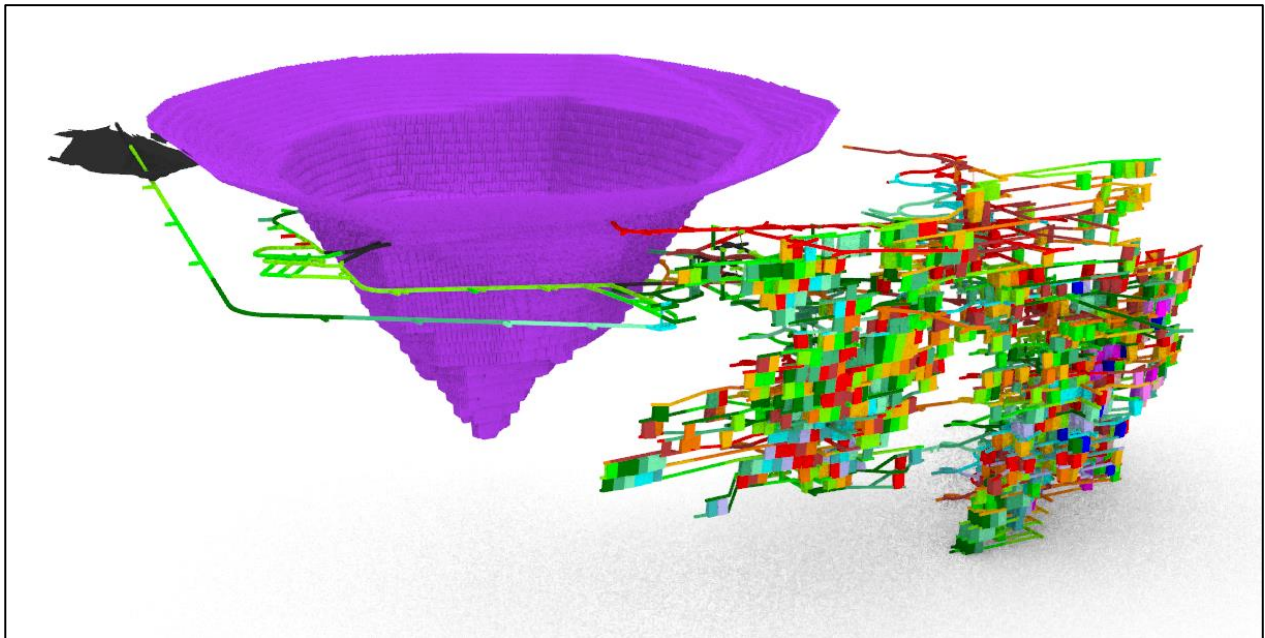


**Figure 1-1:** Perspective view showing LOM geometry.

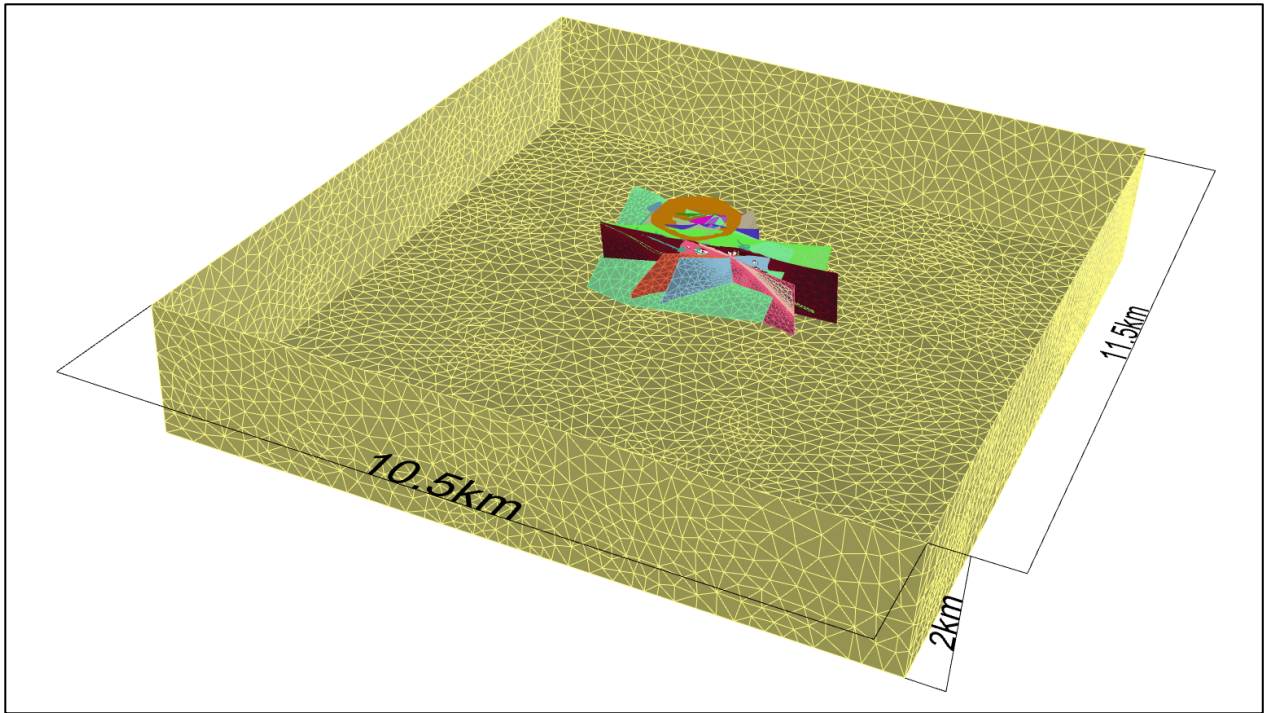


**Figure 1-2:** Perspective view showing the model geometry.

## **2 PROJECT WORKFLOW, BACKGROUND DATA & MODEL COMPOSITION**

This section summarises the available background data and assumptions relevant to the project and describes how these data and assumptions have been incorporated into the workflow.

1. Modelling workflow.
2. Geological interpretation and topography.
3. In situ stress field.
4. Stope filling methodology and fill properties.
5. Hydrogeological conditions and simulation parameters.

### **2.1 Project workflow & modelling framework**

This workflow for the FE modelling undertaken as part of this project was:

1. Initial mining engineering and rock mechanics appreciation of the project including compilation of all relevant geometric data into a 3D CAD database using commercial software.
2. Discontinuum finite element (FE) mesh construction using commercial software and in-house scripting tools. Higher-order finite elements were used for all volume elements.
3. Assignment of geotechnical domains, material properties, initial conditions, boundary conditions and the mining and fill sequences to the FE mesh.
4. Solution of the stress, strain and displacement fields and released elastic energy for each step in the modelled mining sequence using the Abaqus Explicit FE solver. Abaqus Explicit is a commercial, general purpose, 3D, non-linear, continuum or discontinuum FE analysis package designed specifically for analysing problems with significant plasticity, large strain gradients, high deformation levels and large numbers of material domains. Commercial software and in-house post-processing scripts are used to process the Abaqus output and visualise the results.

The Levkovitch-Reusch 2 (LR2) discontinuum constitutive framework was applied in Abaqus to describe the mechanical behaviour of the rockmass and structures. The Appendix contains further details of the LR2 framework. In summary, the LR2 framework includes:

1. 3D geometry, with excavations sequenced in a sufficient number of separate excavation steps to capture the necessary temporal resolution for the project scope.
2. Strain-softening dilatant constitutive model for the rockmass and structures with a generalised Hoek-Brown yield criterion. Different material properties are assigned to each geotechnical domain.
3. Discontinuum formulation using cohesive finite elements to simulate discrete structures. Cohesive finite elements are free to dislocate and dilate and can realistically capture the behaviour of thin structures which tetrahedral finite elements cannot achieve as effectively. The complete interpreted structural model at the required resolution can be included, and where appropriate, can be supplemented with one or more discrete fracture networks (DFNs) to improve the structural resolution.
4. Structures less persistent than those modelled explicitly can be represented by "smearing" the effects of structures within the continuum regions of the modelled rockmass.
5. Hydromechanical coupling, where necessary, to capture the effects of pore water pressure on the rockmass yield surface, or to estimate water flow rates. Hydro-coupling was not

The LR2 modelling framework aims for physical similitude, by making the fewest possible assumptions about the governing physics of the entire mine system within a single physics-based numerical model, at the required scale of the analysis. This results in a realistic but complex model, since complexity is the reality of all mines. Building a realistic mine model by including the governing physics means that rockmass behaviour evolves naturally in the model, and is therefore essential for developing a detailed understanding of the likely rockmass response to mining.

**2.2 Geological setting**

The geological domains provided by Evolution Mining are shown in Figure 2-1. The same lithology boundaries provided by Evolution Mining were built into the numerical model as shown in Figure 2-2.

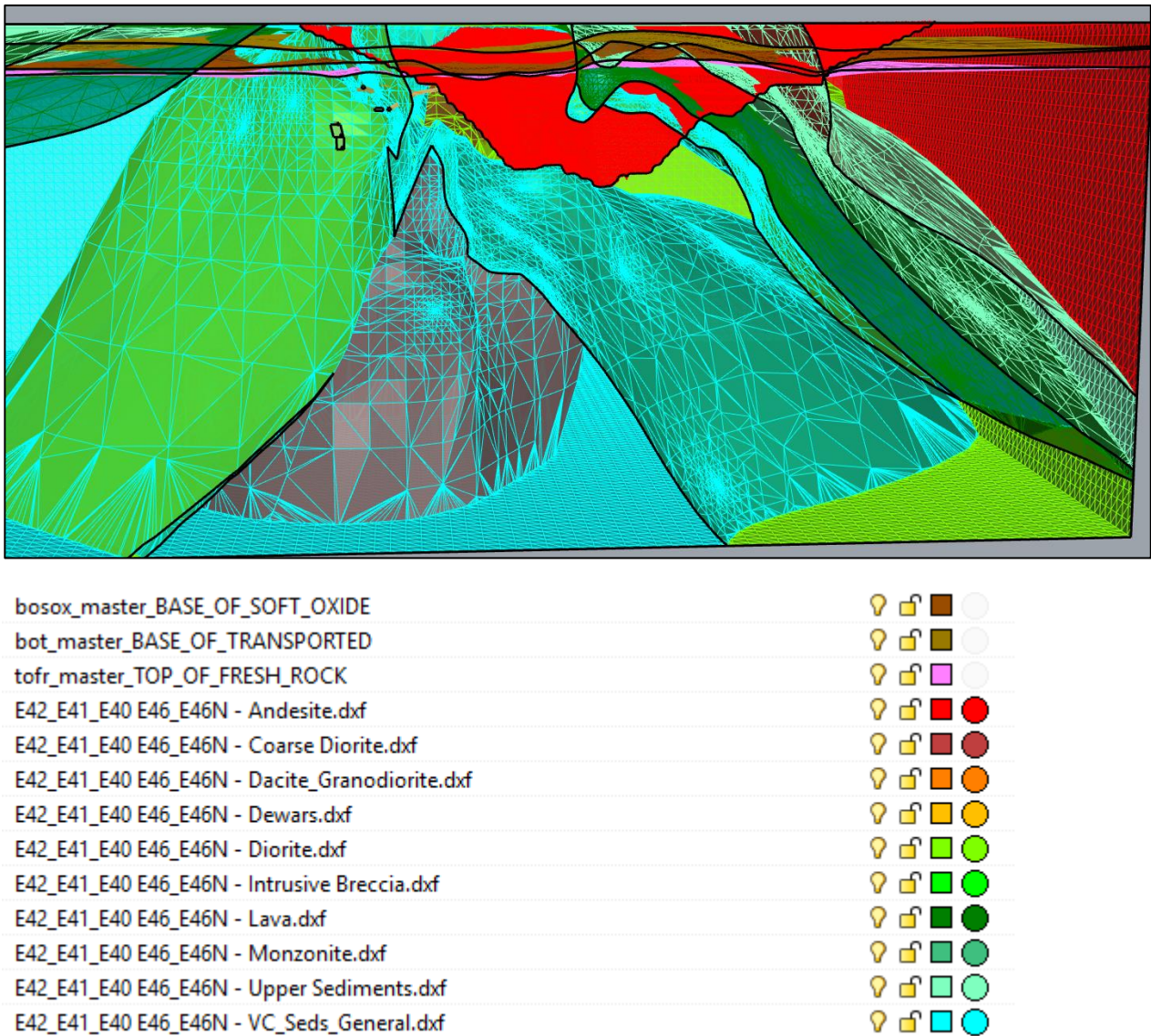


**Figure 2-1: Cross section through the open pit showing geological domains at Lake Cowal.**



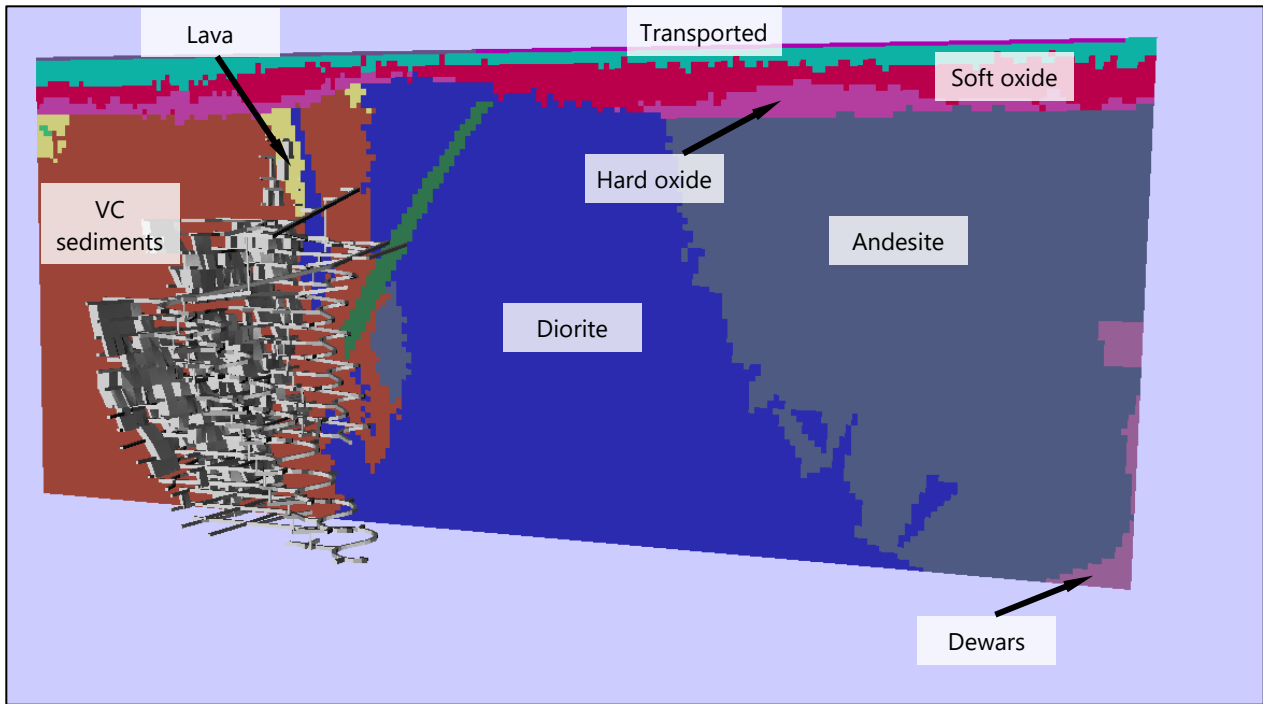


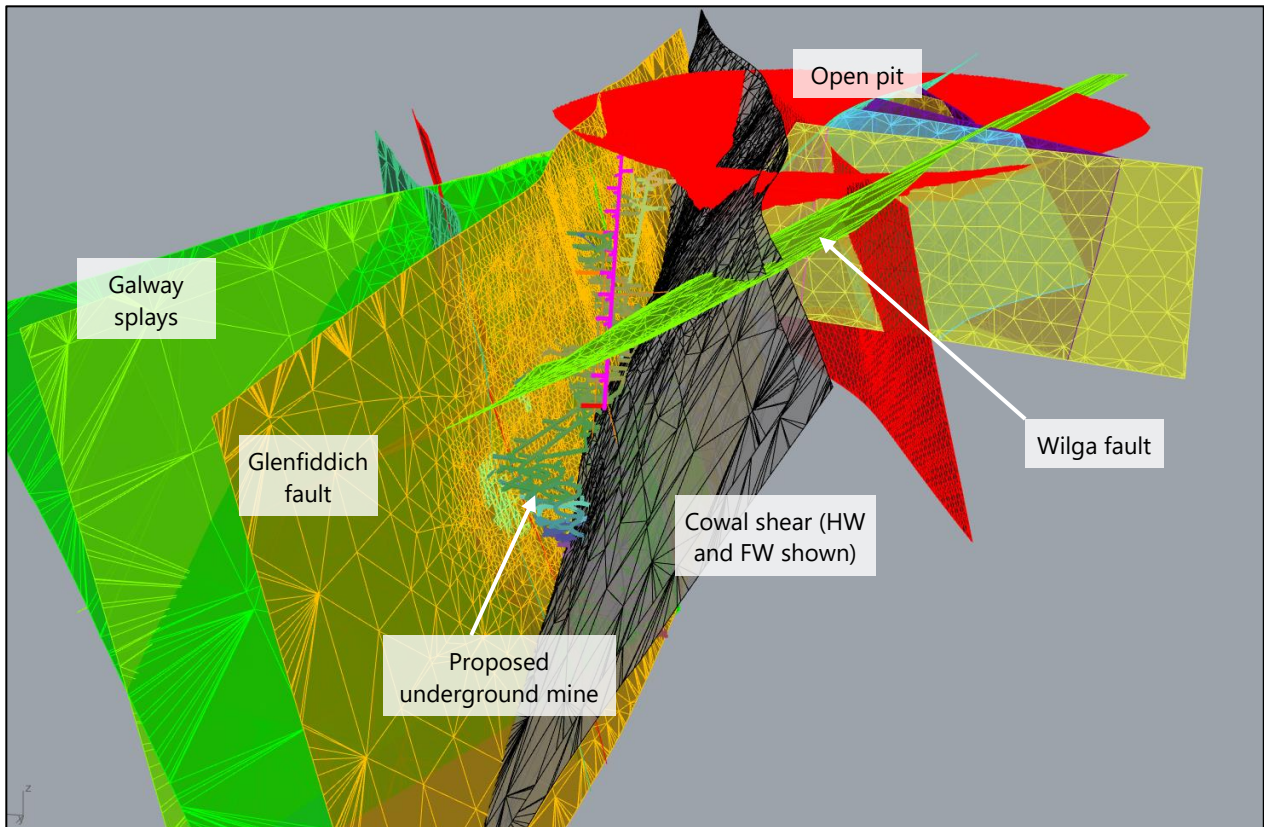
**Figure 2-2: Cross section through the numerical model showing lithology domains in the underground mining precinct.**

### 2.3 Structures

A description of each fault was provided by Evolution Mining as shown in Figure 2-3. Figure 2-4 shows the structures as built in the FE mesh.

Fault Name	Estimated Av Thickness	Estimated Strength	Comments
Ardbeg	Up to 1m	Mod to Weak	Clay sericite filled. - Typically sericite altered. Contained within broader Se alteration zone.
Central	Up to 2m	Weak	Strongly sheared and brecciated fault zone. Weak pervasive si-ser alteration overprinting weak background ch-c alteration. Moderate clay gouge abundant towards base of zone noted in some holes. Minor brecciated clasts.
Cowal	Variable	Mod to Weak	Strongly sheared zone with associated competent dyke. Se altered. Gouge clay on shear and fracture planes with minor brecciated clasts. Occasional slickensides. Moderate clay gouge abundant towards base of zone noted in some holes.
Galway3	Up to 2m	Mod	Phyllic altered zone of shearing. Strong sericite alteration. Some 5mm pug filled faults within zone.
Galway7	Up to 2m	Mod to weak	Phyllic altered zone shear zone with some fractured rock. Gouge filled planes to 10mm noted in some holes at top and bottom of unit.
Glenfiddich	Broader zone up to 1m wide, containing discrete clay filled planes.	Mod to weak	Discrete clay filled planes (to 10mm) within zone of sheared and sometimes fractured rock. Minimal alteration halo. Sometimes healed.
Manna	Up to 1m	Mod to Weak	Clay sericite filled. - Typically sericite altered. Contained within broader Se alteration zone.
Nerang	Up to 2m	Mod	Variable broad mylonitic shear zone to brittle discrete fault zone, broken and sheared host rock, qz cb infill fault gouge and clay on shear surfaces within zone.
Western4	Up to 2m	Strong to mod	Often strongly healed brittle zone with brecciated wall rock material cemented within fine fault gouge. Variable strong phyllic alteration.
Wyrra	Up to 1m	Mod	Discrete fault zone with slickensides, gouge present. Phyllic halo.

**Figure 2-3: Fault details provided by Evolution Mining.**



Ardbeg Fault.dxf - Copy	<input type="checkbox"/>	<input type="checkbox"/>	<input type="checkbox"/>	<input type="checkbox"/>
Bodels	<input type="checkbox"/>	<input type="checkbox"/>	<input type="checkbox"/>	<input type="checkbox"/>
Bulldog	<input type="checkbox"/>	<input type="checkbox"/>	<input type="checkbox"/>	<input type="checkbox"/>
Central_extended.dxf - Copy	<input type="checkbox"/>	<input type="checkbox"/>	<input type="checkbox"/>	<input type="checkbox"/>
cowl shear fw	<input type="checkbox"/>	<input type="checkbox"/>	<input type="checkbox"/>	<input type="checkbox"/>
cowl shear hw	<input type="checkbox"/>	<input type="checkbox"/>	<input type="checkbox"/>	<input type="checkbox"/>
EastCorringal	<input type="checkbox"/>	<input type="checkbox"/>	<input type="checkbox"/>	<input type="checkbox"/>
Galway Splay 3.dxf - Copy	<input type="checkbox"/>	<input type="checkbox"/>	<input type="checkbox"/>	<input type="checkbox"/>
Galway Splay 7.dxf - Copy	<input type="checkbox"/>	<input type="checkbox"/>	<input type="checkbox"/>	<input type="checkbox"/>
Girral	<input type="checkbox"/>	<input type="checkbox"/>	<input type="checkbox"/>	<input type="checkbox"/>
Glenfiddich revised.dxf - Copy	<input type="checkbox"/>	<input type="checkbox"/>	<input type="checkbox"/>	<input type="checkbox"/>
Manna Fault.dxf - Copy	<input type="checkbox"/>	<input type="checkbox"/>	<input type="checkbox"/>	<input type="checkbox"/>
Nerang	<input type="checkbox"/>	<input type="checkbox"/>	<input type="checkbox"/>	<input type="checkbox"/>
Wamboyne	<input type="checkbox"/>	<input type="checkbox"/>	<input type="checkbox"/>	<input type="checkbox"/>
WestCorringal	<input type="checkbox"/>	<input type="checkbox"/>	<input type="checkbox"/>	<input type="checkbox"/>
Western	<input type="checkbox"/>	<input type="checkbox"/>	<input type="checkbox"/>	<input type="checkbox"/>
Wilga.dxf - Copy	<input type="checkbox"/>	<input type="checkbox"/>	<input type="checkbox"/>	<input type="checkbox"/>
Wyrra	<input type="checkbox"/>	<input type="checkbox"/>	<input type="checkbox"/>	<input type="checkbox"/>

Figure 2-4: Perspective views showing structures built in FE mesh together with meshed LOM geometry.

The resolution of the available structural information allows mine-scale interpretations of the model results. This means that average strains across the rockmass between modelled structures can be simulated and interpreted, but locally higher strains due to structures smaller than those modelled explicitly cannot develop in the model. For interpretations of potential peak strains, which may be needed to assess the potential for locally high deformation levels around individual stopes for example, a model incorporating structures with persistence smaller than the scale of the stopes themselves would be needed.

With the current model, we therefore cannot forecast the stability of individual stopes, because stope stability forecasts depend largely on stope-scale structures<sup>1</sup>. Likewise, we cannot forecast the stability of individual drives because such forecasts depend on drive-scale<sup>2</sup> structures. The model does allow general interpretations of stope and drive stability based on, for example, forecast deformation arising from weaker rockmass conditions, adverse geometric configurations and sequences, but explicit forecasts are not possible.

## 2.4 Estimated material properties for modelling

The material properties used in the model are given in Table 2-1. The following nomenclature is used in Table 2-1:

UCS	= uniaxial compressive strength.
GSI	= geological strength index.
$\epsilon_0$	= 0 = plastic strain at start of peak strength stage (see Figure 2-6).
$\epsilon_1$	= plastic strain at start of transitional strength stage (see Figure 2-6).
$\epsilon_2$	= plastic strain at start of residual strength stage (see Figure 2-6).
$E$	= Young's modulus for the rockmass.
$\nu$	= Poisson's ratio for the rockmass.
$s, m, a$	= generalised HB yield parameter for the rockmass.
$d$	= rockmass dilation parameter.
$\kappa$	= $s\sigma_c^{1/a}$ = Generalised HB cohesion parameter for the rockmass. Units are $\text{MPa}^{1/a}$ .
$\Phi$	= $m\sigma_c^{1/a-1}$ = Generalised HB friction parameter for the rockmass. Units are $\text{MPa}^{1/a-1}$ .

Material properties for this project were taken from previously modelling projects by AMC and Itasca (see Figure 2-5). We note the previously developed fault properties do not necessarily match the description provided in Figure 2-3.

The material properties for this project were taken from those developed by AMC and Itasca as part of previous open pit assessments, as advised by Evolution mining. The faults, transported and soft oxide material properties previously described use a Mohr-Coulomb strength criterion. A Hoek-Brown strength criterion was applied in the FE material model framework with input parameters closely matched to the Mohr-Coulomb strength criterion developed by Itasca as shown in Figure 2-5.

---

<sup>1</sup> Stope-scale structures have a persistence similar to the stope dimensions.

<sup>2</sup> Drive-scale structures have a persistence of ~5m and larger.

**EVOLUTION: LAKE COWAL UNDERGROUND MINE SUBSIDENCE ASSESSMENT**

Soils	Density (t/m <sup>3</sup> )	Cohesion (MPa)	Phi (deg)	Tensile Strength (MPa)	E <sub>rm</sub> (GPa)	Hoek's D	Poisson's Ratio							
Transported	1.85	0.026	26.7	1.0	0.4	-	0.30							
SOx	1.95	0.028	24.0	1.0	0.4	-	0.30							
								Segment 1	Segment 2					
Rock	Density (t/m <sup>3</sup> )	E <sub>i</sub> (GPa)	UCS (MPa)	GSI	m <sub>i</sub>	Hoek's D	Cohesion (MPa)	Phi (deg)	C (MPa)	Phi (deg)	Tensile (MPa)	E <sub>rm</sub> (GPa)	Poisson's Ratio	
Hox	2.00	67	127	34	14	1.0	0.21	38	-	-	0.017	3.62	0.27	
Andesite	2.77	65	125	73	21	0.7	2.38	60	3.34	55	0.524	24.82	0.21	
						1.0	1.80	60	2.16	56	0.455	16.08		
Diorite	2.80	70	132	75	24	0.7	2.75	62	3.78	57	0.580	28.74	0.21	
						1.0	2.12	61	2.51	58	0.509	18.90		
Lava	2.76	70	159	74	22	0.7	3.14	61	4.10	57	0.697	27.74	0.21	
						1.0	2.41	60	2.78	57	0.608	18.11		
UVc	2.77	67	127	74	14	0.7	3.03	55	3.80	51	0.874	26.55	0.21	
						1.0	2.34	54	2.63	51	0.763	17.33		
LVc	2.77	67	127	75	14	0.7	3.27	55	4.03	51	0.957	27.51	0.21	
						1.0	2.55	54	2.83	52	0.839	18.09		
EVC	2.77	67	127	66	14	0.7	1.69	56	2.48	49	0.426	18.72	0.22	
						1.0	1.19	55	1.49	50	0.356	11.60		
Cowal Fault Zone	2.80	70	132	25	24	0.7	0.16	52	0.70	37	0.006	2.12	0.28	
						1.0	0.06	48	0.25	33	0.004	1.77		
	2.80	70	132	40	24	0.5	0.38	61	1.27	49	0.032	5.38	0.26	
						0.7	0.31	59	1.09	45	0.025	4.08		
						1.0	0.15	56	0.44	44	0.018	2.79		
Single Faults	Cohesion (kPa)	Phi (deg)	Tensile Strength (MPa)	Shear Stiffness (GPa/m)	Normal Stiffness (GPa/m)									
	50	30	0	1	10									

**Figure 2-5: Material properties used by Itasca (and AMC) for numerical modelling undertaken in 2015/16**

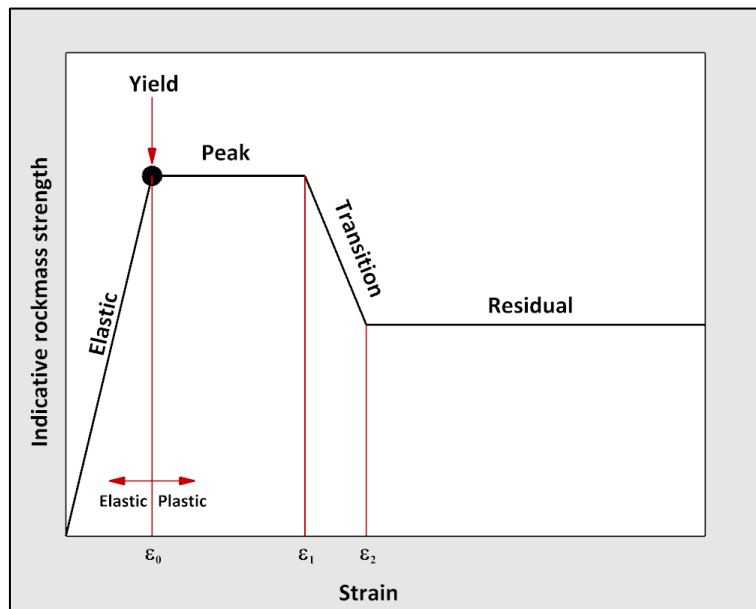


**Figure 2-6:** Indicative rockmass softening curve demonstrating the plastic strain transition points  $\epsilon_1$  and  $\epsilon_2$ .

Table 2-1: Rock mass properties used in the FE model.

## LAKE COWAL

### Material property set M03

Number	Domain	Code	Density (kg/m <sup>3</sup> )	UCS (MPa)	GSI	Stage	Plastic strain	E (GPa)	v	s	m	α	d	κ	Φ
1	HARD OXIDE	TRANS	2,000	60	35	Peak	ε <sub>0</sub> = 0.0%	12.5	0.24	5.05E-04	0.64	0.500	0.15	1.8	38
						Transition	ε <sub>1</sub> = 2.8%	12.5	0.24	5.05E-04	0.64	0.500	0.15	1.8	38
						Residual	ε <sub>2</sub> = 4.9%	12.5	0.24	4.01E-04	0.70	0.500	0.05	1.4	42
2	ANDERSITE	ANDST	2,770	125	73	Peak	ε <sub>0</sub> = 0.0%	26.1	0.28	6.10E-03	2.55	0.500	0.31	95	320
						Transition	ε <sub>1</sub> = 1.9%	26.1	0.28	6.10E-03	2.55	0.500	0.31	95	320
						Residual	ε <sub>2</sub> = 3.3%	26.1	0.28	2.09E-03	1.45	0.500	0.11	33	180
3	DIORITE	DIOR	2,800	132	75	Peak	ε <sub>0</sub> = 0.0%	27.6	0.28	7.57E-03	2.81	0.500	0.33	130	370
						Transition	ε <sub>1</sub> = 1.8%	27.6	0.28	7.57E-03	2.81	0.500	0.33	130	370
						Residual	ε <sub>2</sub> = 3.2%	27.6	0.28	2.36E-03	1.53	0.500	0.12	41	200
4	GRANODIORITE	GRAN	2,800	127	70	Peak	ε <sub>0</sub> = 0.0%	26.5	0.28	6.17E-03	2.49	0.500	0.32	100	320
						Transition	ε <sub>1</sub> = 1.9%	26.5	0.28	6.17E-03	2.49	0.500	0.32	100	320
						Residual	ε <sub>3</sub> = 3.3%	26.5	0.28	2.17E-03	1.47	0.500	0.11	35	190
5	DEWARS	DEWAR	2,800	127	70	Peak	ε <sub>0</sub> = 0.0%	26.5	0.28	6.17E-03	2.49	0.500	0.32	100	320
						Transition	ε <sub>1</sub> = 1.9%	26.5	0.28	6.17E-03	2.49	0.500	0.32	100	320
						Residual	ε <sub>2</sub> = 3.3%	26.5	0.28	2.17E-03	1.47	0.500	0.11	35	190
6	INTRUSIVE BRECCIA	BREC	2,800	127	70	Peak	ε <sub>0</sub> = 0.0%	26.5	0.28	6.17E-03	2.49	0.500	0.32	100	320
						Transition	ε <sub>1</sub> = 1.9%	26.5	0.28	6.17E-03	2.49	0.500	0.32	100	320
						Residual	ε <sub>2</sub> = 3.3%	26.5	0.28	2.17E-03	1.47	0.500	0.11	35	190
7	LAVA	LAVA	2,760	159	72	Peak	ε <sub>0</sub> = 0.0%	33.2	0.30	1.51E-02	3.53	0.500	0.40	380	560
						Transition	ε <sub>1</sub> = 1.5%	33.2	0.30	1.51E-02	3.53	0.500	0.40	380	560
						Residual	ε <sub>2</sub> = 2.7%	33.2	0.30	3.59E-03	1.84	0.500	0.14	91	290
8	MONZONITE	MONZ	2,760	127	70	Peak	ε <sub>0</sub> = 0.0%	26.5	0.28	6.17E-03	2.49	0.500	0.32	100	320
						Transition	ε <sub>1</sub> = 1.9%	26.5	0.28	6.17E-03	2.49	0.500	0.32	100	320
						Residual	ε <sub>2</sub> = 3.3%	26.5	0.28	2.17E-03	1.47	0.500	0.11	35	190
9	UPPER SEDIMENTS	UP_SED	2,770	127	65	Peak	ε <sub>0</sub> = 0.0%	26.5	0.28	5.73E-03	2.31	0.500	0.32	92	290
						Transition	ε <sub>1</sub> = 1.9%	26.5	0.28	5.73E-03	2.31	0.500	0.32	92	290
						Residual	ε <sub>2</sub> = 3.3%	26.5	0.28	2.17E-03	1.47	0.500	0.11	35	190
10	VC SEDIMENTS GEN	GEN_SED	2,770	127	65	Peak	ε <sub>0</sub> = 0.0%	26.5	0.28	5.73E-03	2.31	0.500	0.32	92	290
						Transition	ε <sub>1</sub> = 1.9%	26.5	0.28	5.73E-03	2.31	0.500	0.32	92	290
						Residual	ε <sub>2</sub> = 3.3%	26.5	0.28	2.17E-03	1.47	0.500	0.11	35	190

LAKE COWAL - Material property set M03

COWAL2019NOV14\_MATPROPS\_RECORD.xlsm

### Cover sequence

The properties listed below were applied to the weathered cover sequence domains as specified by Evolution (2019):

Transported (inputs from Figure 2-5)

c = 26 kPa, phi = 26.7 deg, E<sub>(rm)</sub> = 0.4 GPa, v = 0.3

Soft Oxide (inputs from Figure 2-5)

c = 28 kPa, phi = 24 deg, E<sub>(rm)</sub> = 0.4 GPa, v = 0.3

Hard Oxide

GSI = 35, UCS = 60, Mi = 14, E<sub>(intact)</sub> = 20 GPa,

Note the UCS values provided here differ significantly from the data used the AMC and ITASCA modelling of 2014 and 2015. This change was requested by Evolution's Group Geotechnical Engineer following discussions of the relative strength of the hard oxide compared to the fresh rock.

### Fault properties

Strength properties for faults were grouped into two categories following discussions with Evolution's Group Geotechnical Engineer. Previously, only one set of strength parameters were applied to all of the faults at Lake Cowal. However, this is counter intuitive as the faults have significantly different strength characteristics

and applying a single strength criterion would be contradictory to the information and range of fault properties provided in Figure 2-3. A complete catalogue of fault properties was not provided for the project. Following discussion with Evolution's Group Geotechnical Engineer, it was decided that two sets of fault properties would be adopted in the fresh rock, and a weaker fault strength applied for the faults in the oxide domain. The two sets of properties in fresh rock were for the "weak" and "moderate/strong faults" as described in Figure 2-3. All faults described as weak or moderate to weak, were given the properties of "weak" faults listed below. Faults categorised as moderate or strong to moderate, were given the "strong" properties listed below. Please note the terminology is in relative terms only and may not be comparable to fault properties at other mines.

Faults in the weathered oxide zone are known to be weaker compared to fresh rock. BE noted that the fault properties used in previous modelling in 2014 and 2015 were actually stronger than the soft oxide, which is counter intuitive and unrealistic. Discussions with Evolution's Group Geotechnical Engineer lead to the fault properties in the oxide domains as listed below:

- Faults in the oxide zone – Cohesion = 25 kPa, friction angle = 20 degrees
- "Weak" faults – Cohesion = 50 kPa, friction angle = 30 degrees
- "Moderate/Strong" faults – Cohesion = 85 kPa, friction angle = 38 degrees

The Wilga fault was found to be an important fault with significant response in the previous model iterations. The Wilga fault is not listed in Figure 2-3. The moderate/strong properties were applied to the Wilga fault. A Mohr-Coulomb strength criterion for the faults was used for the simulation at the request of Evolution.

### **Rockmass properties**

The intact rock properties applied for the fresh rock domains have been taken from the 2014 and 2015 simulations conducted by AMC and ITASCA (respectively). One difference is that a D factor, or blasting factor has not been applied in the BE model simulation. The D factor is an empirical factor used to reduce the strength of a rockmass due to blasting damage or disturbance.

This factor is not relevant for the subsidence assessment conducted as the area of interest is not subject to blast damage. The D factor has been used successfully in literature for downgrading rockmass properties close to the excavation boundary, such as pit wall and for slope stability assessments. However, the factor should not be applied prior to mining or throughout all of the rockmass within the model (regardless the distance from blasting), as per previous model simulations. This point was discussed and agreed with Evolution prior to model simulation.

### 2.5 Stress field

No in-situ stress testing has been undertaken at the CGO to date. The stress field applied in the numerical model was taken from a nearby underground mine with extensive in situ stress testing. The in-situ stress regime for the nearby mine is provided in Figure 2-7. The major principal stress direction also corresponds to the regional stress regime for the district, as shown in Figure 2-8.

Principal stress component	Magnitude gradient (MPa/km)	Dip (degrees)	Dip azimuth (degrees)	$\sigma_i/\sigma_{zz}$
$\sigma_1$	57.8	0	290	2.14
$\sigma_2$	30.3	0	200	1.60
$\sigma_3$	23.6	90	090	1.00

Stress gradients applied from reference  $z = 5,100\text{mRL}$ .

Cartesian stress tensor at 1,000m:

$$\begin{bmatrix} \sigma_{xx} & \sigma_{xy} & \sigma_{zx} \\ \sigma_{xy} & \sigma_{yy} & \sigma_{yz} \\ \sigma_{zx} & \sigma_{yz} & \sigma_{zz} \end{bmatrix} = \begin{bmatrix} \sigma_{EE} & \sigma_{EN} & \sigma_{UE} \\ \sigma_{EN} & \sigma_{NN} & \sigma_{NU} \\ \sigma_{UE} & \sigma_{NU} & \sigma_{UU} \end{bmatrix} = \begin{bmatrix} 56 & -4.8 & 0 \\ -4.8 & 45 & 0 \\ 0 & 0 & 27 \end{bmatrix} \text{MPa}$$

Ratio of average horizontal stress to vertical stress:  
(Brady & Brown 2006, p. 159)

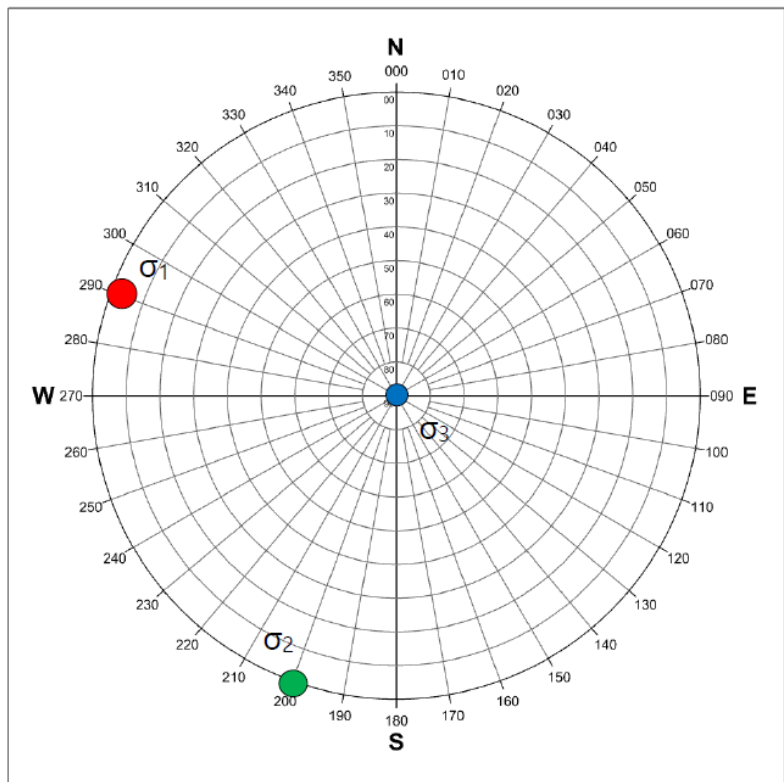
$$k = \frac{k_x + k_y}{2} = \frac{\sigma_{xx} + \sigma_{yy}}{2\sigma_{zz}} = 1.87$$


Figure 2-7: In situ stress applied in the FE model

Stress Province	Principal Stresses (at a depth of 1000m, for stress measurements > 500m)	
	$\sigma_1$ Orientation	Magnitudes (MPa); $\sigma_1 : \sigma_2 : \sigma_3$
1 Yilgarn	Variable, WSW-ENE (?)	90 : 50 : 35
2 Gawler-Curnamona	WNW-ESE	55 : 40 : 30
3 Lachlan	WNW-ESE	55 : 35 : 30
4 Arunta	WSW-ENE	55 : 40 : 25
5 Kimberley	SW-NE (?)	50 : 40 : 25 (?)
6 Mt Isa Inlier	WSW-ENE	40 : 30 : 20

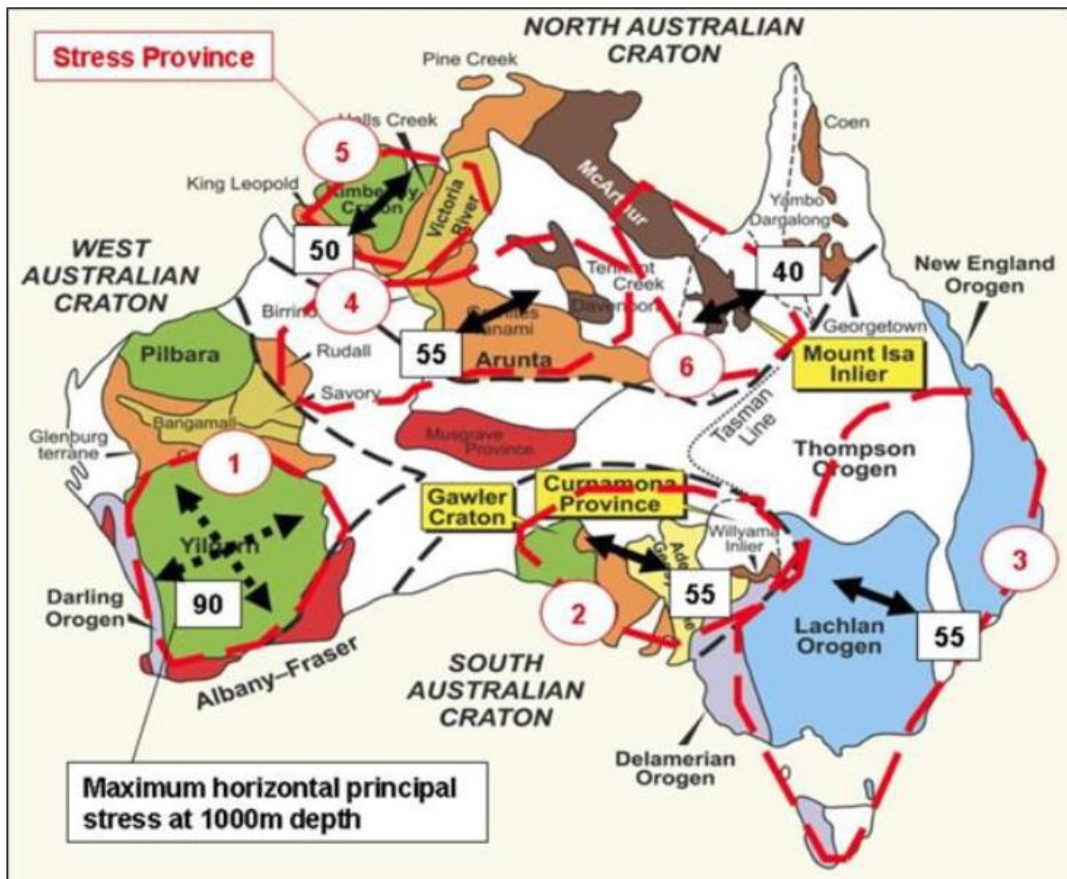


Figure 2-8: Stress provinces in the Australian continent (after Lee et al. 2010)

## 2.6 Hydrogeological conditions

The effects of groundwater drawdown on surface subsidence have not been included in the numerical simulation to assess surface subsidence as we understand the underground mining sequence is effectively drained due to open pit drawdown of the water table.



**2.7 Stope filling methodology and fill properties**

In the model, stopes to be mined in frame  $i$  starting at time  $t_i$  are excavated over the period  $t_i$  to  $t_i + 0.1s$  by ramping down the Young’s modulus from the rockmass value to the void value of 0.1 MPa. Stopes are filled at the end of the frame (at  $t_i + 3.0s$ ) by setting the elastic constants of the stope void to fill properties. In practice, the mine could leave stopes open for longer than modelled and may not always achieve tight-filling.

The following elastic constants were applied for fill:

- Young’s modulus  $E_{fill} = 100$  MPa.
- Poisson’s ratio  $\nu_{fill} = 0.25$ .

**2.8 Mining geometry and sequence**

The model included the complete as-built and planned geometry for CGO’s UG, comprising:

- The current as-built open pit and future open pit mining.
- All underground lateral and vertical development.
- All stopes.
- Surface dumps, tailings dam and the dam wall for the lake.

Table 2-2 summarises the modelled sequence.

**Table 2-2:** Summary of model sequence Q01 with corresponding calendar dates.

Model step	Year/ Quarter	Model step	Year/ Quarter	Model step	Year/ Quarter
1	Y2007_Q01	31	Y2025	61	Y2031
2	Y2009_Q01	32	Y2025_Q01	62	Y2031_Q01
3	Y2011_Q01	33	Y2025_Q02	63	Y2031_Q02
4	Y2013_Q01	34	Y2025_Q03	64	Y2031_Q03
5	Y2015_Q01	35	Y2025_Q04	65	Y2031_Q04
6	Y2017_Q01	36	Y2026	66	Y2032_Q01
7	Y2019_Q01	37	Y2026_Q01	67	Y2032_Q02
8	Y2019_Q02	38	Y2026_Q02	68	Y2032_Q03
9	Y2020_Q01	39	Y2026_Q03	69	Y2032_Q04
10	Y2020_Q02	40	Y2026_Q04	70	Y2033_Q01
11	Y2020_Q03	41	Y2027	71	Y2033_Q02
12	Y2020_Q04	42	Y2027_Q01	72	Y2033_Q03
13	Y2021	43	Y2027_Q02	73	Y2033_Q04
14	Y2021_Q02	44	Y2027_Q03	74	Y2034_Q01
15	Y2021_Q03	45	Y2027_Q04	75	Y2034_Q02
16	Y2021_Q04	46	Y2028	76	Y2034_Q03
17	Y2022	47	Y2028_Q01	77	Y2034_Q04
18	Y2022_Q02	48	Y2028_Q02	78	Y2035_Q01
19	Y2022_Q03	49	Y2028_Q03		
20	Y2022_Q04	50	Y2028_Q04		
21	Y2023	51	Y2029		
22	Y2023_Q01	52	Y2029_Q01		
23	Y2023_Q02	53	Y2029_Q02		
24	Y2023_Q03	54	Y2029_Q03		
25	Y2023_Q04	55	Y2029_Q04		
26	Y2024	56	Y2030		
27	Y2024_Q01	57	Y2030_Q01		
28	Y2024_Q02	58	Y2030_Q02		
29	Y2024_Q03	59	Y2030_Q03		
30	Y2024_Q04	60	Y2030_Q04		

Review of the latest mine design identified 19 stopes that were located in close proximity to the weathered cover sequence geology, or within the cover sequence layers (see Figure 2-9 and Figure 2-10). Seven of these stopes extend into the hard oxide (a weak to moderate strength rockmass that has been weathered) and some are in close proximity to the top of fresh rock contact with a small crown pillar thickness in strong fresh rock. Some stopes also extend close to the base of the soft oxide, which is very weak. These stopes have a significantly elevated risk of chimneying to surface due to the close proximity of the weak cover layers. Chimneying to surface would have potentially catastrophic effects to the lake and to the underground mine should stope failure reach the surface or groundwater table. Furthermore, these stopes do not have planned top access for cablebolting or to ensure tight filling, which are two of the recommended controls for mitigating stope overbreak and chimneying hazard. Due to the elevated risk of crown pillar instability and chimneying potential of these stopes, BE recommended these stopes be removed from the mine design. This recommendation was followed and an updated mine design without these stopes was provided. The updated mine design was used for this assessment.

We also note the groundwater table is likely to be present in the soft oxide and possibly into the hard oxide. We understand groundwater modelling is being completed as part of the EIS to confirm the phoretic surface during underground mining. Stope interaction with groundwater has two potential impacts to underground mining. One is an increase in pumping due to drainage of groundwater into the mine, the other is stope instability due to the presence of water.

Prior to building the latest numerical model, it was recommended that that a minimum crown pillar thickness between the top of any planned stope and the top of the fresh rock surface be used to update the current design. A minimum stope width to crown pillar thickness of 1:2 was recommended. This corresponds to a minimum crown pillar thickness of ~20m to 30m for the 10 to 15m wide stopes. We note that some stopes are up to 20m wide and the crown pillar thickness should be adjusted, or the stope dimensions on upper levels reduced (i.e. large stopes split into two smaller stopes). The crown pillar is to be in fresh rock, and not within the oxide layers. It is noted this crown pillar requirements is preliminary only and additional geotechnical assessment would be required during the detailed mine design and mine operation once more geotechnical information is available, such as additional drilling information, development mapping and experience in the general underground mining conditions. It was recommended that a total of 19 stopes be removed from the proposed mine design on the two upper most production levels. The mine design was subsequently updated by Evolution following communication of this issue in mid May 2020. As a result, the 19 stopes shown in green in Figure 2-11 have not been included in the model geometry or subsidence assessment in this report. The adjusted mine design has a similar depth of stoping below the top of fresh rock layer as the previous underground mine design.

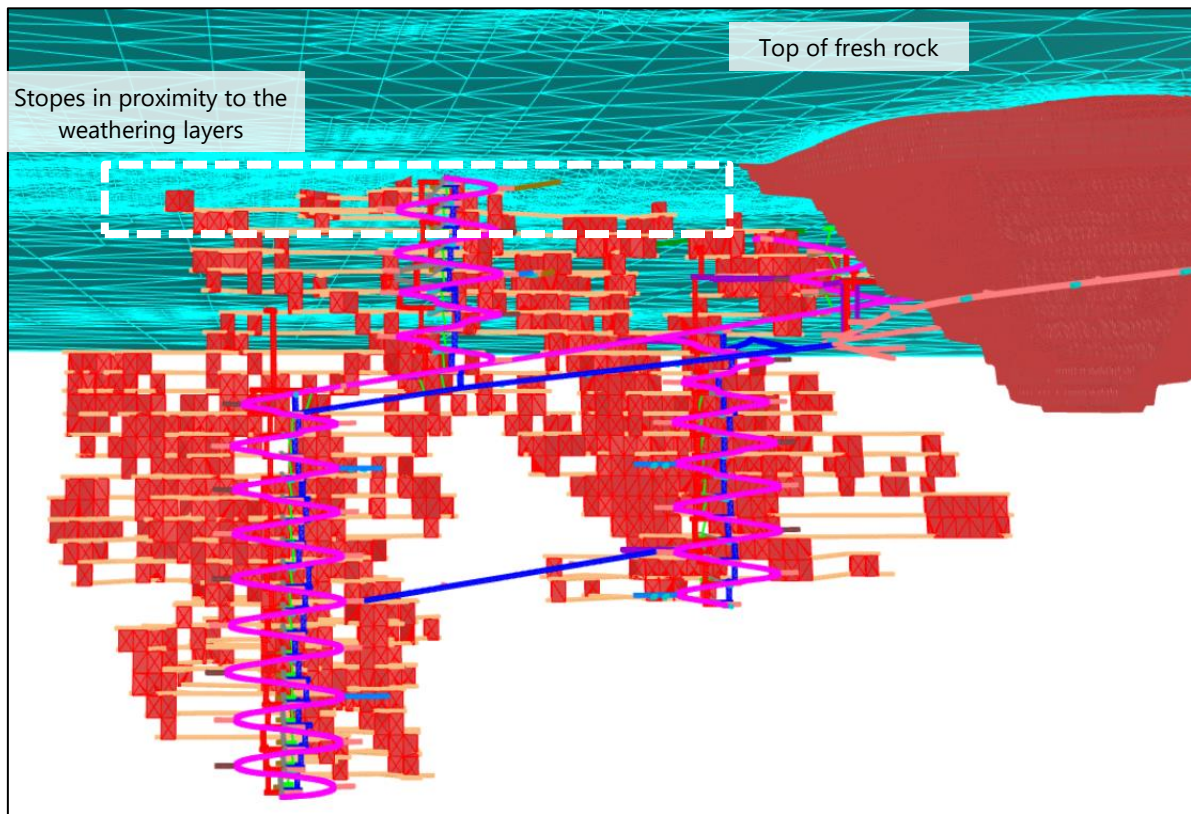


Figure 2-9: Stopes in proximity and intersecting the weathered layers in the latest underground mine design

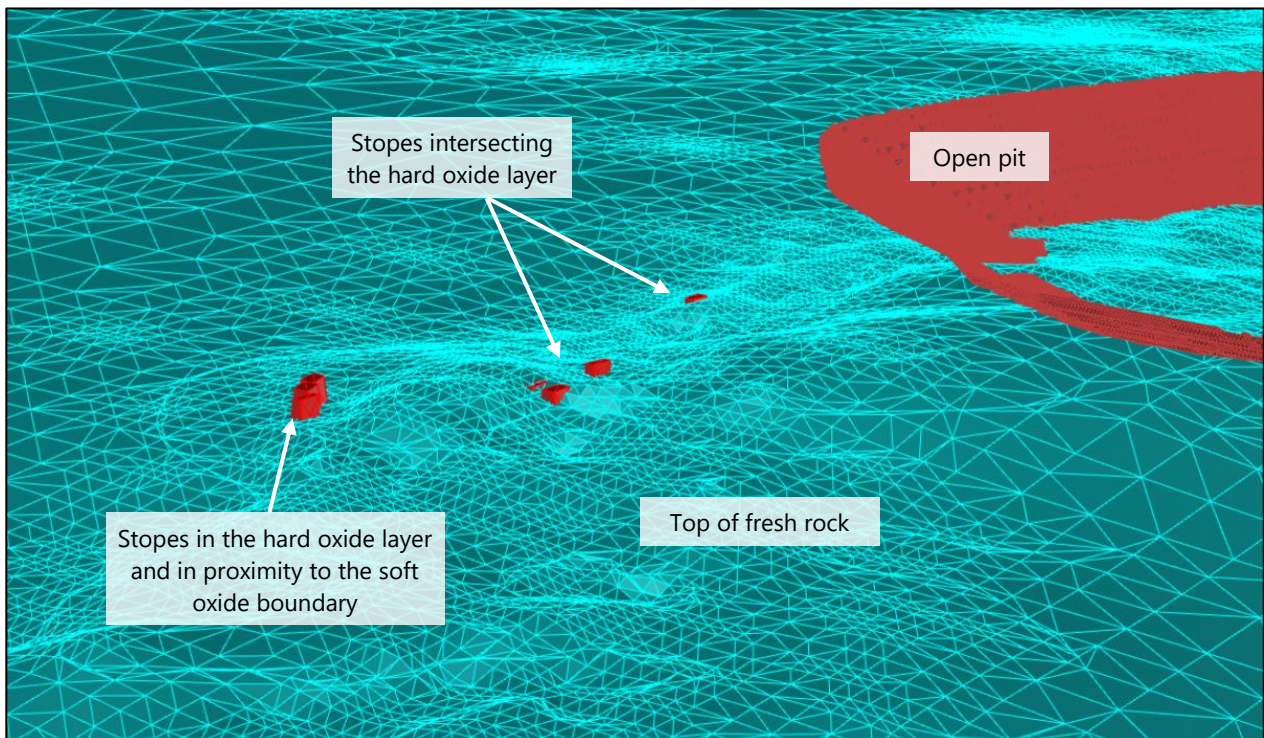
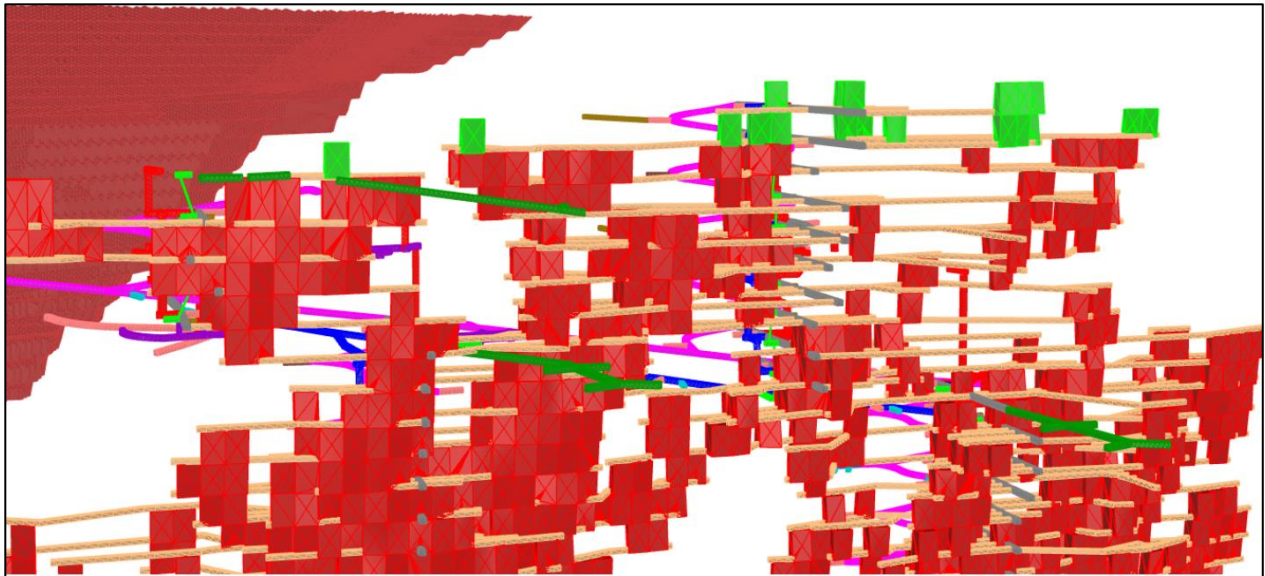


Figure 2-10: Upper levels of stoping intersecting the top of fresh rock boundary



**Figure 2-11: Stopes shown in green were recommended not to be included in the underground mine design due to chimneying potential**

## 2.9 Rockmass damage scale

The rockmass damage scale is used to describe (plastic) strain in the rockmass. The damage scale is shown in Figure 2-12. It uses a logarithmic quantity, called  $\log P$ , defined by

$$\log P = \log_{10}(1000\epsilon_p + 1).$$

Here,  $\epsilon_p$  is the deviatoric equivalent plastic strain. Damage levels in development are well defined by Sandy et al. (2010). In open stopes:

1. Minor rockmass damage indicates a low likelihood of instability.
2. Moderate rockmass damage indicates an increased likelihood of instability, particularly in hangingwalls and crowns.
3. Significant rockmass damage is characterised by relatively high frequency of instability, leading to reduced recovery and productivity and higher dilution and costs.
4. Very significant rockmass damage is characterised by severe stability problems for open stopes and usually necessitates other mining methods.

It is essential to note that these damage categories are indicative only because persistent structures usually control the stability of open stopes.

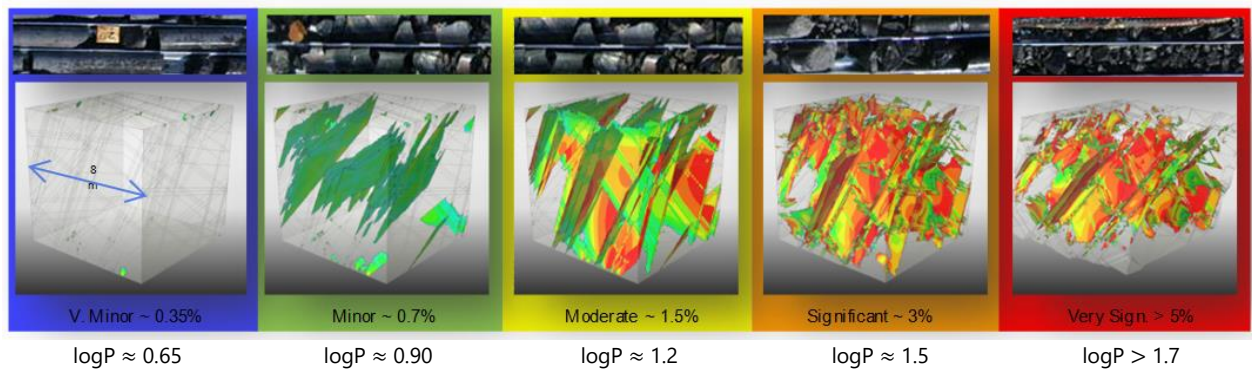


**Figure 2-12: Rockmass damage scale.**

### **3 FORECASTS, INTERPRETATION & DISCUSSION**

This section summarises the model results and our interpretation of the surface impacts due to underground mining and extension of the open pit over the mine life according to the current LOM plan. The results are best reviewed and interpreted using 3D visualisation software such as Voxler, so here we present a comparatively brief summary of the results and our interpretation of the expected behaviour, possible impacts on mining activities and possible risk mitigation measures.

#### **3.1 Surface impacts**

The underground mine is to the north of the existing open pit and below Lake Cowal, which is periodically filled with water after seasonal / heavy rainfall. The underground mine is approximately 130m to 150m below the surface on the uppermost level. This does not include the 19 planned stopes and access development removed by Evolution from the preliminary mine design provided for the numerical model and subsidence assessment. The cover above the underground mine consists of transported sediments, soft oxide and hard oxide material and then fresh rock as shown in Figure 3-1 and Figure 3-2. The underground mine precinct relative to the pit and lake is shown in Figure 3-3.

Forecasts for surface deformation and subsidence include:

1. Forecast vertical movement above the underground mining precinct from 2019 to end of mine life are negligible and generally less than 15mm. Maximum vertical displacement of 25mm are forecast in isolated areas above the underground. This movement is upwards (upsidence, or uplift) is due to displacement along the Glenfiddich fault, which becomes slightly mobilised in the model forecasts due to nearby underground mining. Vertical displacement and total displacement forecasts are shown in Figure 3-6 to Figure 3-10
2. Most surface deformation is elastic in nature and was caused by open pit mining prior to 2019. This is due to the large volume of material removed in the open pit to date, relative to planned mining in the future.
3. Surface displacements are considered negligible (see reference in Figure 3-4) and are within the same order of magnitude as the effects of water (shrink/swell action) and erosion. The forecast levels of surface movement are well within the limits and precision of current geological understanding, material properties and model capabilities at a mine-scale.
4. The model forecasts the Glenfiddich fault is activated by underground mining. Extraction of stopes results in slight upwards displacement of the hangingwall (~15mm) as shown in Figure 3-10 movement is due to a reduction in confinement on the fault as a result of nearby stoping.
5. A plot of total displacement and displacement vectors demonstrates that most movement in proximity to the underground mine is horizontal closure, where the hangingwall and footwall of the underground mine move closer together due to extraction of the orebody (see Figure 3-11). The horizontal displacement forecast is low, but significantly higher than the vertical component. This is normal for long and relatively narrow underground gold mines.
6. Figure 3-12 to Figure 3-16 show examples of surface movement and damage forecast in the model for specific locations along the dam wall and above the underground mine. These reports provide details of forecast movement throughout the planned life of mine for each location indicated on the map. The damage classification scheme is provided in Figure 3-5.

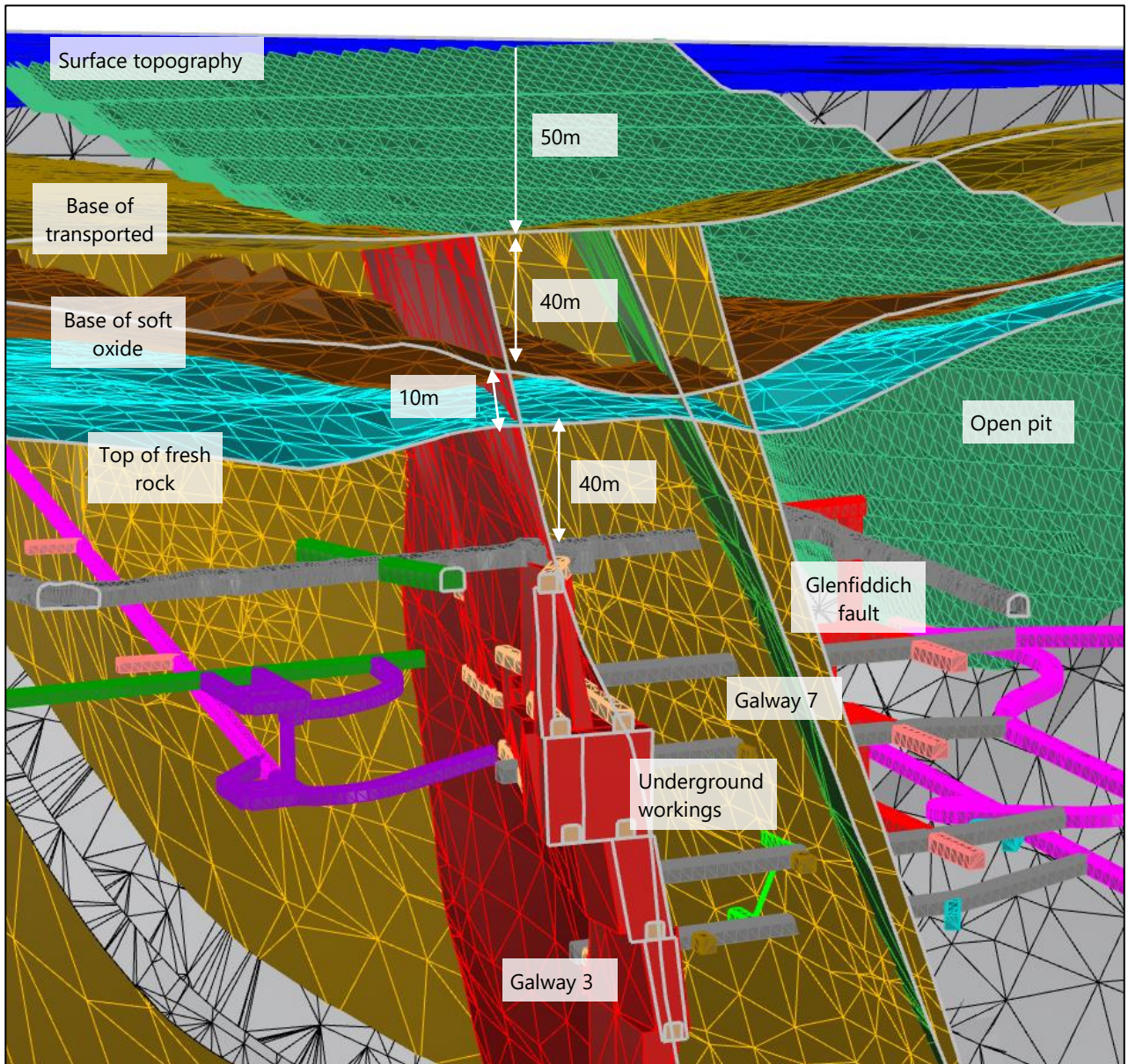


Figure 3-1: Cross section through the proposed underground mine showing indicative thickness of the cover units relative to the underground mine.

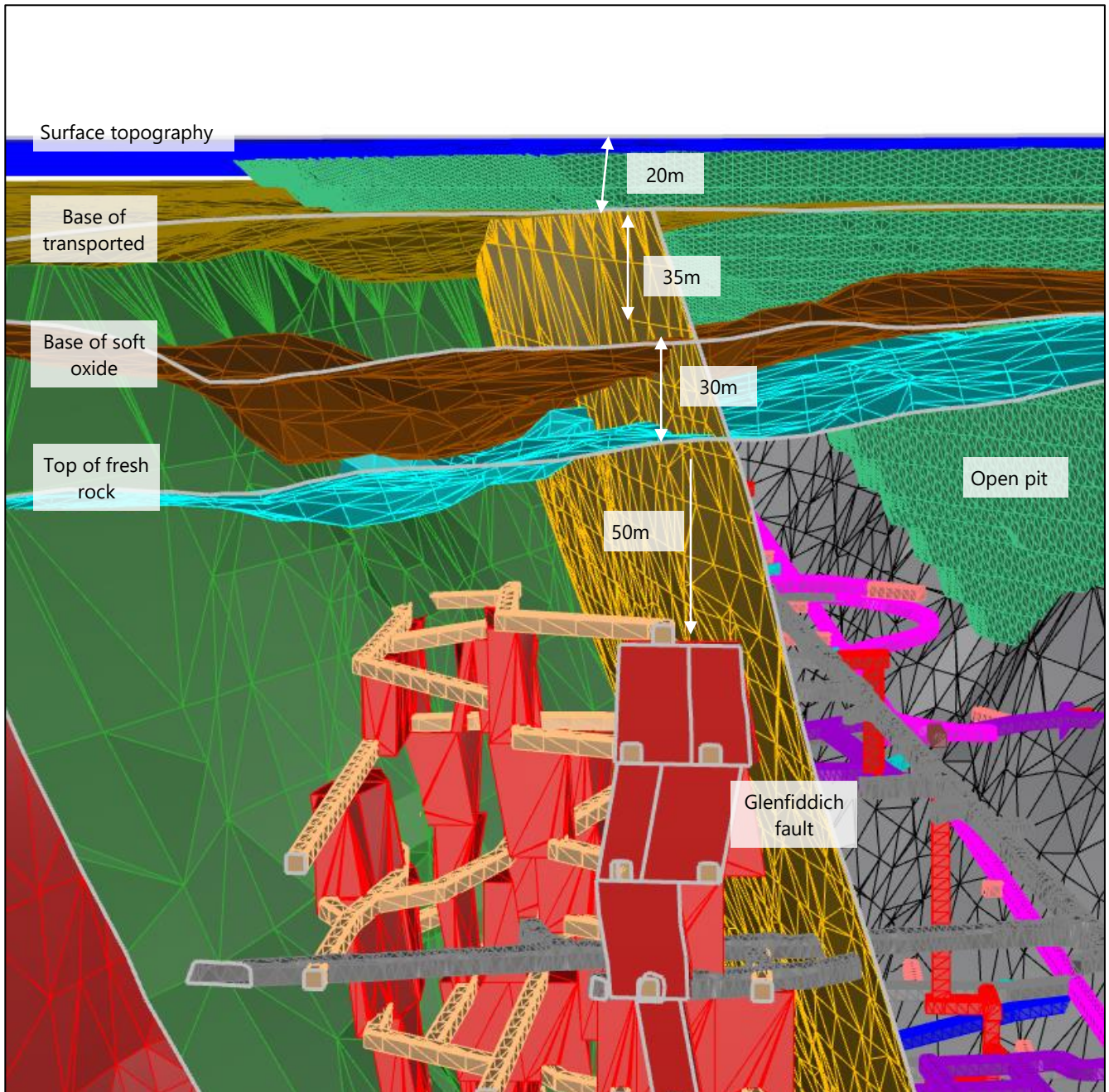


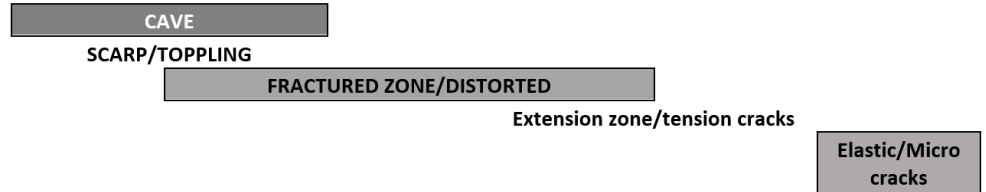
Figure 3-2: Cross section through the proposed underground mine showing indicative thickness of the transported material and soft oxide cover units relative to the underground mine.



Figure 3-3: Aerial photo of the pit and Lake Cowal, with respect to the planned underground mine footprint



Description				
Very Significant movement with Moderate to heavy fracturing with <u>scarp</u> formation and toppling	Very Significant movement with Moderate fracturing with localised heavy fracturing or scarp formation	Moderate movement with Minor Fracturing	Minor movement with Sparse local cracks	Minor Movement (= affected)



Degree of Influence	Very Severe	Severe to Very Severe	Moderate to Severe	Slight to moderate	Negligible	
Subsidence or Horizontal movement	>5-10m	>2m	>1m	>0.5m	>0.2	<0.2m
Horizontal Strain	$\sim 10^{-1}$	$\sim 10^{-2}$	$>3 \times 10^{-3}$	$>1.5 \times 10^{-3}$	$>0.5 \times 10^{-3}$	$<0.5 \times 10^{-3}$
Angular Distortion	$\sim 10^{-1}$	$\sim 10^{-2}$	$>7 \times 10^{-3}$	$>3 \times 10^{-3}$	$>1 \times 10^{-3}$	$<1 \times 10^{-3}$
Plastic Strain	>5%	1-5%	1%	0.70%	0.1-0.3%	<0.1-0.3%

**Figure 3-4: Subsidence classes and criteria**

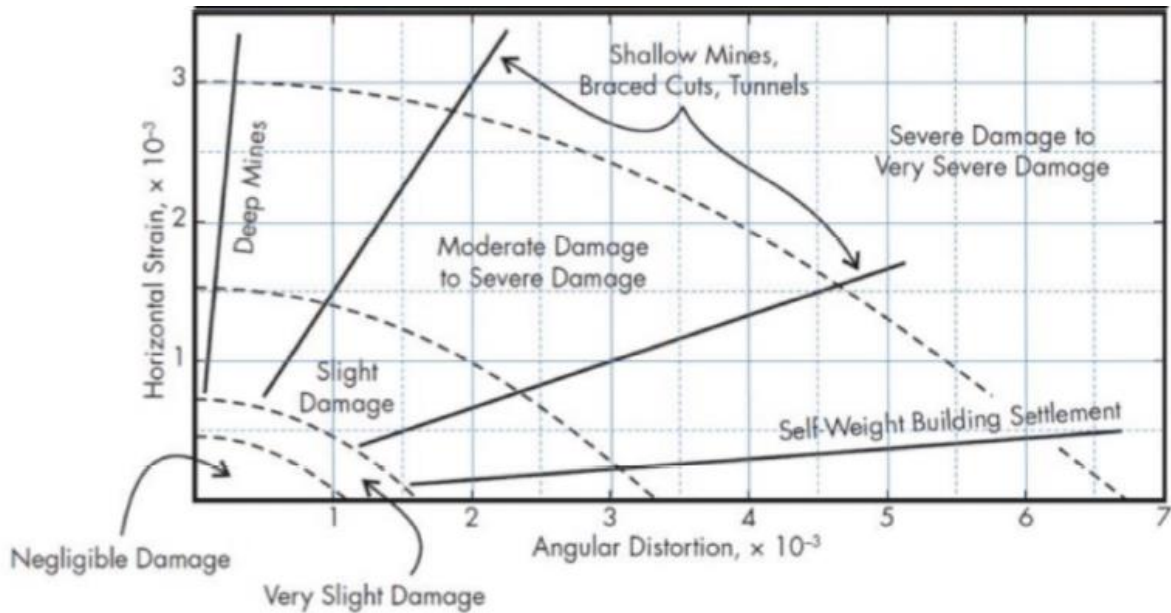


**Figure 3-5: Damage limits and classification for surface infrastructure (after Harrison)**

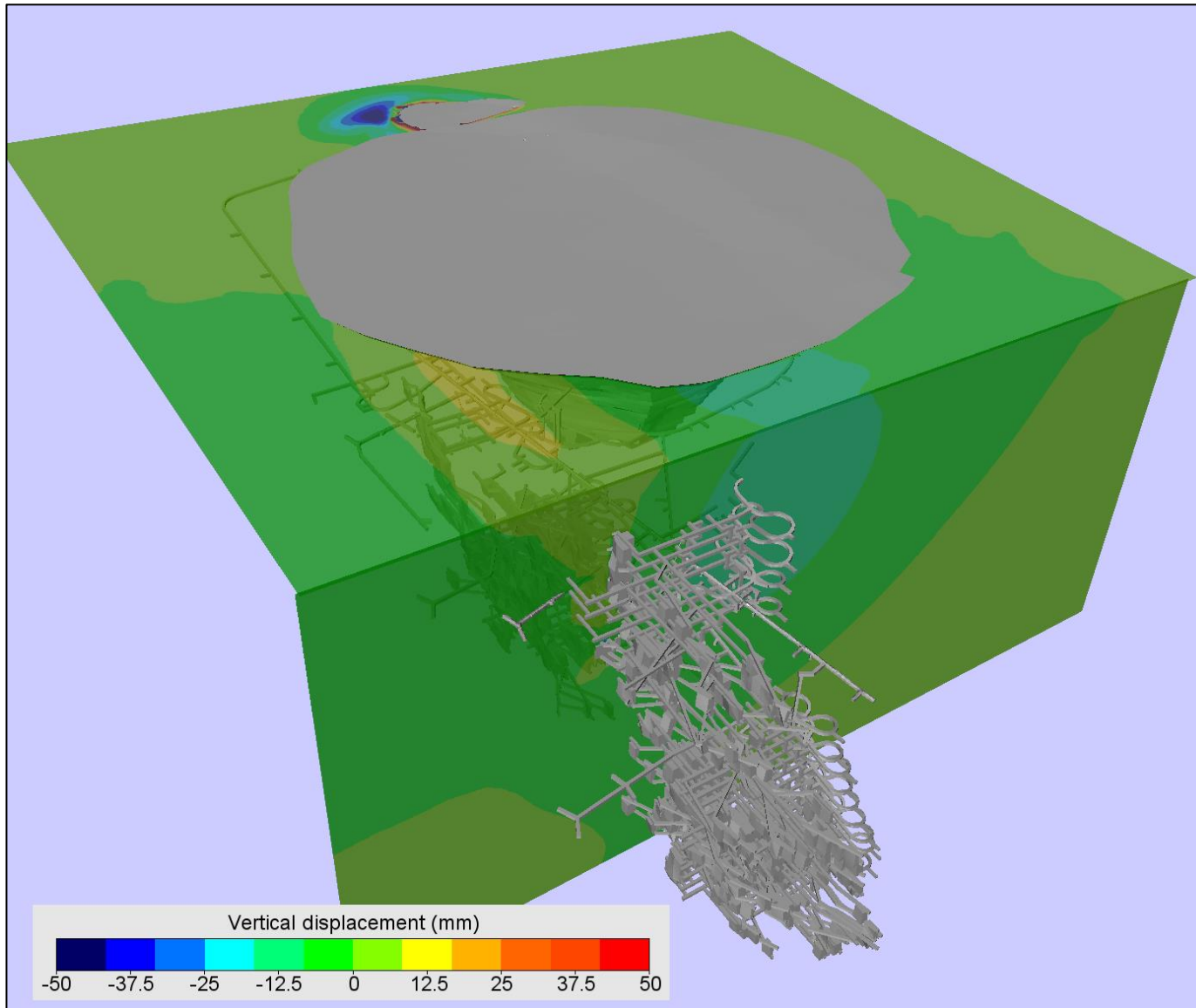


Figure 3-6: Forecasts vertical displacement from the end of 2019 to the end of mine life above the proposed underground mine (horizontal and vertical cross sections through the model)

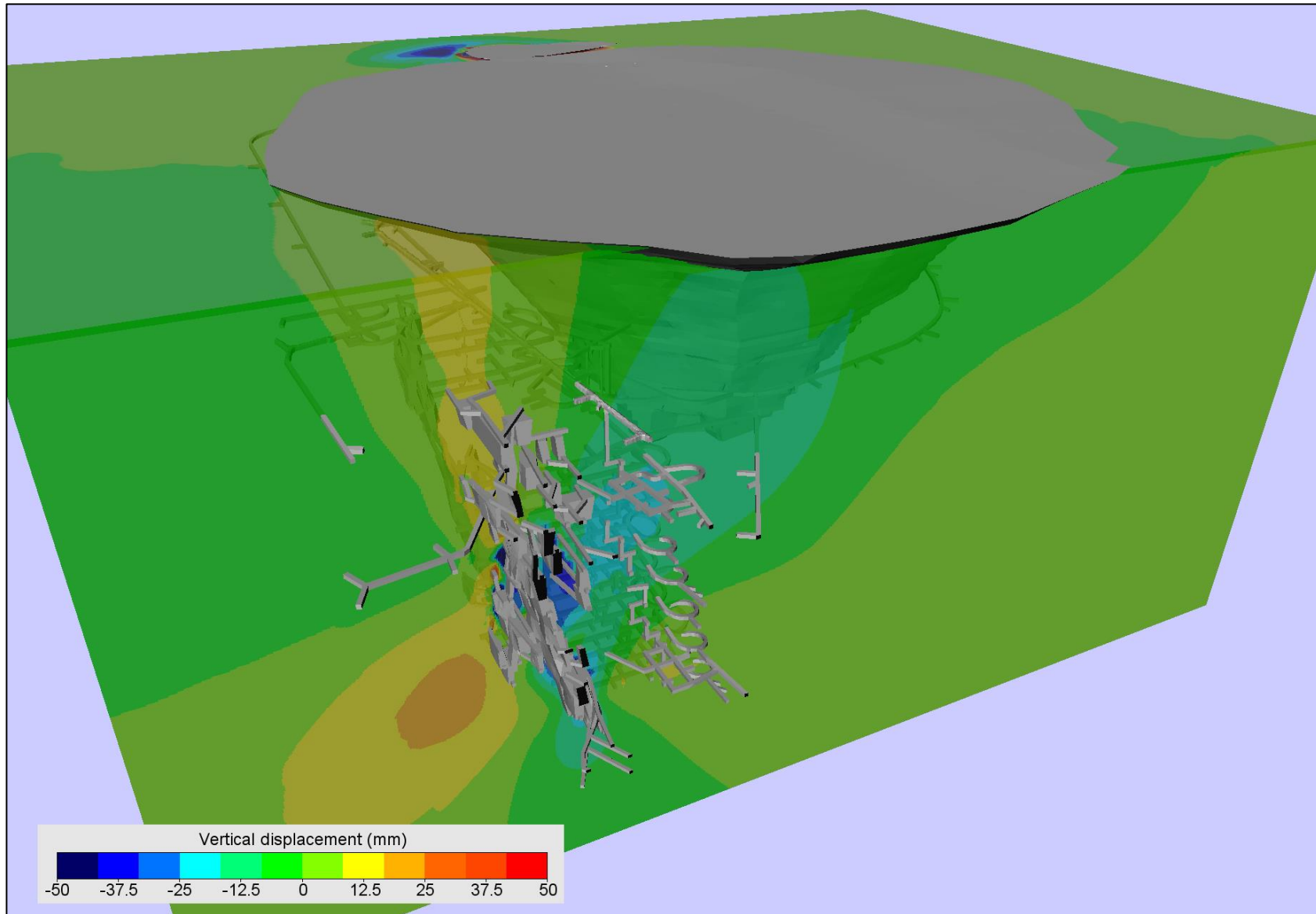


Figure 3-7: Forecasts vertical displacement from the end of 2019 to the end of mine life above the proposed underground mine (horizontal and vertical cross sections through the model)

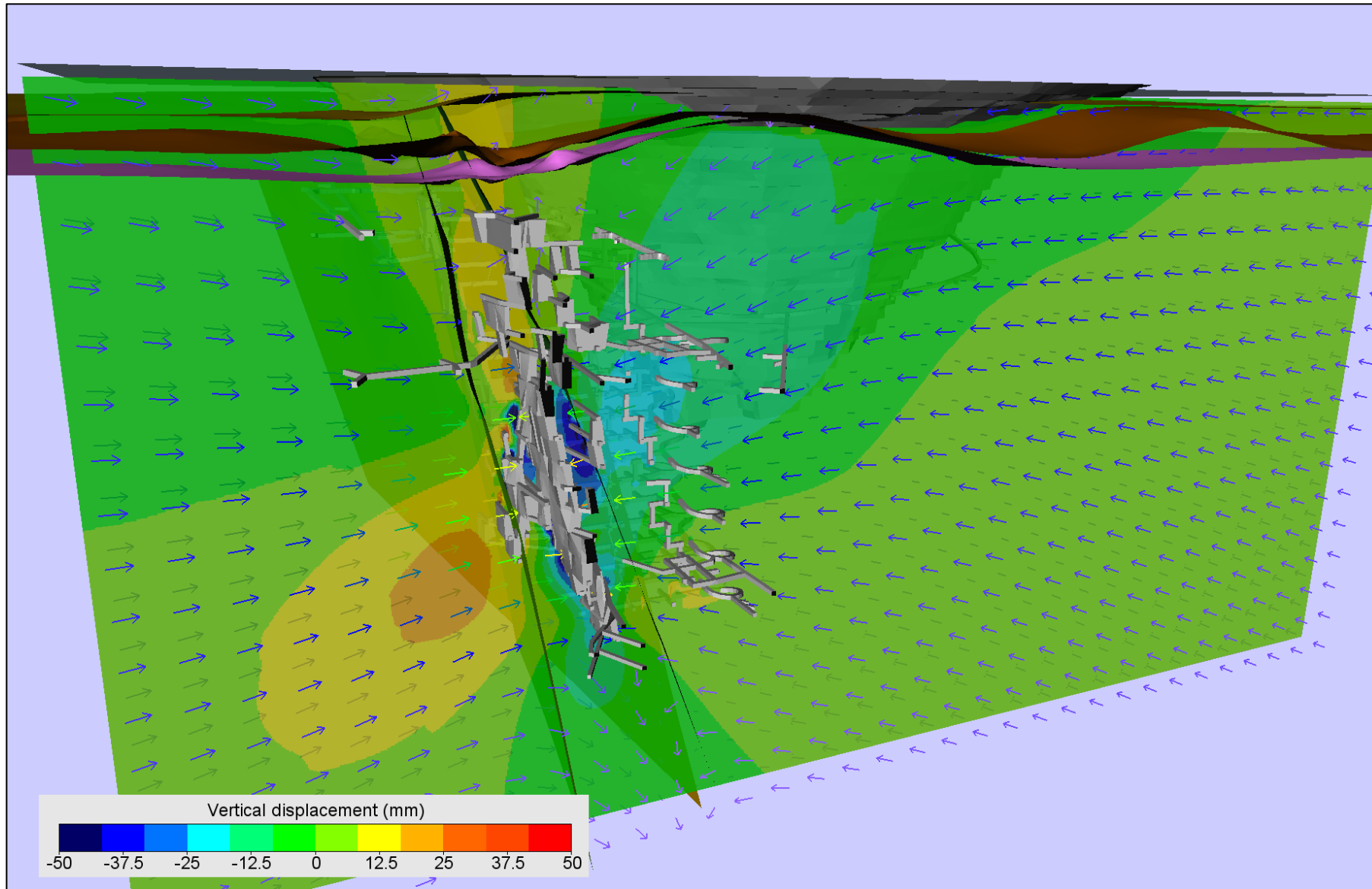


Figure 3-8: Forecasts vertical displacement from the end of 2019 to the end of mine life above the proposed underground mine (vertical cross section through the model). Arrows indicate the direction of movement

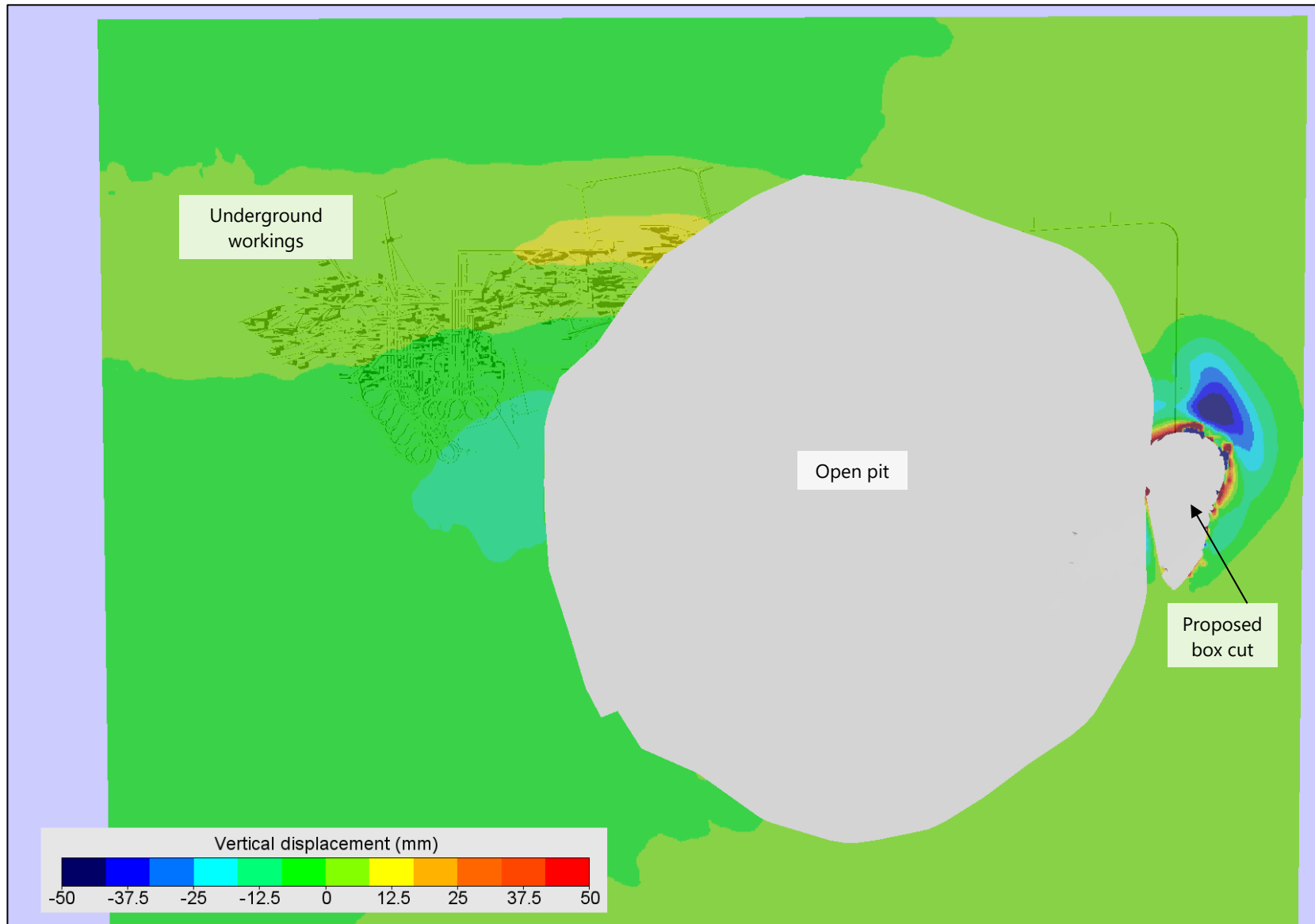


Figure 3-9: Forecasts vertical displacement from the end of 2019 to the end of mine life above the proposed underground mine (plan view on surface)

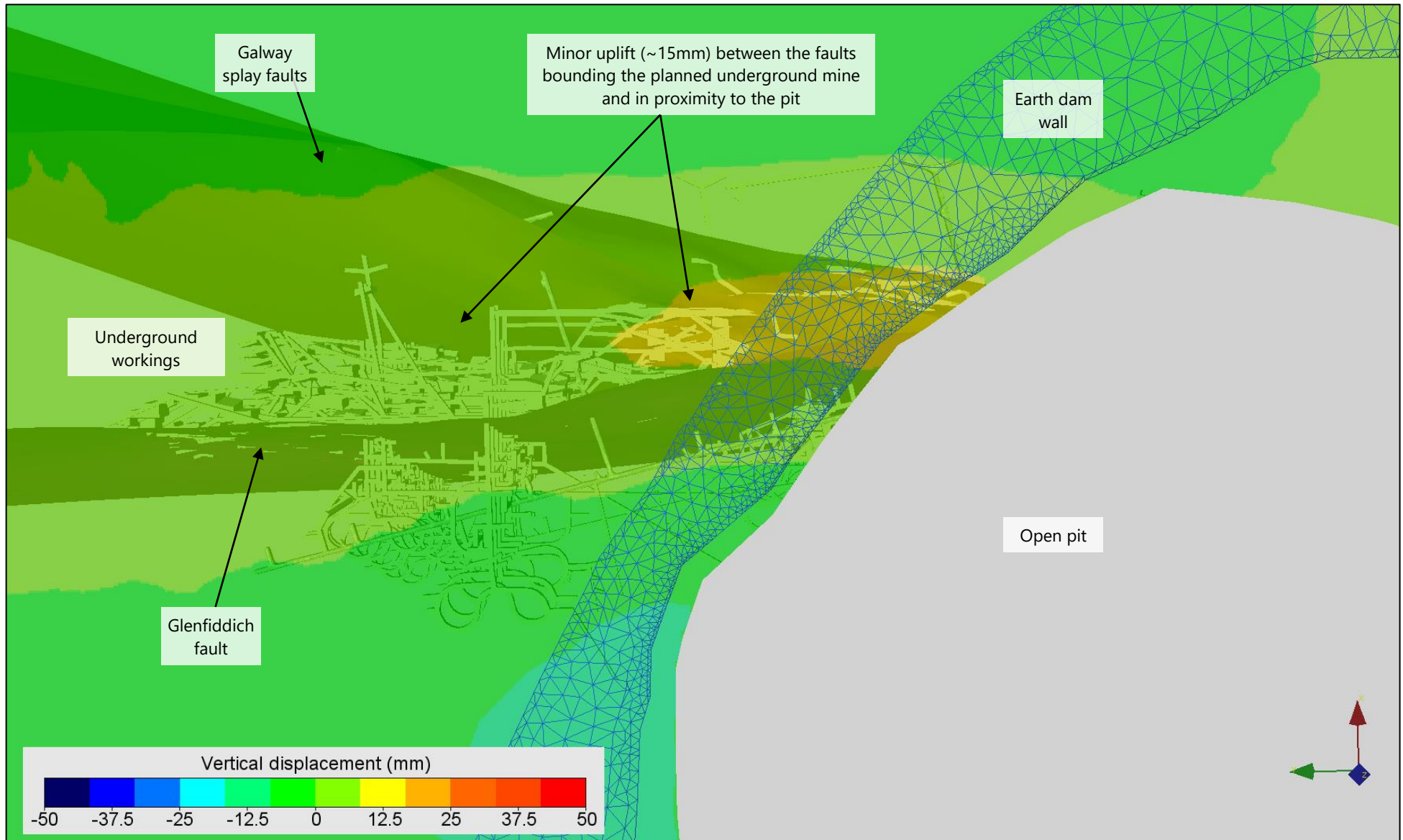


Figure 3-10: Vertical movement forecast from the end of 2019 to the end of mine life. Movement is between the Galway splays and Glenfiddich fault which bound the proposed underground stope production.

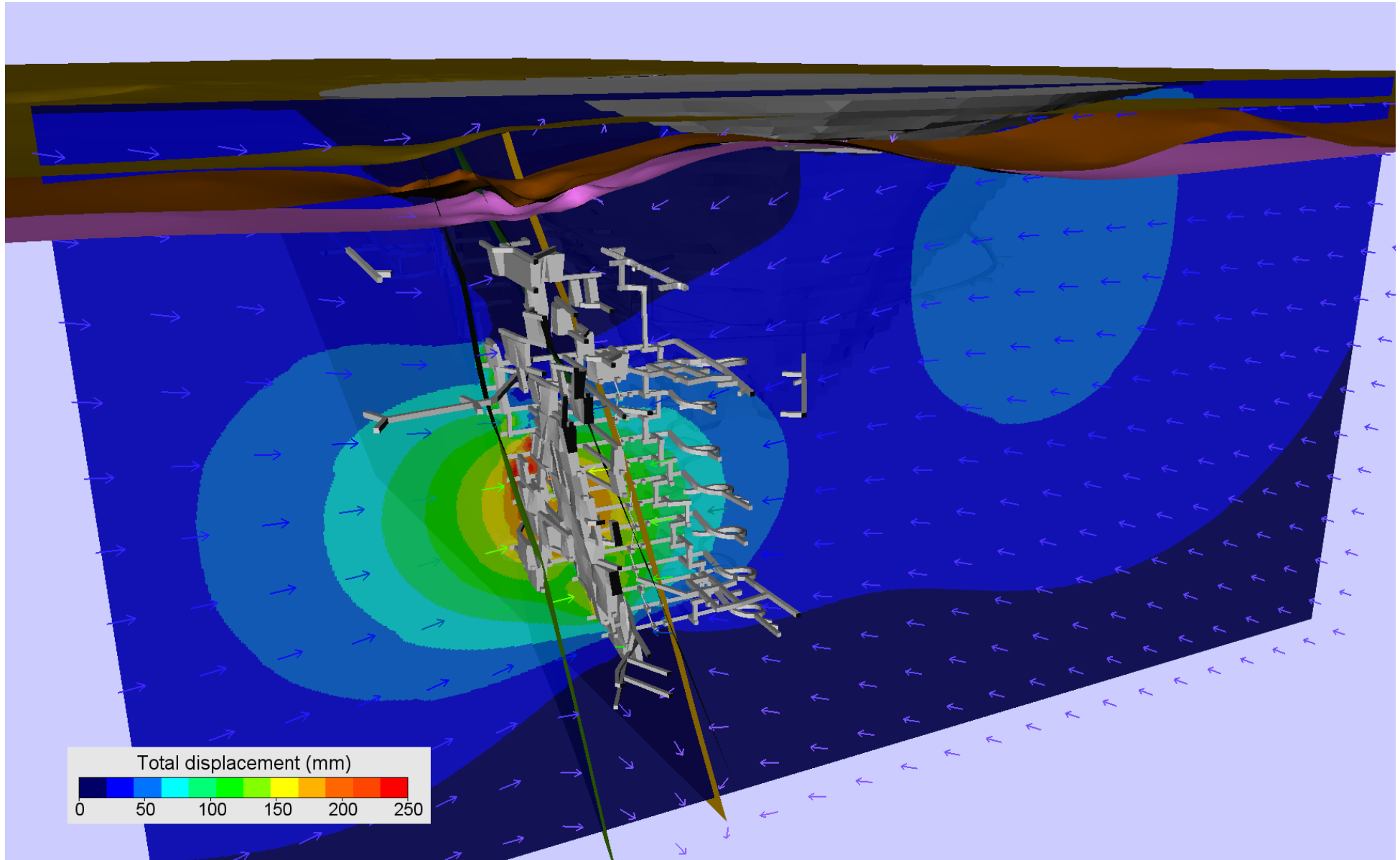
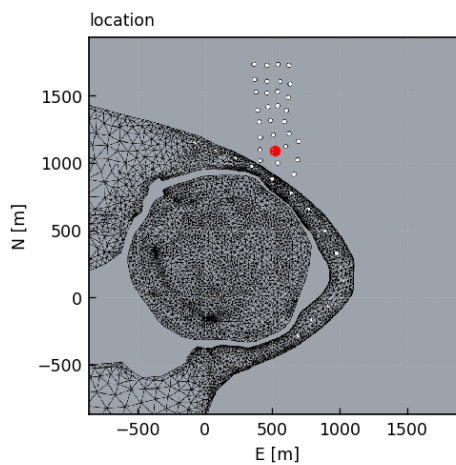
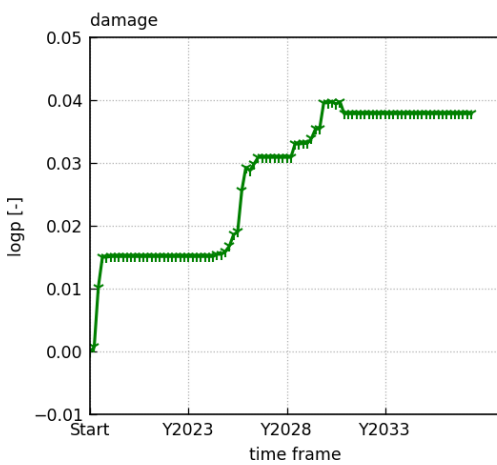
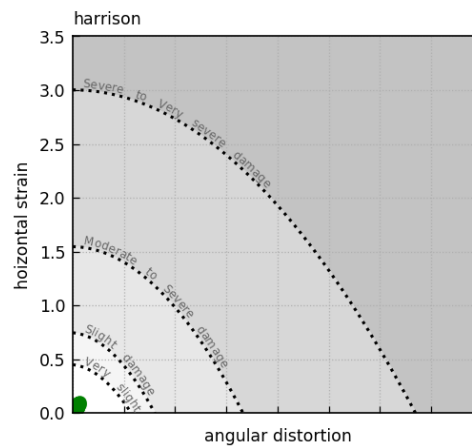
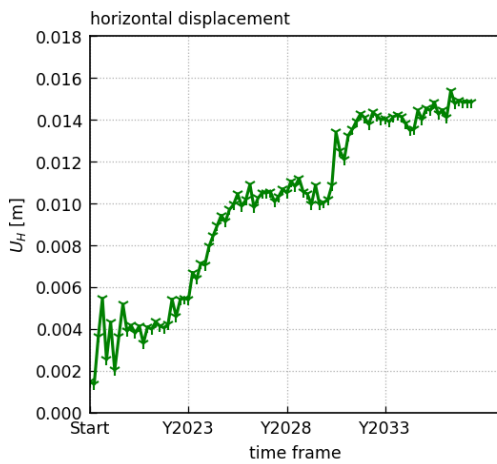
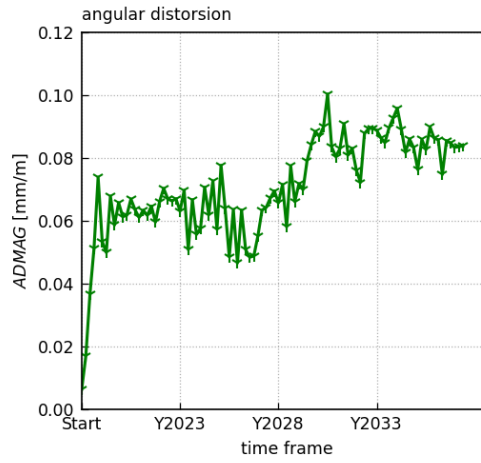
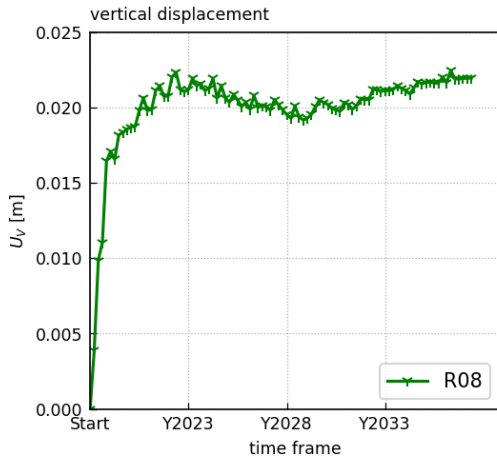


Figure 3-11: Cross section through the model showing forecast total displacement from the end of 2019 to the end of mine life for the proposed underground mine

**EVOLUTION: LAKE COWAL UNDERGROUND MINE SUBSIDENCE ASSESSMENT**

Project	
Site Name	Control Points Pit Wall
Site Number	P033_UG_SURFACE

East	518 m
North	1093 m
RL	1203 m



**Figure 3-12: Detailed report for movement and damage over time above the planned underground mine**



**EVOLUTION: LAKE COWAL UNDERGROUND MINE SUBSIDENCE ASSESSMENT**

Project	
Site Name	Control Points Pit Wall
Site Number	P043_UG_SURFACE

East	469 m
North	1416 m
RL	1203 m

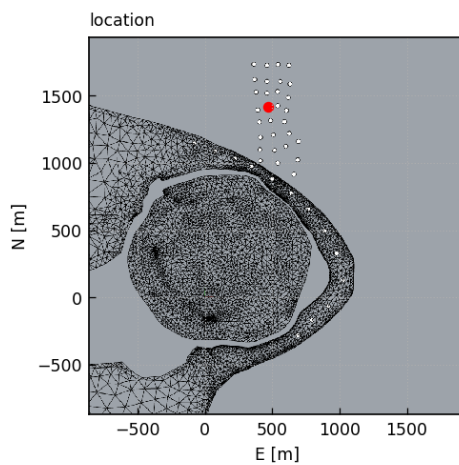
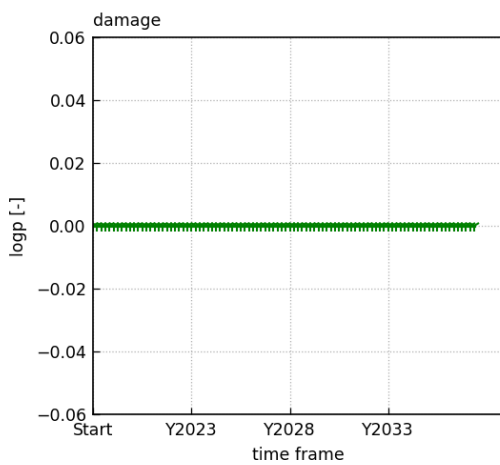
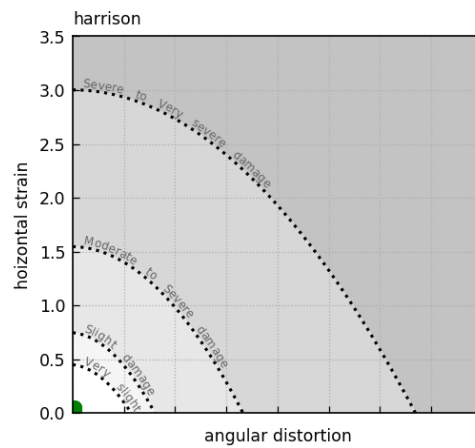
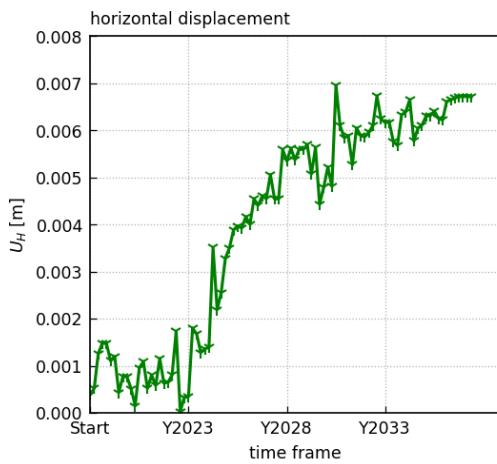
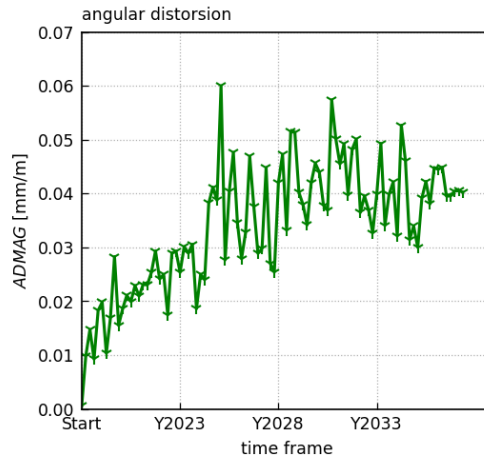
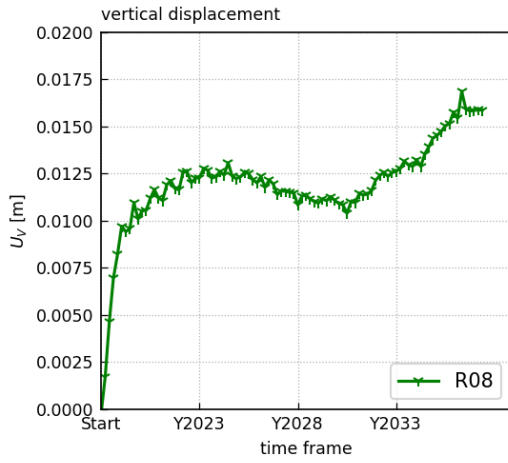


**Figure 3-13: Detailed report for movement and damage over time above the planned underground mine**

**EVOLUTION: LAKE COWAL UNDERGROUND MINE SUBSIDENCE ASSESSMENT**

Project	
Site Name	Control Points Pit Wall
Site Number	P064_FLOOR

East	501 m
North	880 m
RL	1202 m

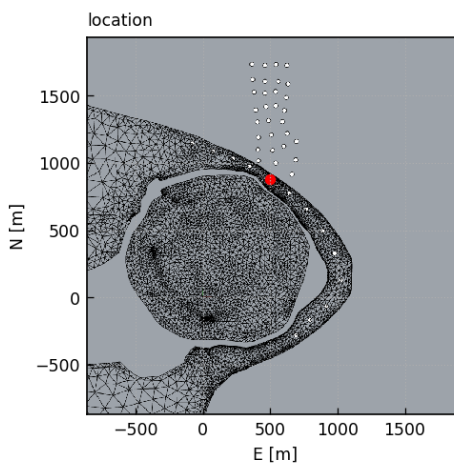
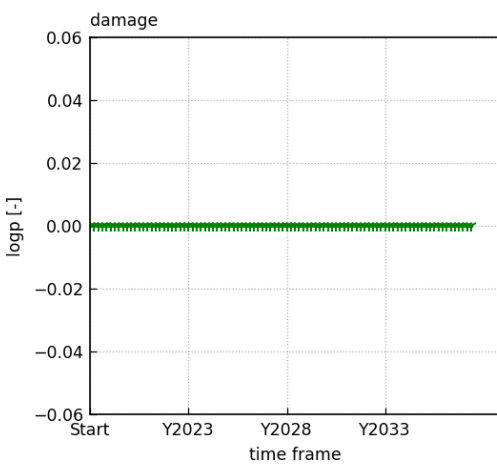
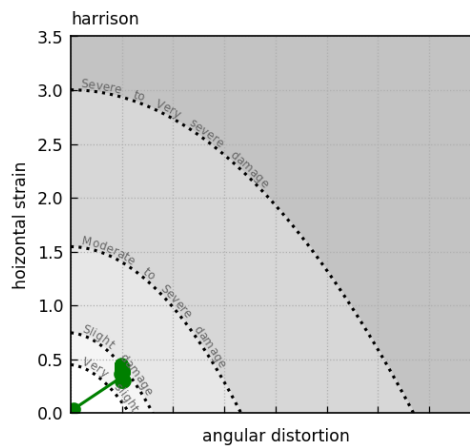
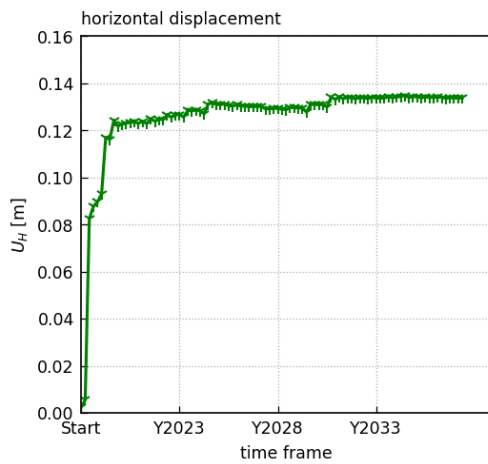
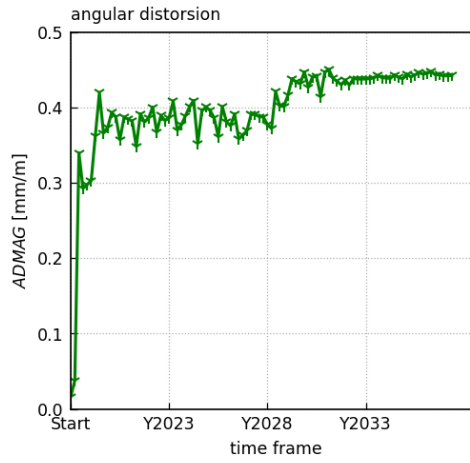
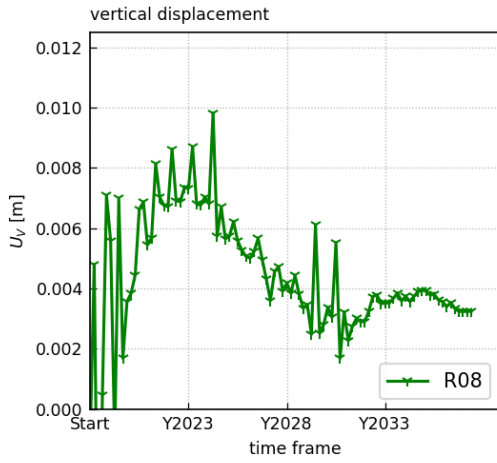


**Figure 3-14: Detailed report for movement and damage over time on the dam wall to the north of the open pit**

Project	
Site Name	Control Points Pit Wall
Site Number	P063_FLOOR

East	346 m
North	971 m
RL	1202 m

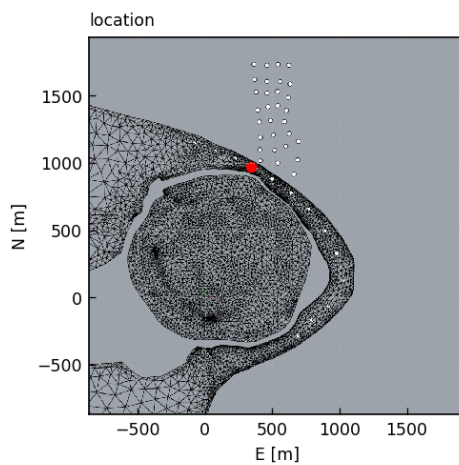
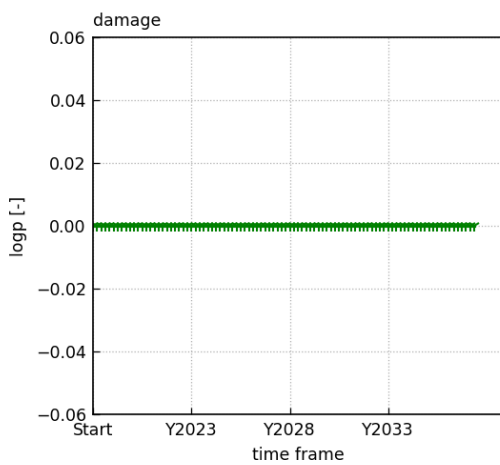
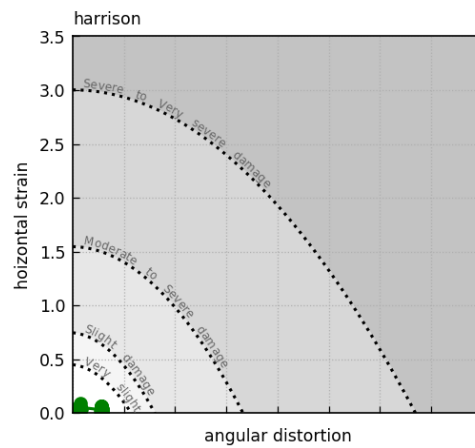
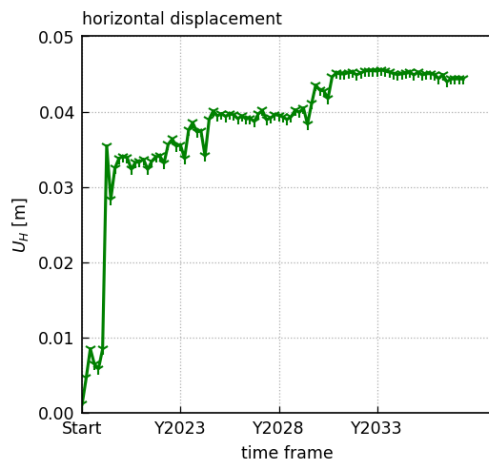
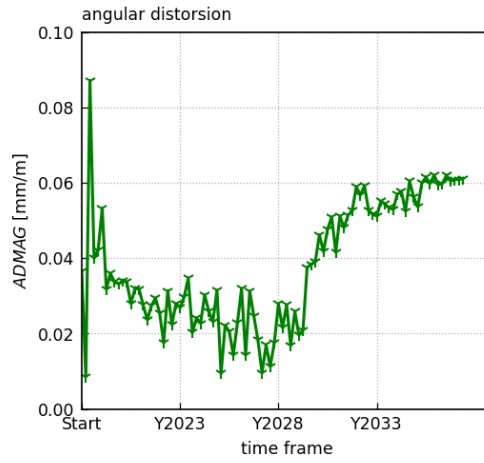
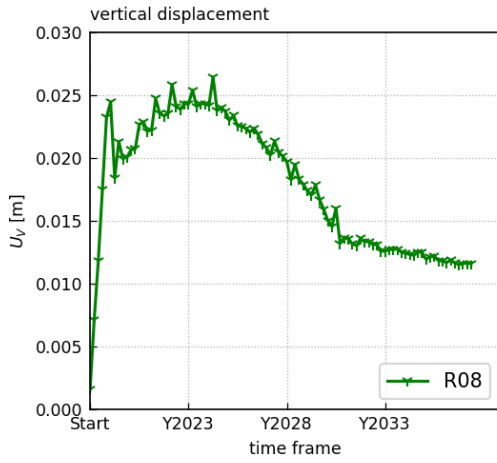


**Figure 3-15: Detailed report for movement and damage over time on the dam wall**

**EVOLUTION: LAKE COWAL UNDERGROUND MINE SUBSIDENCE ASSESSMENT**

Project	
Site Name	Control Points Pit Wall
Site Number	P069_FLOOR

East	1030 m
North	125 m
RL	1202 m

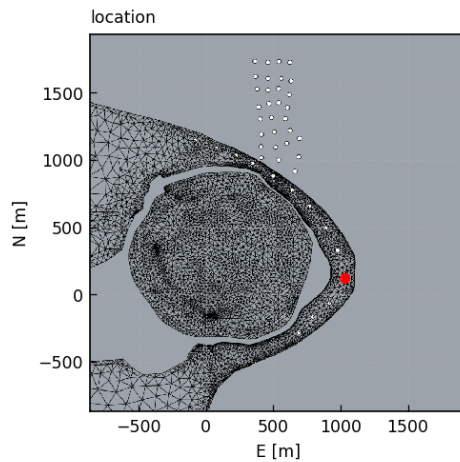
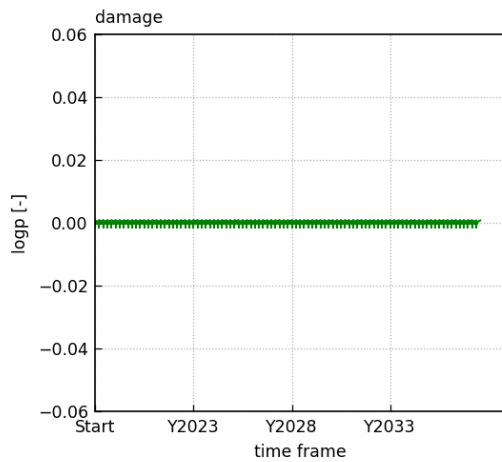
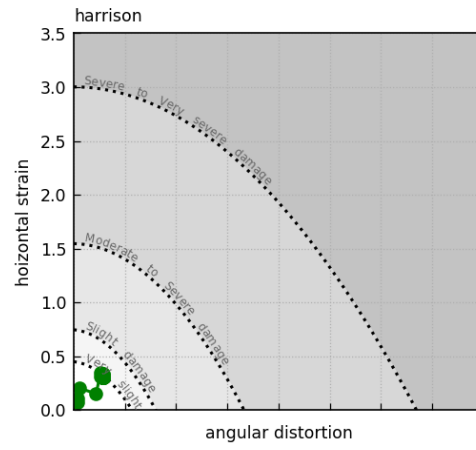
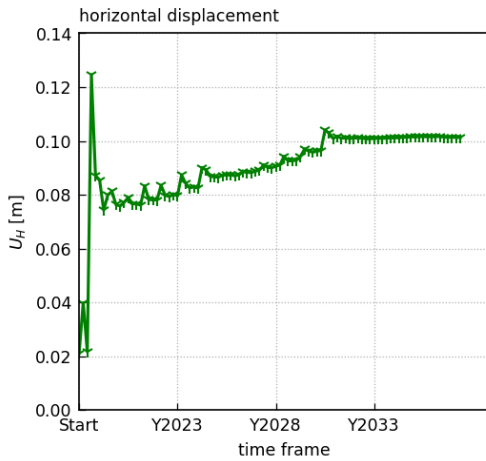
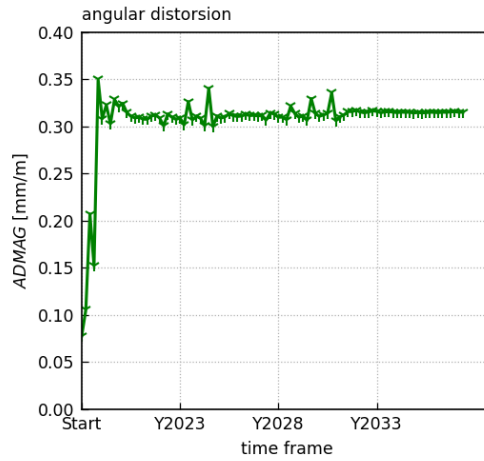
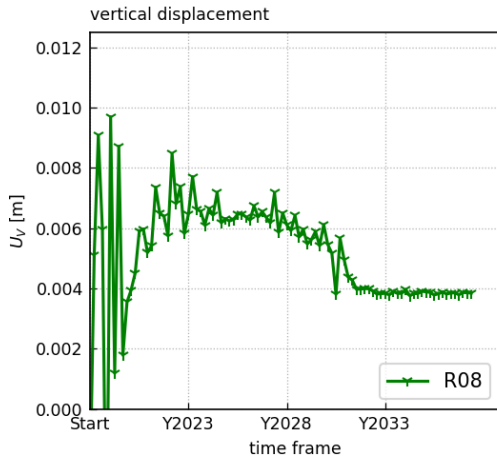


**Figure 3-16: Detailed report for movement and damage over time on the dam wall to the east of the open pit**

### **3.2 Open pit and underground interaction**

Forecasts for open pit and underground mine interaction include:

1. Figure 3-17 to Figure 3-19 show cross sections through the underground mine showing total displacement forecast in the model. As expected, minor levels of horizontal closure are forecast in the underground mine, particularly in deeper and thicker sections of planned stoping. Displacement in proximity to the pit is inwards (horizontal closure) and slightly upwards due to removal of open pit material.
2. Rockmass damage (a function of plastic strain in the FE model) and major principal stress are shown in Figure 3-20 to Figure 3-24 . The model forecasts show:
  - a. Low damage in the rockmass above the upper stoping levels.
  - b. Moderate to locally significant damage and displacement along faults in the immediate vicinity of the open pit. This damage does not extend as far as the underground workings.
  - c. Generally minor to moderate levels of damage are forecast around underground workings. This is normal and would normally be controlled using ground support and via design modifications during mine construction as additional geological data becomes available.
  - d. Some locally significant deformation and rockmass damage is forecast in close out pillars close to the central access drives due to the diminishing pillars in the current mining sequence.
  - e. Moderate to significant levels of rockmass damage are forecast along the boundary between bottom of the hard oxide and the top of fresh rock, as well as the weak cover sequence units in proximity to the pit. This does not impact the stability of the underground mine, but may correspond to an increase in the hydraulic conductivity of the damaged zone.
  - f. Low to moderate stress above upper stopes in each block. Forecast stress conditions are unlikely to result in significant crown overbreak or stope instability unless impacted by major faults such as the Glenfiddich fault in the hangingwall or intermediate scale structures at a local scale that are not included in the model. A detailed crown pillar stability assessment should be conducted to confirm crown pillar stability.
3. Assessment of model forecasts for displacement, rockmass damage (plastic strain) and stress demonstrates very low and negligible interaction between the open pit and underground mine. We note some minor interaction occurs in the weak sediments and soft oxide layers, however these effects are mostly due to previous open pit mining.

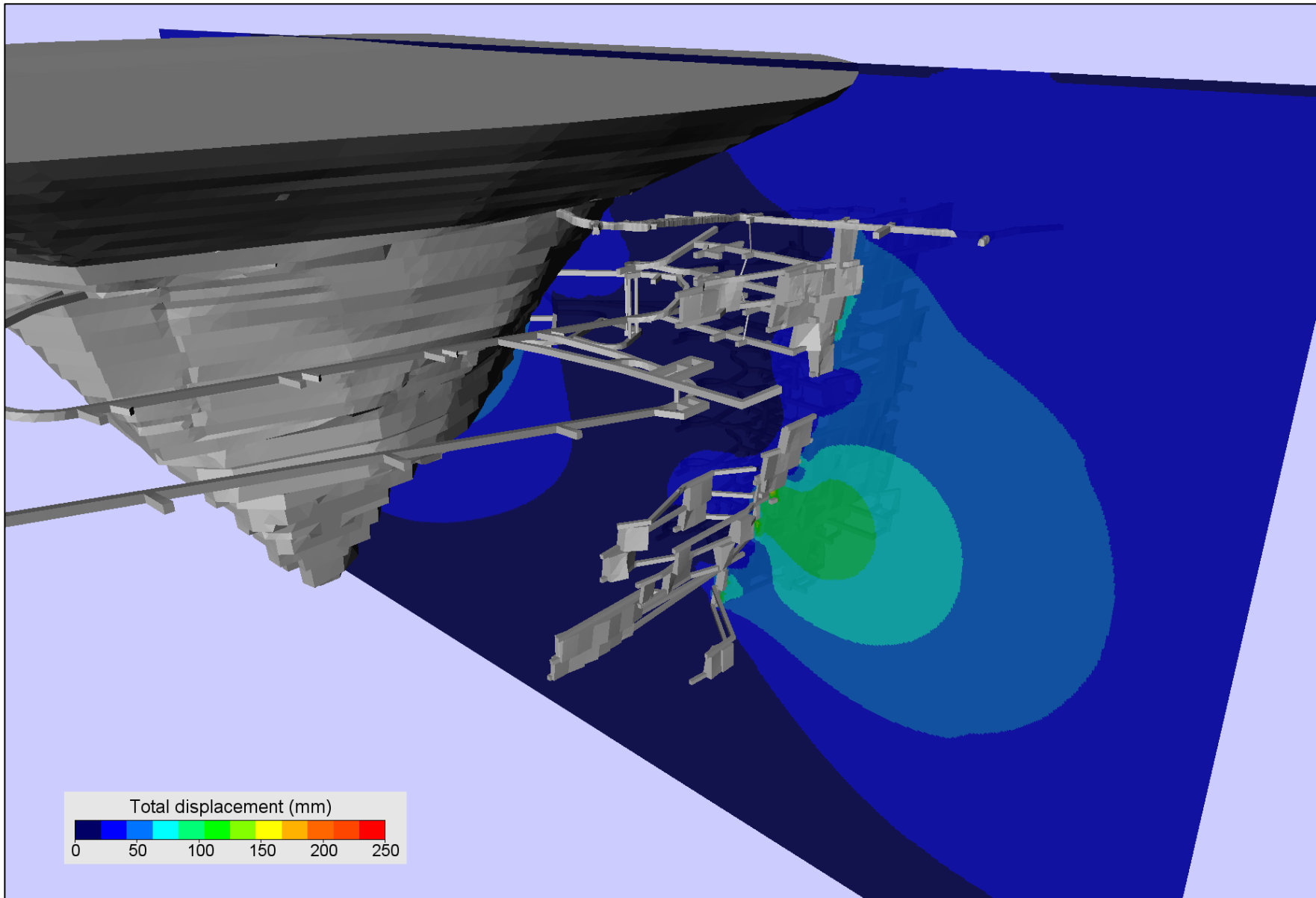


Figure 3-17: Cross section of total displacement through the underground mine (displacement shown is from end of 2019 to end of mine life)

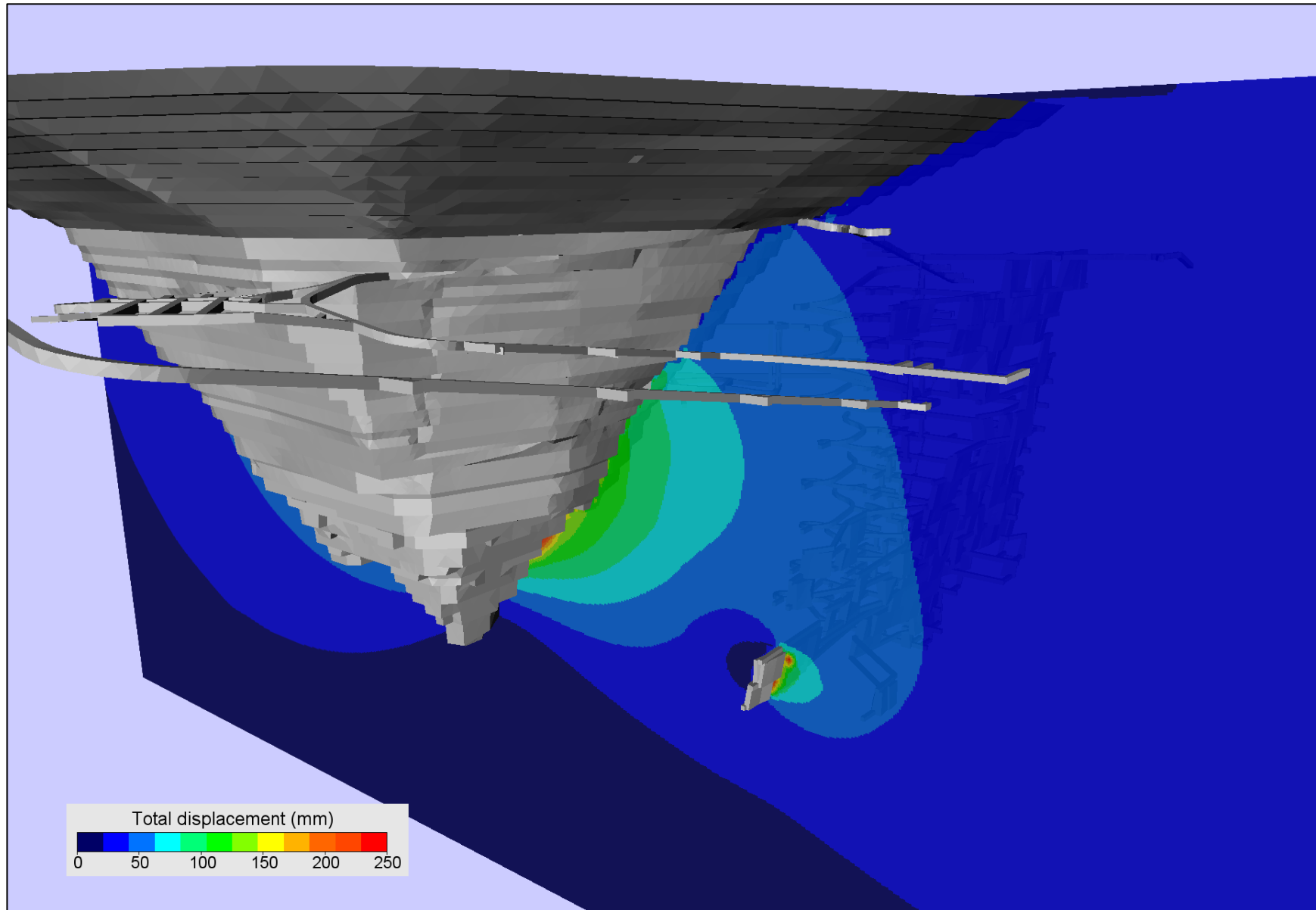


Figure 3-18: Cross section of total displacement through the underground mine (displacement shown is from end of 2019 to end of mine life)

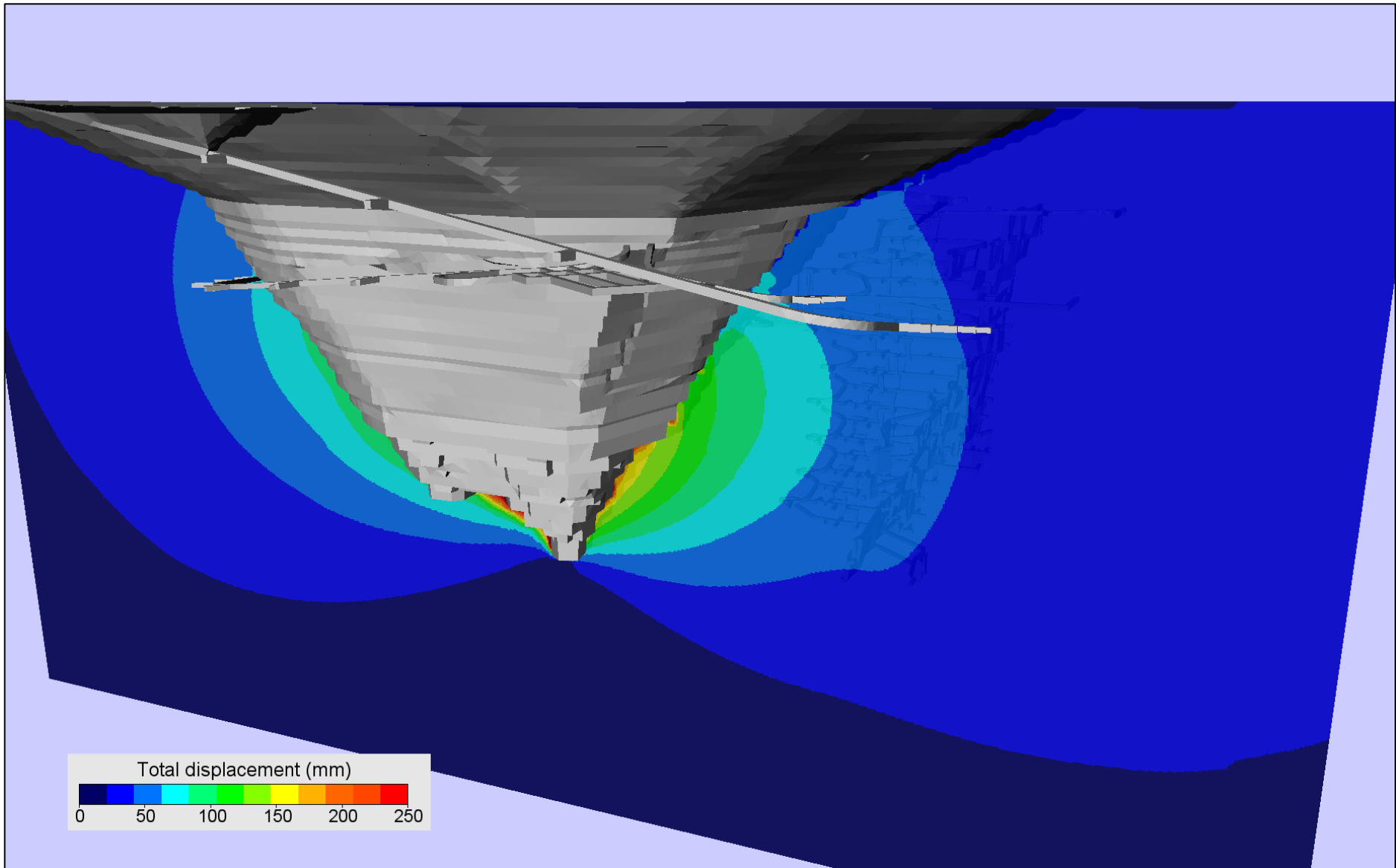


Figure 3-19: Cross section of total displacement through the underground mine (displacement shown is from end of 2019 to end of mine life)



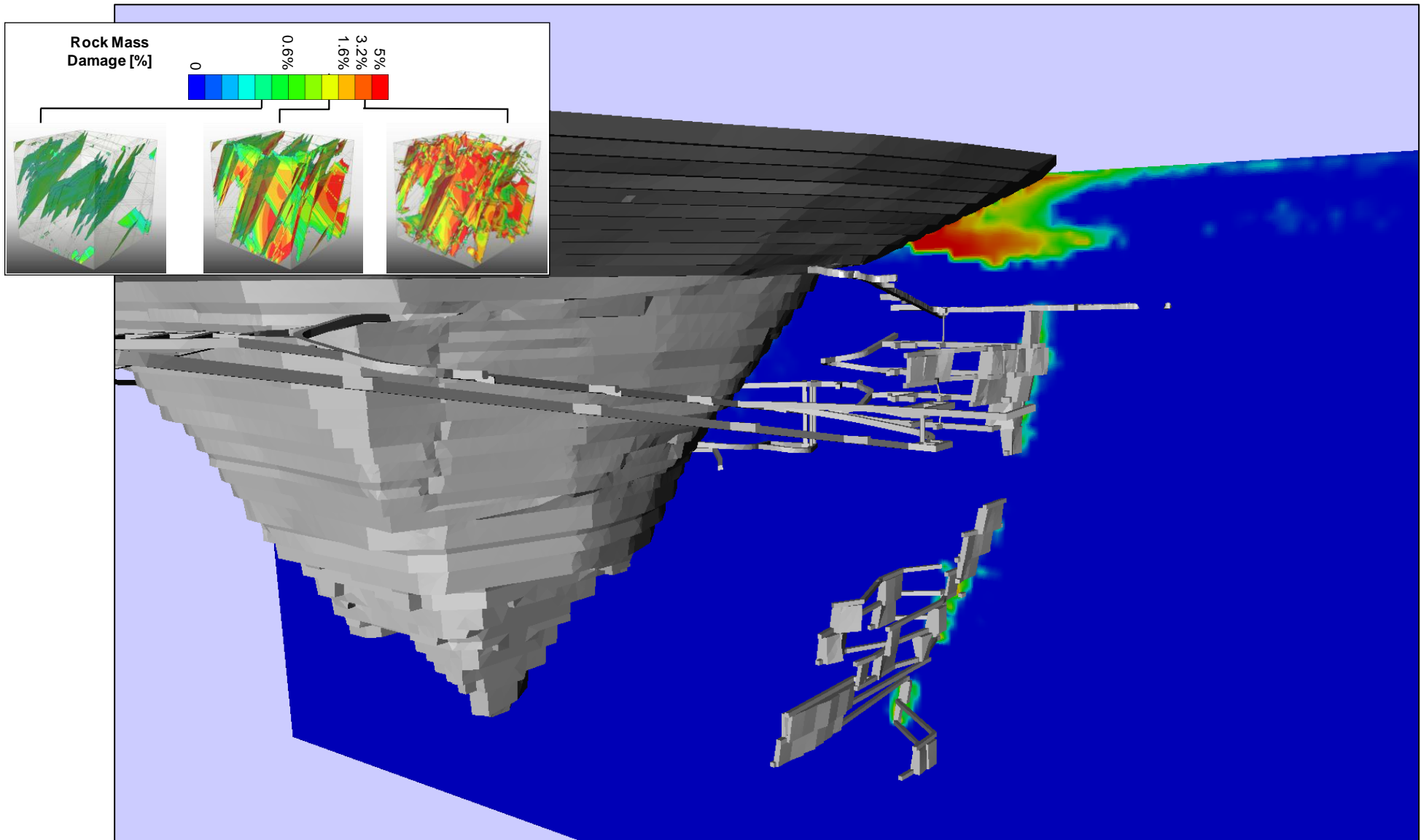


Figure 3-20: Cross section of rockmass damage forecast in the underground mine precinct. Note the most significant damage is in the transported and soft oxide layers in proximity to the open pit

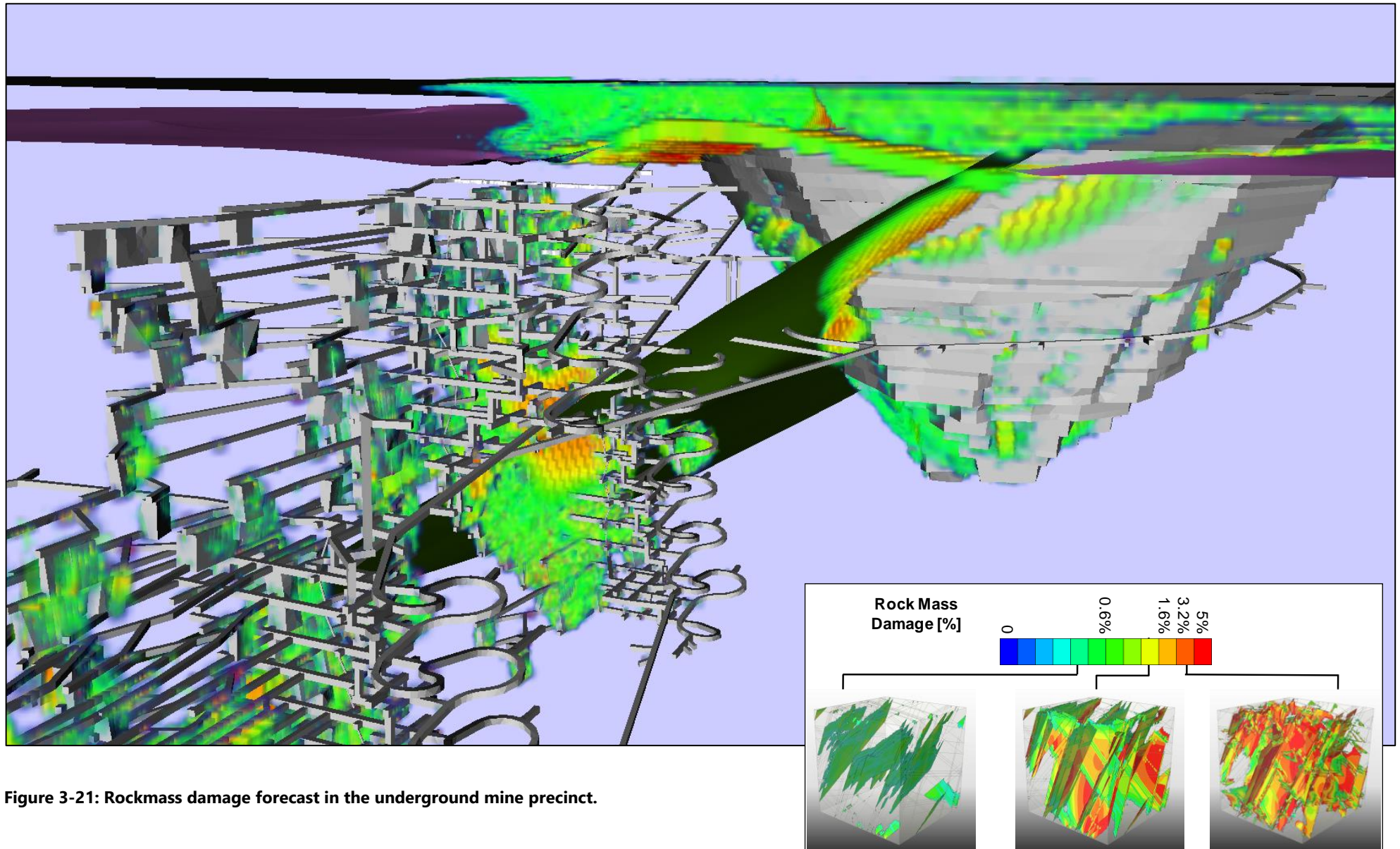


Figure 3-21: Rockmass damage forecast in the underground mine precinct.

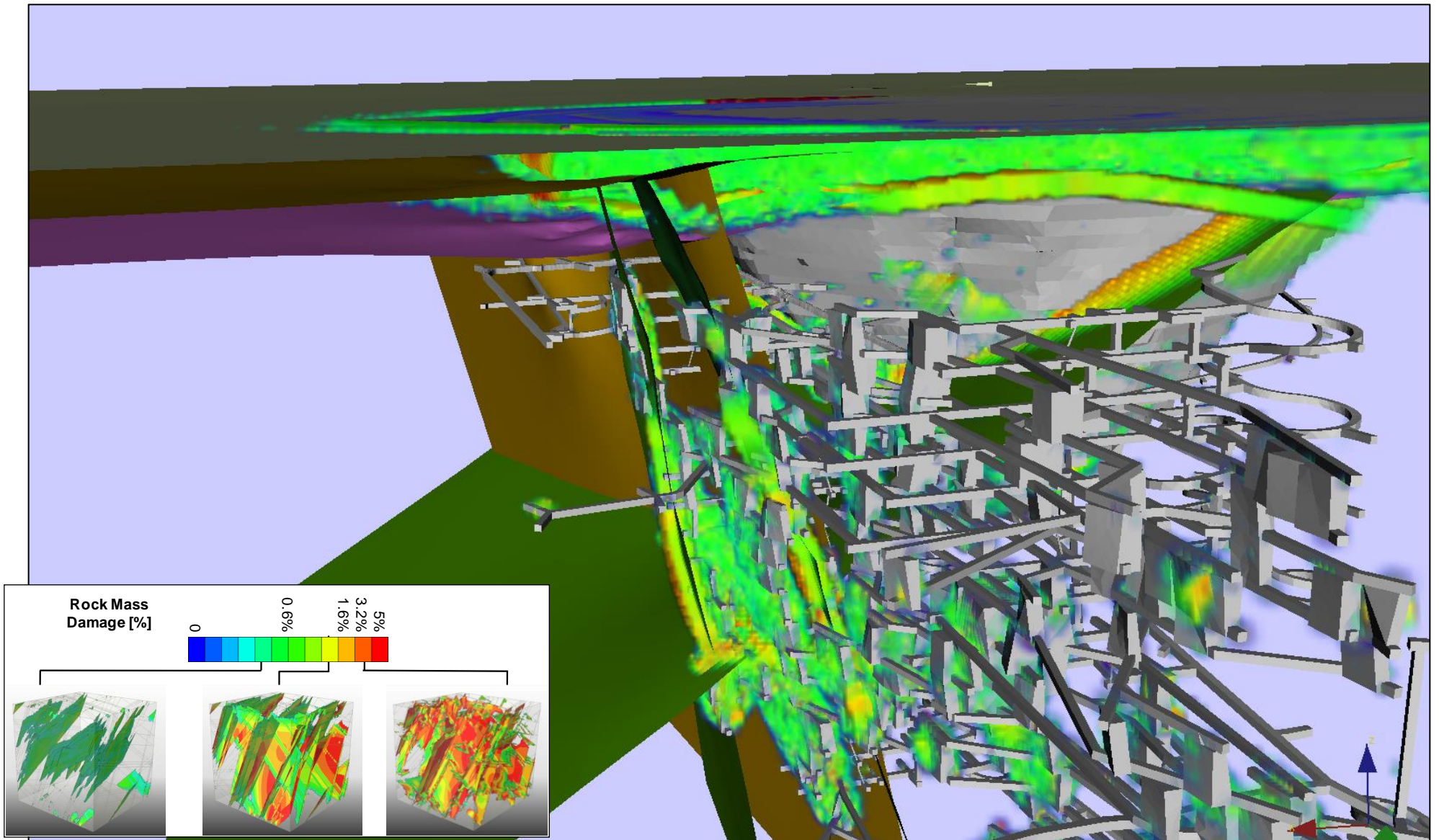


Figure 3-22: Rockmass damage forecast in the underground mine precinct.

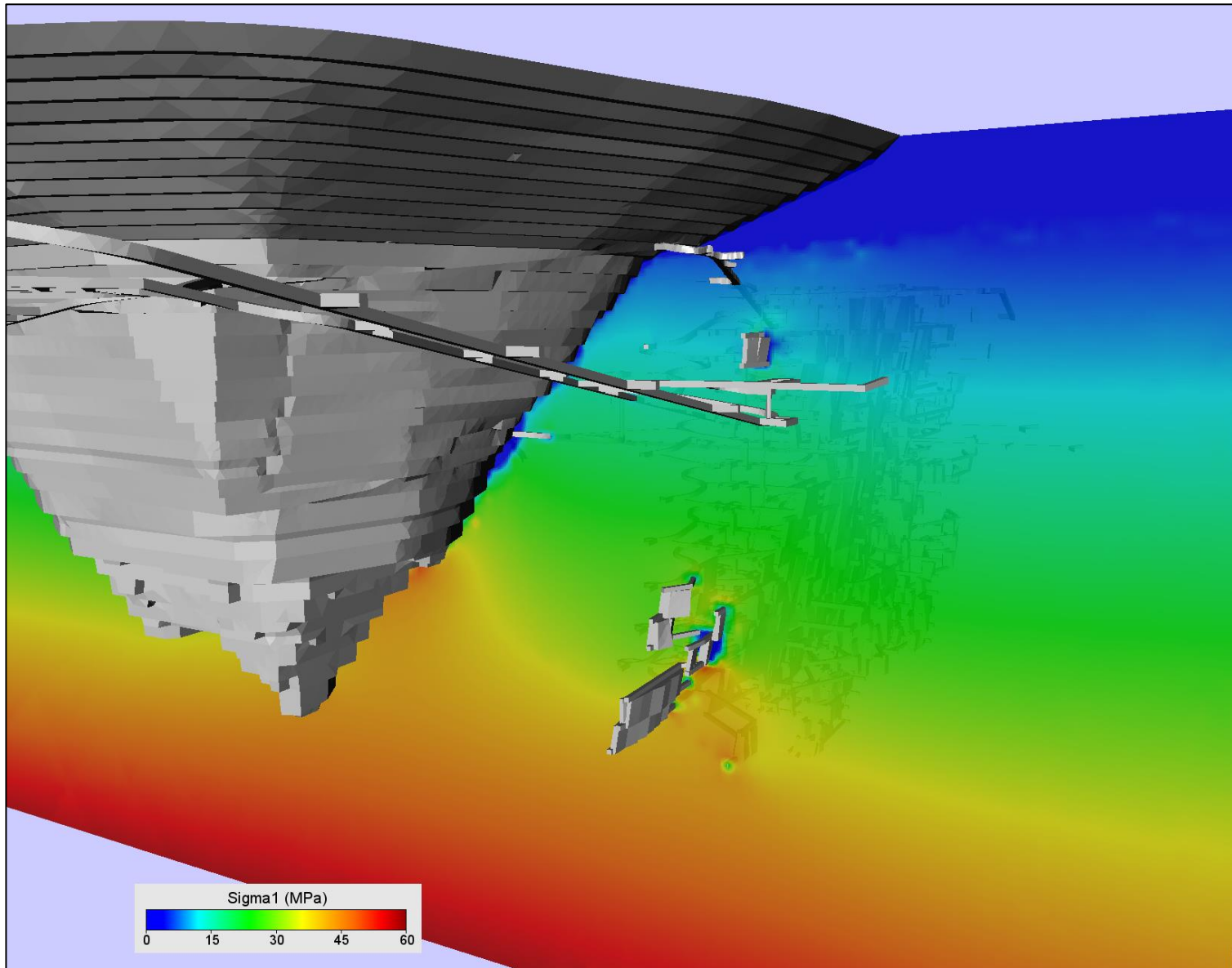


Figure 3-23: Cross section showing major principal stress.

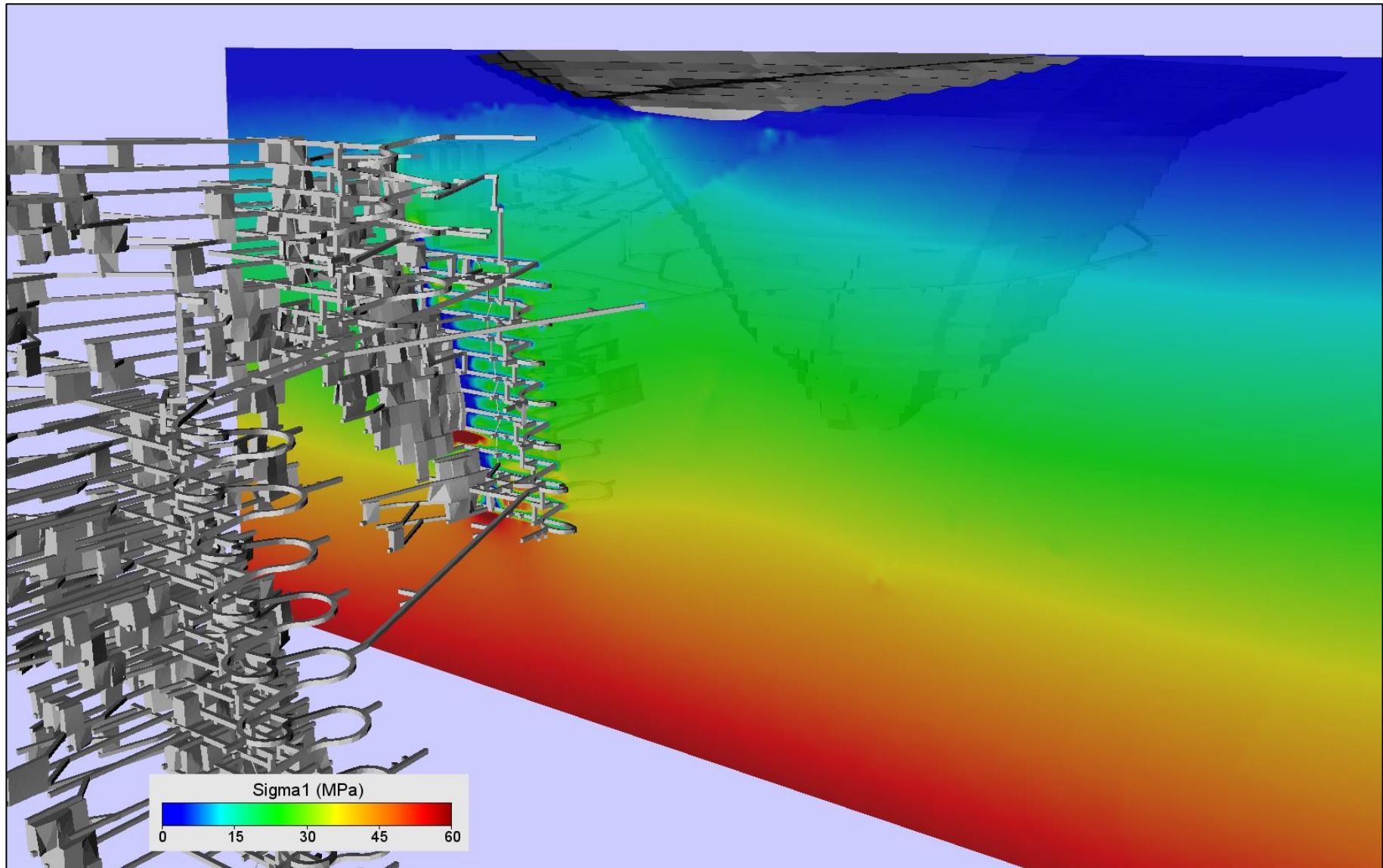


Figure 3-24: Cross section showing major principal stress.

### **3.3 Stope overbreak and chimney failure potential**

Stope failure to surface is a hazard for all underground (stopping) mines. An example of a stope that has chimneyed to surface is provided in Figure 3-25. This stope chimneyed approximately 200m (sub vertically) along a major fault to break through to surface. Breakthrough was unplanned and occurred ~1 month after the stope had failed and was partially backfilled. Backfilling was delayed due to the unplanned failure and stope was only partially filled due to the level of the filling horizon. The stope continued to fail along the fault and broke through to surface near an access road, haul road and surface infrastructure. The breakthrough was around 10m x 15m wide and widened to approximately 20m prior to being filled from surface. Notably, this stope was larger than the planned stopes at Lake Cowal, but also considerably deeper and in stronger rock.

Chimneying failure of stopes at Lake Cowal must be appropriately addressed to mitigate the potential for stope failure to surface. This is particularly important given the presence of Lake Cowal above the underground mining precinct. In our opinion, the most likely cause of (potential) chimney failure of the stopes closest to surface are the major faults in proximity to planned stopes. These faults include the Glenfiddich fault, Galway splay faults (see Figure 3-26) and any other larger to intermediate scale structures that have not been identified to date. Although the likelihood of stope overbreak and chimneying to failure is very low (with appropriate controls), the consequence to the underground mine would be catastrophic.

We note the rockmass in proximity to the underground mine is generally strong with weak fault conditions. Low rockmass damage is forecast in proximity to the uppermost stoping block and very low damage is forecast in the stope crowns (see Figure 3-27). Failure and chimney potential will likely be governed by faults in proximity to planned stoping and also effected by any weak or jointed rockmass conditions, ground water, stress among other factors.

We note the potential for the rockmass in proximity to stoping to be bedded and highly anisotropic based on the faulting in the geological model provided. This rockmass condition would result in stopes being more prone to unravelling and chimney type failures, as shown in Figure 3-28 and Figure 3-29. We also note the potential for ground water to weaken the faults and the rockmass in the crown pillar region, as shown in Figure 3-30.

A detailed crown pillar stability assessment must be conducted for each stope on the upper mining levels. We note that 19 high risk stopes in the preliminary mine design update were recommended to be removed from the mine design. These 19 stopes are not part of this assessment following a design update by Evolution and should not be planned unless it is demonstrated the crown pillars will remain stable. Stopes within the oxide and transported layers are not likely to be stable and should not be planned at this stage of the project.

A number of empirical and numerical methods exist for assessing crown pillar stability. A schematic of key components of a crown pillar stability assessment is provided in Figure 3-31. A useful guideline for assessing risk of crown pillars is provided by Carter and shown in Table 3-1. It is recommended that crown pillar stability of the uppermost stopes be continuously evaluated during mine design updates and as additional geological information becomes available.

The mine should also consider delaying the mining of the upper most row of stopes in the upper most stoping blocks. Mining these stopes first, or very early in the mine life is when the mine has the least geological knowledge (relative to other stages of underground mining). This includes the understanding of the hydraulic properties of the faults and water inflows.

Other recommendations and control measures to minimise the potential for stope overbreak or chimney failure are listed below. Depending on local geological conditions encountered, the mine should review the list below, and select the controls appropriate to the conditions encountered.

- Detailed crown pillar stability assessment for each stope and panels of stopes on the uppermost production levels

- Mine single lift stopes in the upper levels. A smaller stope void increases the potential for stope overbreak and failure material to fill the void due to the swell of the broken material, prior to extensive failure or chimneying to surface.
- Stope sequencing to minimise risk of failure and unravelling along faults, particularly where stopes are bounded by multiple faults. Multiple stopes in close proximity should not be mined at the same time.
- Top down drilling of the upper stopes will provide access to the top of the stope (the overcut drive) which enables cablebolting of the stope crown and hangingwall and access for rapid tight filling with paste.
- Tight fill stopes, as far as practical.
- Developing the overcut drive with a downwards grade from the access. This will enable the stopes to be tight filled to the backs with paste.
- Backfilling stopes in a timely manner.
- Ensuring paste lines and other backfill infrastructure is in place prior to firing stopes with potential for instability or in proximity to major faults.
- Reducing the strike length of stopes to reduce potential instability. A review of the stope dimensions should be conducted following stope development and structural mapping of the area.
- Cablebolting of stope crowns, when appropriate.
- Review of a stand-off between stope walls and major faults, such as the Glenfiddich fault is appropriate based on local conditions
- Employing a continuous mining sequence. Secondary stopes have a higher risk of instability (generally).
- Avoid mining stopes where major faults confluence in proximity to the stope, particularly near vertical faults such as the Glenfiddich fault and Galway splays.
- Mine stopes on the upper levels when Lake Cowal is dry.

We note than many stope failures at other mines are self arrested and do not propagate to surface due to the bulking of the broken overbreak material. However, this does not always occur and some stopes unravel with a very low bulking factor. The example shown in Figure 3-25 is an example where site engineers were aware of the stope failure, filled the stope with paste as high as possible and expected the remaining void to be filled with the bulked overbreak material. The stope breakthrough to surface occurred approximately 1 month later in proximity to a haul road, access road and critical infrastructure.



**Figure 3-25: A stope that has chimneyed approximately 200m vertically through to surface at an underground mine in QLD. The surface breakthrough was approximately 10m x 20m across**



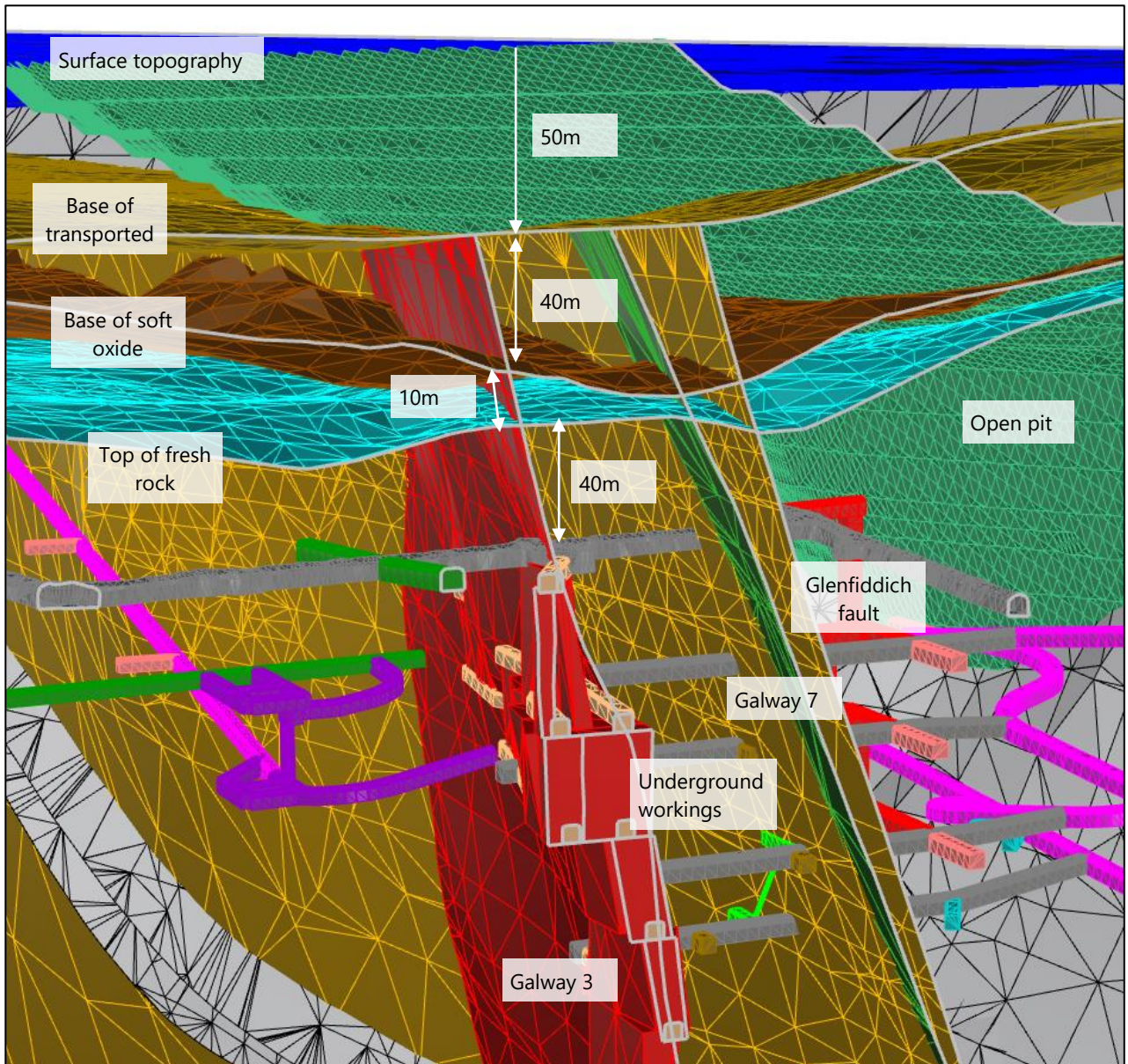
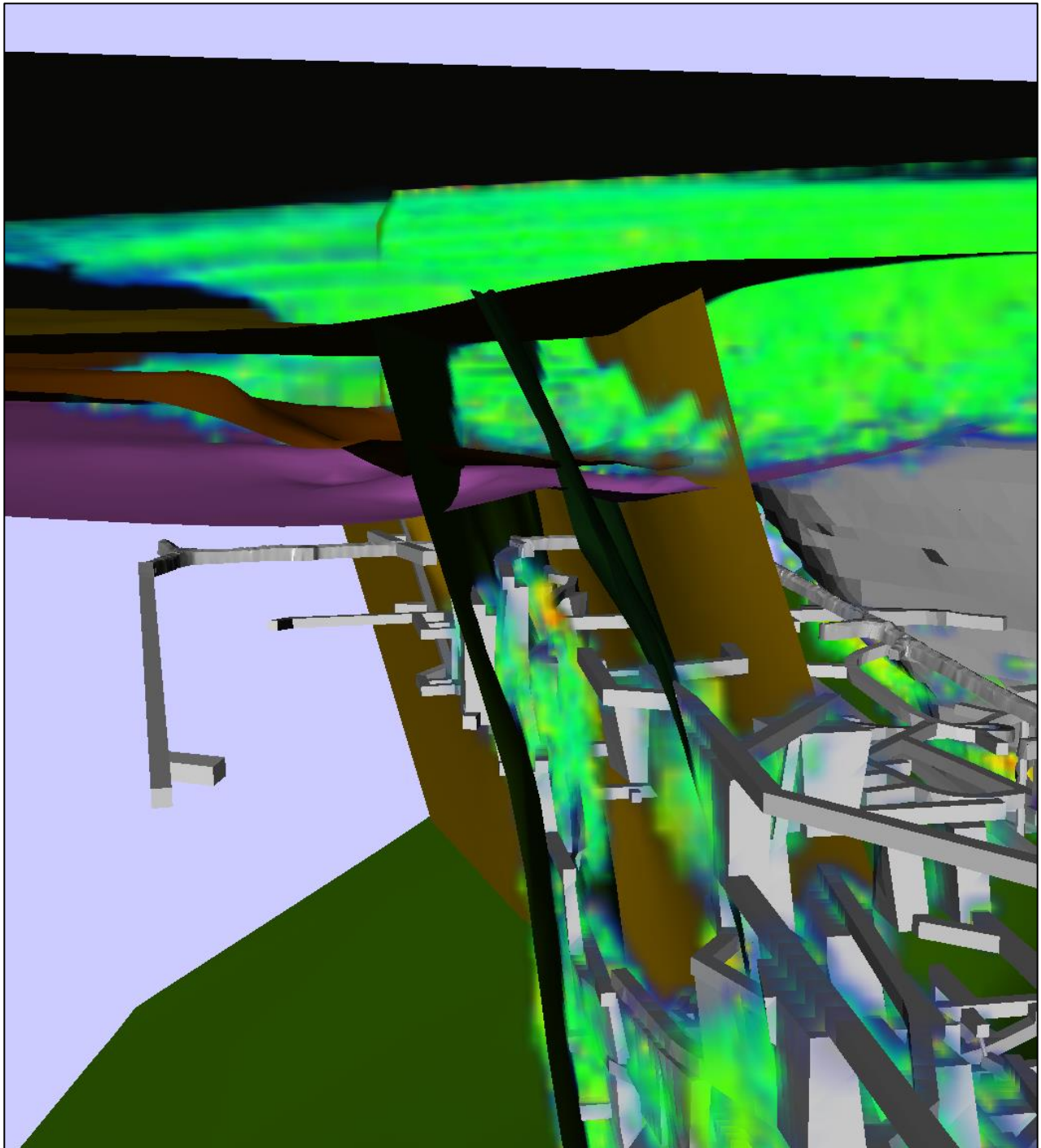


Figure 3-26: Cross section through the proposed underground mine showing indicative thickness of the cover units relative to the underground mine.



**Figure 3-27: Forecast rock mass damage in the vicinity of the upper stopping blocks (showing the Galway and Glenfiddich faults)**

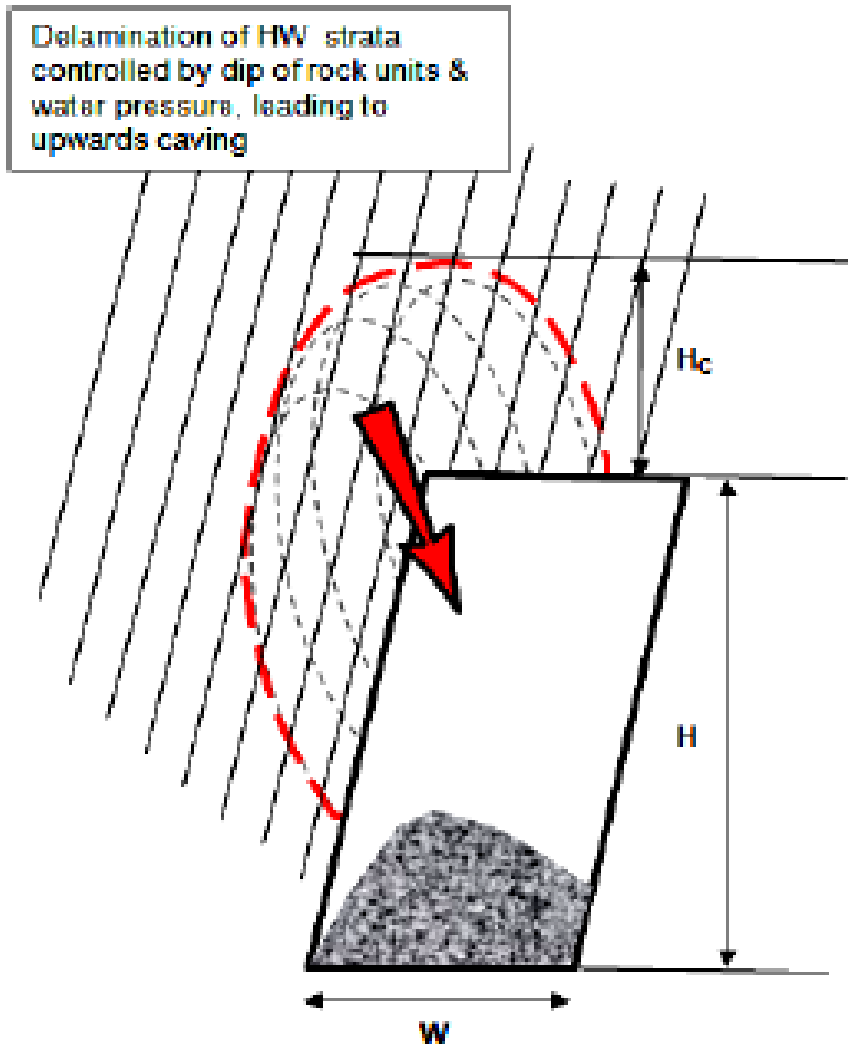


Figure 3-28: Example of crown pillar failure mechanism in steeply dipping rockmass (After Carter)

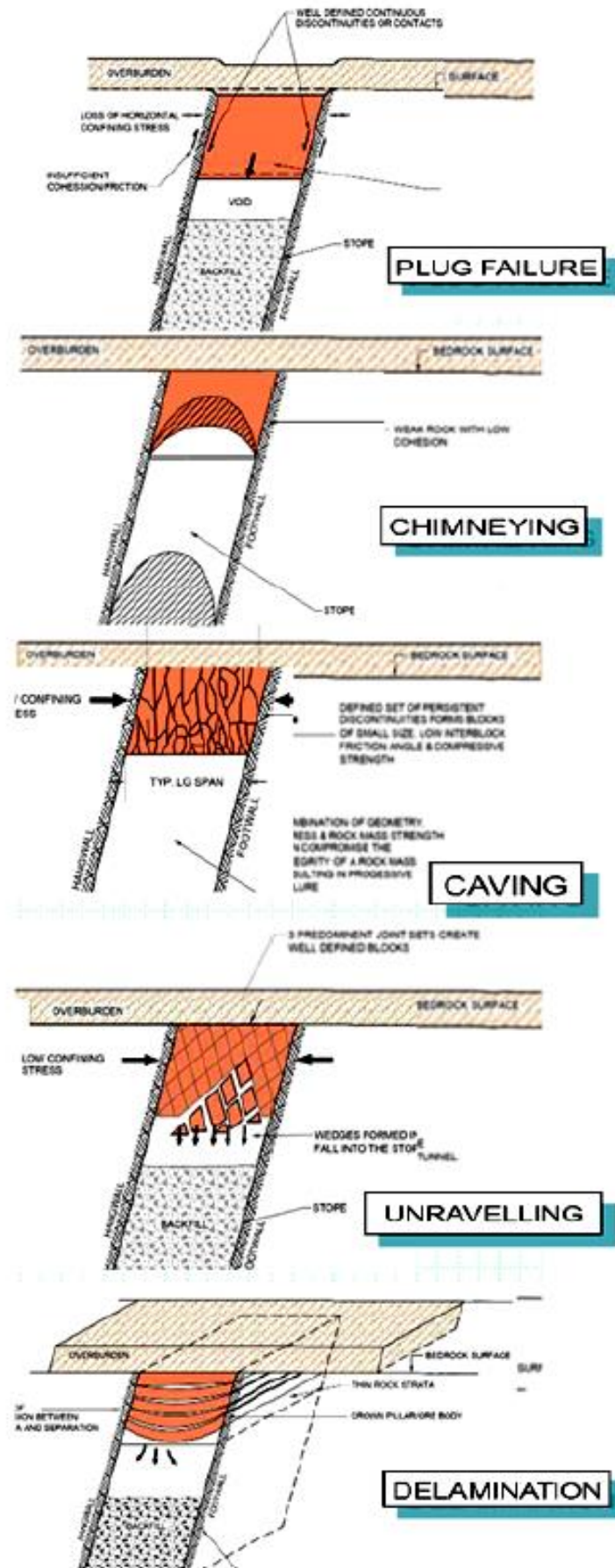


Figure 3-29: Principal surface crown pillar failure mechanisms (after Carter)

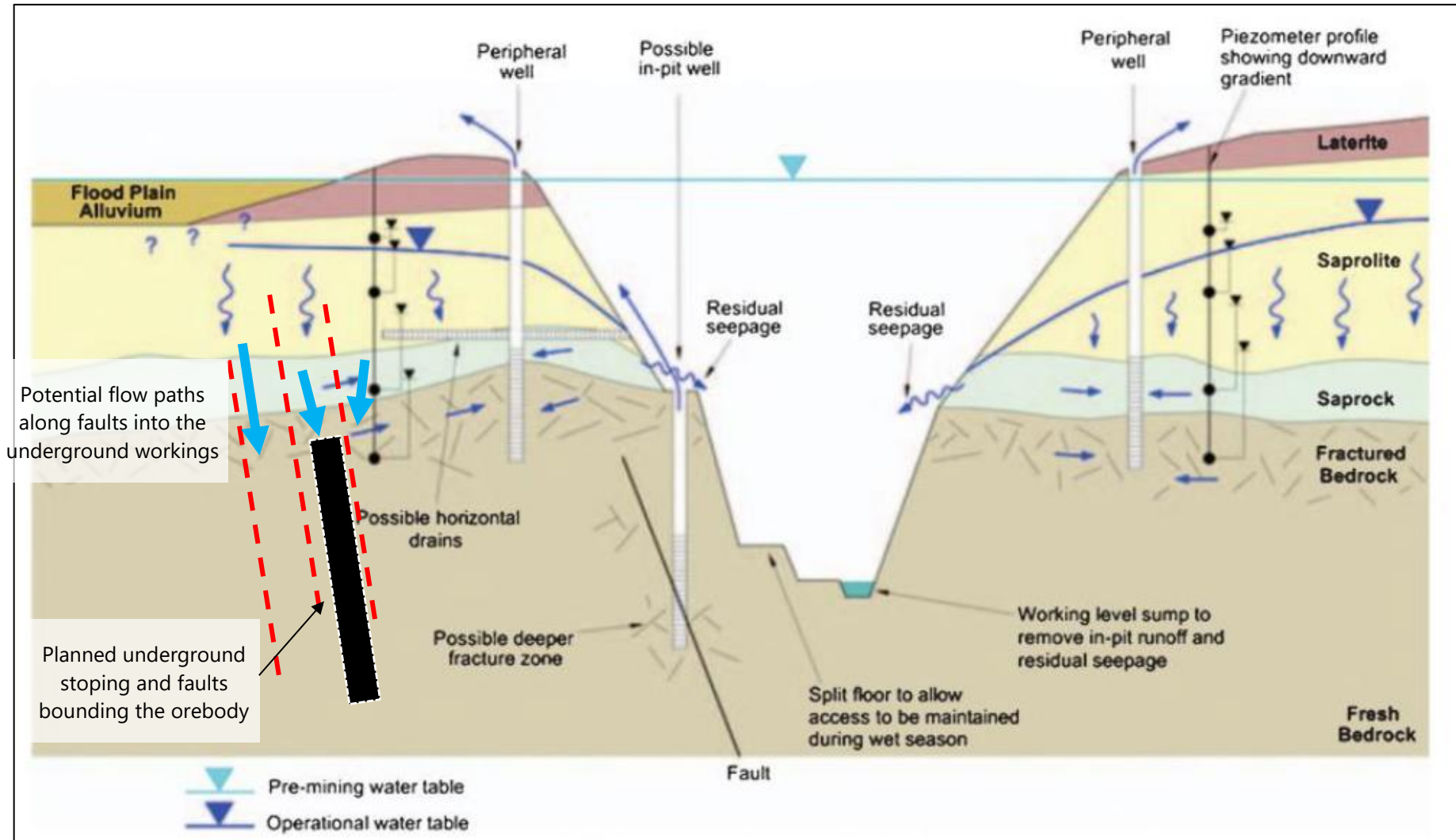


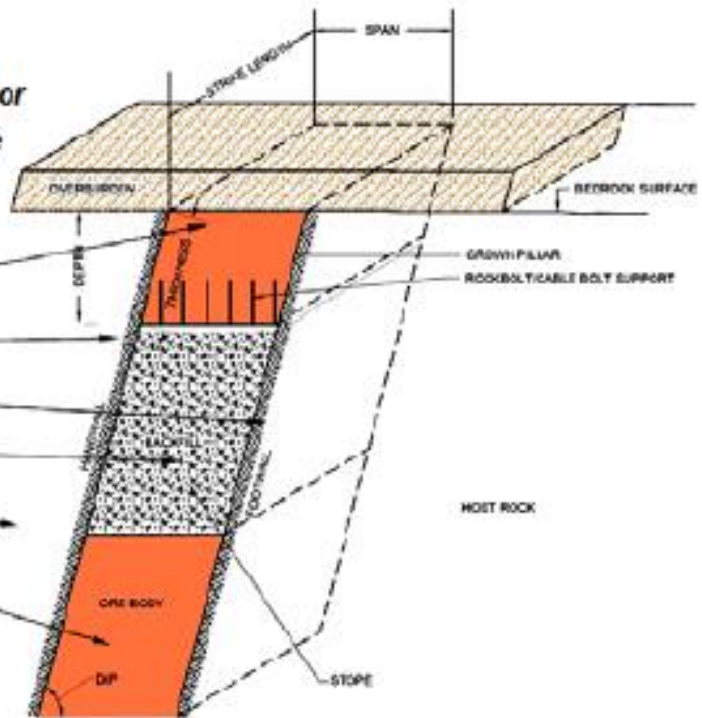
Figure 3-30: Schematic of groundwater distribution at Lake Cowal, showing potential effects of underground mining and water flow along faults intersecting the water bearing cover units and the underground workings.

> Cover Issues

- > Overburden, Tailings
- > Other Mine workings – Pit Floor
- > Existing/Future Infrastructure
- > Water bodies

> Mine Workings - Geometry

- > Crown Pillar
- > Hangingwall
- > Footwall
- > Stope
- > Host Rock
- > Ore Body



Given the typical stope geometry and geological and rockmass conditions comprising a typical crown pillar situation, such as shown in Figure 12, it was recognized that:

$$\text{Crown Stability} = f\left(\frac{T\sigma_h\theta}{SL\gamma u}\right) \quad (2)$$

where *increased stability* for any rock mass quality would be reflected by an increase in:

- $T$ , the rock crown thickness
- $\sigma_h$ , the horizontal insitu stress
- and/or...in  $\theta$ , the dip of the foliation or of the underlying opening, and;

where *decreased stability* for any crown would result from increases in:

- $S$ , the crown span
- $L$ , the overall strike length of the opening
- $\gamma$ , the mass (specific gravity) of the crown
- and/or...in  $u$ , the groundwater pressure.

Figure 3-31: Schematic of crown pillar with nomenclature

Table 3-1. Acceptable risk exposure guidelines (after Carter et al, 2008)

Class	Probability of Failure %	Minimum Factor of Safety	Maximum Scaled Span, $C_s (= S_c)$	ESR (Barton et al. 1974)	Design Guidelines for Pillar Acceptability/Serviceable Life of Crown Pillar				
					Expectancy	Years	Public Access	Regulatory position on closure	Operating Surveillance Required
A	50 – 100	<1	$11.31Q^{0.44}$	>5	Effectively zero	< 0.5	Forbidden	Totally unacceptable	Ineffective
B	20 – 50	1.0	$3.58Q^{0.44}$	3	Very, very short-term (temporary mining purposes only ; unacceptable risk of failure for temporary civil tunnel portals)	1.0	Forcibly Prevented	Not acceptable	Continuous sophisticated monitoring
C	10 – 20	1.2	$2.74Q^{0.44}$	1.6	Very short-term (quasi-temporary stope crowns ; undesirable risk of failure for temporary civil works)	2 – 5	Actively prevented	High level of concern	Continuous monitoring with instruments
D	5 – 10	1.5	$2.33Q^{0.44}$	1.4	Short-term (semi-temporary crowns, e.g. under non-sensitive mine infrastructure)	5 – 10	Prevented	Moderate level of concern	Continuous simple monitoring
E	1.5 – 5	1.8	$1.84Q^{0.44}$	1.3	Medium-term (semi-permanent crowns, possibly under structures)	15–20	Discouraged	Low to moderate level of concern	Conscious superficial monitoring
F	0.5 – 1.5	2	$1.12Q^{0.44}$	1	Long-term (quasi-permanent crowns, civil portals, near-surface sewer tunnels)	50–100	Allowed	Of limited concern	Incidental superficial monitoring
G	<0.5	>>2	$0.69 Q^{0.44}$	0.8	Very long-term (permanent crowns over civil tunnels)	>100	Free	Of no concern	None required

## **4 CONCLUSIONS, RECOMMENDATIONS & LIMITATIONS**

The main conclusions and recommendations arising from this project are outlined below, as well as the main limitations.

### **Main findings**

This report details the findings from model iteration R07. This simulation includes the most recent mine underground mine design, including a box cut, portal and additional decline. A review of the mine design provided identified 19 stopes that were located in close proximity to the weathered cover sequence geology, or within the cover sequence layers. These stopes have a significantly elevated risk of chimneying to surface due to the close proximity of the weak cover layers. Prior to building the numerical model, it was recommended that a minimum crown pillar thickness between the top of any planned stope and the top of the fresh rock surface be used to update the current design. A minimum stope width to crown pillar thickness of 1:2 was recommended. This corresponds to a minimum crown pillar thickness of ~20m to 30m for the 10 to 15m wide stopes. The mine design as subsequently updated by Evolution and the 19 stopes removed from the mine plan used for the R07 numerical model.

Our main findings for the latest model iteration (R07) are:

1. Vertical displacement forecasts on the surface above the proposed underground mine are generally less than 15mm and considered negligible. This amount of displacement is well within the limits and precision of current geological understanding, material properties and capabilities of a mine-scale model.
2. Forecast surface movement is slightly upwards (upsidence, not subsidence). This is due to displacement along the Glenfiddich fault, which becomes slightly mobilised due to nearby underground mining. There is also minor uplift in proximity to the pit due to continued mining of the pit and removal of 'dead-weight' (or overburden pressure).
3. Unlike caving methods or mining methods used for underground coal mining, such as longwall mining, surface subsidence is generally minimal, and often negligible for most stoping operations, particularly stoping operations targeting near vertical and relatively thin gold orebodies such as Lake Cowal underground.
4. The updated underground mine design and layout is appropriate for minimising (potential) surface subsidence. This is because of the planned sequence, relatively small stope dimensions with planned paste backfill, 20-30m crown pillar thickness in fresh rock and planned cablebolt ground support for the stope crowns. Of course, these controls do not completely eliminate the potential for any impact to surface as there are potentially unknown geological conditions present. The proposed underground mine design is considered feasible for minimising any impacts to surface and is forecast to have negligible impact to the surface topology provided stopes/crown pillars do not fail. It is noted that some geological conditions cannot be completely characterised and understood until development in planned mining blocks, particularly the upper stoping blocks, has been completed. Additional monitoring, measurement and risk mitigation measures addressing stope stability are addressed in the recommendations section. Failure of stope crown pillars is a key hazard that must be managed by the mine.
5. A potential hazard for the underground mine is stope failure or chimney failure of the upper stopes in the mine. The model does not forecast significant rockmass damage or major instability above these stopes. However, local geological conditions encountered in this domain may be different from the current understanding. Chimney failure and stope instability is a potential hazard in all stoping mines and must be managed appropriately. Chimney failure of a stope to surface at Lake Cowal would likely result in any surface water in the lake to report to the underground workings.



The mine will need to carefully manage this hazard through mine design, sequence, timely paste fill and (possibly) cablebolt stope walls and crowns. We have provided recommendations to mitigate this hazard.

6. Some stope hangingwalls are in close proximity to the Glenfiddich fault, which is in proximity to much of the mineralised zone on the hangingwall side. There is increased potential for hangingwall overbreak and stope failure / chimneying along the Glenfiddich fault, and other faults in proximity to mining that intersect with the weak oxide and transported material, such as the Galways splays.
7. There is potential for (increased) water inflow into underground workings along faults (i.e. Glenfiddich and Galway splay faults) that are slightly mobilised in proximity to the underground workings. Water inflow to the underground will depend on degree of saturation of overlying cover sediments in proximity to these faults, and the hydraulic conductivity of the individual faults.
8. There is minimal interaction between the underground and open pit mine. The interaction for stress, strain and displacement are considered negligible. This is due to the small footprint of the underground mine in proximity to the pit.

### Recommendations

Our recommendations arising from this project are outlined below. BE would be pleased to assist EMM and Evolution with implementing the recommendations if required.

1. Stopes within the oxide and transported layers are not likely to be stable and should not be planned at this stage of the project. Current geological interpretation demonstrates the depth and thickness of the transported and oxide layers is variable. The mine should continue to update the interpretation of these boundaries with information from ongoing drilling programmes. The location of the top of fresh rock is most important for the underground mine design.
2. Geotechnical characterisation and development of a detailed geotechnical domains model and structural model, particularly in the upper mining areas of the underground mine. The geotechnical and structural models will require on-going refinement over the mine life which is the normal practice in any mine.
3. The mine should review the planned mining sequence and consider delaying the mining of the upper most row of stopes in the upper most stoping blocks. Mining these stopes first, or very early in the mine life is when the mine has the least geological knowledge and understanding of stope performance (relative to other stages of underground mining). This includes the understanding of the hydraulic properties of the faults and (potential) water inflows to the underground mine.
4. Other recommendations and control measures to minimise the potential for stope overbreak or chimney failure that may impact the surface are listed below. Depending on local geological conditions encountered, the mine should review the list below, and select the controls appropriate to the conditions encountered. We understand some of these controls are currently being planned. Additional controls, if required would normally be identified and planned as part of the risk assessment and detailed design process.
  - a. A detailed crown pillar stability assessment must be conducted for each stope on the upper mining levels. We recommend the use of empirical methods as a minimum, or a combination of empirical and numerical methods. The mine must ensure the risk of crown pillar failure is suitably controlled.
  - b. Mine single lift stopes in the upper stoping block. Smaller stopes are more stable than large stopes. A smaller stope void increases the potential for stope overbreak and failure material to fill the void due to the swell of the broken material, prior to extensive failure or chimneying to surface.

- c. Stope sequencing to minimise risk of failure and unravelling along faults, particularly where stopes are bounded by multiple faults. Multiple stopes in close proximity should not be mined at the same time.
  - d. Top down drilling of the upper stopes will provide access to the top of the stope (the overcut drive) which enables cablebolting of the stope crown and hangingwall and access for rapid tight filling with paste.
  - e. Tight fill stopes, as far as practical.
  - f. Backfilling stopes in a timely manner.
  - g. Developing the overcut drive with a downwards grade from the access. This will enable the stopes to be tight filled to the backs with paste.
  - h. Ensuring paste lines and other backfill infrastructure is in place prior to firing stopes with potential for instability or in proximity to major faults.
  - i. Reducing the strike length and width of stopes to reduce potential instability. A review of the stope dimensions should be conducted following stope development and structural mapping of the area.
  - j. Cablebolting of stope crowns, when appropriate.
  - k. Review of a stand-off between stope walls and major faults, such as the Glenfiddich fault is appropriate based on local conditions
  - l. Employing a continuous mining sequence. Secondary stopes have a higher risk of instability (generally).
  - m. Avoid mining stopes where major faults confluence in proximity to the stope, particularly near sub-vertical faults such as the Glenfiddich fault and Galway splays.
  - n. Mine stopes on the upper levels when Lake Cowal is dry.
5. Detailed stope stability assessments using geotechnical information from future drilling programmes, laboratory testing and rock mass characterisation from underground exposures.
  6. Stability monitoring of stopes and TARP to backfill stopes that show early signs of large scale instability.
  7. The mine should develop a TARP and undertake a detailed risk assessment for potential stope instability in areas deemed to have elevated risk or potential for surface break through.
  8. Subsidence monitoring above the underground mining precinct.
  9. In situ stress measurement.
  10. Additional laboratory strength testing of each rock type.
  11. Characterisation of the major faults, including strength properties and hydraulic conductivity/water inflow rates.
  12. Ground water characterisation, including an assessment of the impact of the mechanical rockmass response on ground water flow paths and hydraulic conductivity.

### Limitations

In addition to the normal resolution limitations associated with the current mine-scale finite element model, the main limitations of this project are:

1. The structural model provided is of “low” resolution. We understand there are a large number of mapped faults within the open pit that were not provided for the assessment of the underground mine. A detailed pit stability assessment has not been completed as part of this assessment.
2. The early stage of underground mining at Lake Cowal precludes detailed calibration, which limits the reliability of the forecasts at this stage. This is normal for a mine at this early stage of pre-production development. Despite the lack of calibration, the results are generally consistent with our expectations based on the current interpretation of the conditions.
3. Sensitivity analyses have not been performed to bracket the range of likely outcomes for the surface impacts to mining.
4. Stope crown pillar stability assessment has not been conducted as sufficiently detailed information at present and is outside the scope of the subsidence assessment. Preliminary recommendations for crown pillar thickness have been integrated into the revised underground mine design.
5. The in-situ stress regime has been assumed using data from a nearby mine as there has been no insitu stress testing to date at Lake Cowal. Local conditions may have a different insitu stress orientation and/or gradient.
6. The impact of ground water inflow to the underground mine has not been included in the model. The model does not include:
  - a. Stress increase from porewater pressure
  - b. Overburden pressure from seasonal surface water (although this effect would be small)
  - c. An assessment of changes to ground water flow or surface water percolation due to rock mass damage, including damage within the major faults, caused by underground mining. We note that small amounts of strain above planned stoping or on structures will increase the hydraulic conductivity of the rock mass and may lead to (increased) water inflow to the underground mine.

It is essential to note that the current forecasts of LOM behaviour are still subject to considerable uncertainty due to the limited quantitative data available for model calibration at this early stage of the underground. This is the normal situation for mines in the early stages of underground mining. On-going data collection and further direct experience with stoping at Lake Cowal and improved calibration will help reduce uncertainty.

## **Enquiries**

Please direct further enquiries to the undersigned.

Sincerely,



### **Alex Campbell**

PhD, MEngSc (Mining Geomechanics), BE (Civil), BE (Mining Hons I) MAusIMM (CP), RPEQ  
Principal Engineer, Mining & Rock Mechanics

## 5 REFERENCES

1. Beck DA, Lilley CR, Reusch F, Levkovitch V & Flatten A. **A preliminary, calibrated scheme for estimating rock mass properties for non-linear, discontinuum models.** *Rock Characterisation, Modelling & Engineering Design Methods – 3rd ISRM SINOROCK Symposium*, Eds. Xia-Ting Feng, John A. Hudson & Fei Tan, Shanghai, China, 18–20 June 2013.
2. Brady BHG & Brown ET. **Rock mechanics for underground mining.** 3rd edition with corrections, Springer, 2006.
3. Lee MF, Mollison L, Campbell A & Litterbach N. **Rock Stresses in the Australian Continental Tectonic Plate – Variability and Controls.** *11th IAEG Congress – Geologically Active New Zealand*, Auckland, September 2010.
4. Levkovitch V, Beck DA & Reusch F. **Numerical simulation of the released energy in strain softening rock materials & its application in estimating seismic hazards in mines.** *Proceedings 8th International Symposium on Rockbursts & Seismicity in Mines*, 1–7 September 2013, Saint Petersburg, Russia.
5. Carter, TG, 2019. Retrospective assessment of structurally-controlled crown pillar failures, 53<sup>rd</sup> US Rock Mechanics/Geomechanics Symposium, New York.
6. Carter, TG, 2014. **Guidelines for use of the Scaled Span Method for Surface Crown Pillar Stability Assessment.** Proc. 1st International Conference on Applied Empirical Design Methods in Mining, Lima-Perú, 9-11th June, 2014, 34pp
7. Carter, T.G., Cottrell, B.E., Carvalho, J.L. & Steed C.M., 2008 **Logistic Regression improvements to the Scaled Span Method for dimensioning Surface Crown Pillars over Civil or Mining Openings.** Proc. 42nd US Rock Mechanics Symposium and 2nd Can-US Rock Symp. San Francisco. Paper 08-282 10pp

## **6 APPENDIX – LR2 FRAMEWORK**

### Contents

A.1.	CONSTITUTIVE MODEL AND PHYSICAL COMPOSITION	68
A.1.1.	The LR2 constitutive framework	68
A.1.2.	Constitutive model for the continuum parts	69
A.1.3.	Representation of explicit structure	72
A.1.4.	Model parameter to determine rock strength	73
A.1.5.	Modelling softening behaviour	76
A.1.6.	The common damage scale	77
A.1.7.	Mechanical response in the presence of pore-water pressure	77
A.1.8.	References	78

### **A.1. CONSTITUTIVE MODEL AND PHYSICAL COMPOSITION**

#### **A.1.1. The LR2 constitutive framework**

The Levkovitch-Reusch 2 (LR2) constitutive framework is a package of tools that describe the stress-strain behaviour of rock masses and structures. The main features of LR2 are:

- The continuum regions of the rockmass are modelled as strain-softening dilatant materials. This means that as strain increases the material softens, weakens and dilates. All parameters can vary at different rates with respect to strain changes, and this allows approximation of complex stress-strain behaviour of real rock masses. A generalisation of the Hoek-Brown yield criterion (Hoek et al. 2002) was used for the continuous regions of the rockmass, as described below.
- The behaviour of explicit discontinuities is approximated using cohesive elements. These elements are used because they can capture the mechanical response of thin structures at large deformations, which normal tetrahedral finite elements cannot achieve effectively. Cohesive elements allow simulation of the discrete behaviour associated with structures and can be used to construct a rockmass model comprising continuum regions separated by discontinuities. The structures are free to dislocate, dilate and degrade.
- Small scale structures can be represented in detailed models explicitly as cohesive elements, or ubiquitously by smearing the effects of the joints within the continuum parts of the rockmass.
- Tetrahedral higher-order elements are used for the discretization of the model geometry. These are considered essential for FE models where large gradients of displacements and damage are expected.
- The LR2 framework includes provision for hydromechanical coupling when necessary which means that the material constitutive equations (governing mechanical behaviour) are solved at the same time as the equations governing fluid flow in porous media (Darcy's equation), or solved in sequential or staggered incremental schemes, depending on the problem. This means that the modelling framework can capture the effects of pore water pressure on the strength of the rock (as may caused by groundwater percolation through the rockmass itself).
- Seismic potential can be assessed by considering the modelled rate of energy release (RER), which is the maximum instantaneous rate of energy release within a unit volume during a model frame.

RER can be correlated with seismic potential and has been successfully applied to forecast seismic potential in several projects. This requires calibration using seismic data for quantitative evaluations of seismic potential.

Model outputs include displacement, stress, strain and pore water pressure fields, where the presence of pore-water pressure is implemented. Plastic strain, reported as the plastic strain tensor or as scalar equivalent plastic strain measure, represents the amount of plastic rockmass deformation after yield. The plastic strain can be interpreted as rockmass damage and usually correlates well with most engineers' visual interpretation and intuitive understanding of rockmass damage. BE's damage scale is based on plastic strain (see further below how modelled rockmass damage can be interpreted).

### **A.1.2. Constitutive model for the continuum parts**

The relation between stress, strain, strength and degradation is described by the constitutive model. Generally, constitutive models consist of 3 main parts:

- (i) a stress dependent yield criterion,
- (ii) a plastic strain potential, which describes how the material will deform as a consequence of changes in stress due to damage and
- (iii) a description of how stress and strain are related.

In the LR2 framework, a generic yield criterion is used that can approximate almost any common rock mechanics yield criterion. In BE models, Hoek-Brown is applied as the base case for most problems.

The starting point for the generic criterion that can approximate Hoek Brown, Mohr coulomb or other criteria is the Menetrey/Willam strength criterion (1), described by the following function

$$\left[ \frac{q}{\sigma_{ci}} \right]^2 + m \left[ \frac{1}{3} \frac{q}{\sigma_{ci}} R(\theta, e) - \frac{p}{\sigma_{ci}} \right] - s = 0 \quad \text{A.1-1}$$

The material constants  $s$  and  $m$  are the measures of the cohesive and frictional strength, and  $\sigma_{ci}$  represents the uniaxial compressive strength of intact rock. Further,

$$p = -\frac{1}{3} \mathbf{I} \cdot \boldsymbol{\sigma} \text{ is the hydrostatic pressure,}$$

$$q = \sqrt{\frac{3}{2} \mathbf{S} \cdot \mathbf{S}} \text{ the Mises equivalent stress and}$$

$$r = \left[ \frac{9}{2} \mathbf{S} \cdot (\mathbf{S} \mathbf{S}) \right]^{1/3} \text{ the third stress invariant}$$

with  $\mathbf{S}$  being the deviatoric part of the Cauchy stress  $\boldsymbol{\sigma}$ . The dependence on the third invariant is introduced via the convex elliptic function in the deviatoric stress plane

$$R(\theta, e) = \frac{4(1-e^2) \cos^2 \theta + (2e-1)^2}{2(1-e^2) \cos \theta + (2e-1) \sqrt{4(1-e^2) \cos^2 \theta + 5e^2 - 4e}}. \quad \text{A.1-2}$$

Here, the variable  $\theta$ , defined via  $\cos 3\theta = (r/q)^3$ , is the deviatoric polar angle (also known as Lode angle) and the material constant  $e$  is the deviatoric eccentricity that describes the "out-of-roundedness" of the deviatoric trace of the function  $R(\theta, e)$  in terms of the ratio between the Mises stress along the extension meridian ( $\theta = 0$ ) and the compression meridian ( $\theta = \pi/3$ ). For  $\theta = 0$  and  $\theta = \pi/3$  the function becomes  $1/e$  and 1 respectively. The convexity of  $R(\theta, e)$  requires that  $0.5 \leq e \leq 1$ .

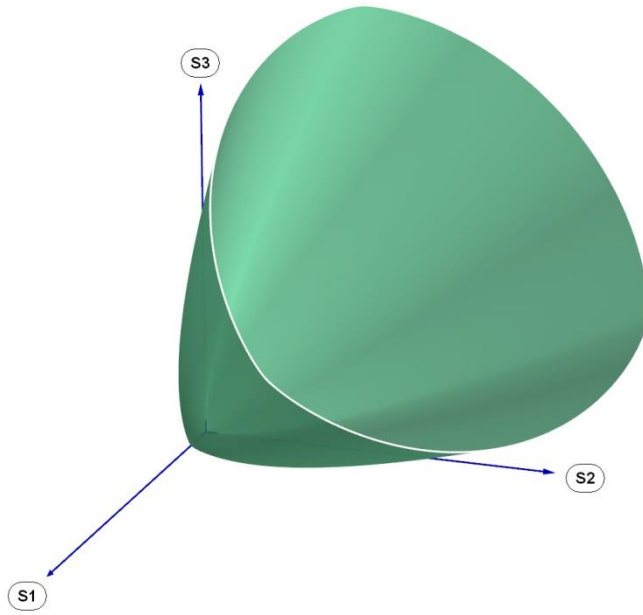


Figure A.1-1 Three dimensional representation of the Menetrey/Willam failure surface in the principal stress space

In the case of  $e = 0.5$  the Menetrey/Willam failure function represents a circumscribed approximation of the Hoek-Brown (2) strength criterion

$$\left(\frac{\sigma_1 - \sigma_3}{\sigma_{ci}}\right)^2 + m \frac{\sigma_3}{\sigma_{ci}} - s = 0, \quad \text{A.1-3}$$

where  $\sigma_1$  and  $\sigma_3$  are the major and minor principal stresses at failure. In order to recognize the similarity between the both criteria we rewrite the principal stresses representation using the relation between the stress invariants and the principal stresses

$$\sigma_1 = -p + \frac{2}{3}q \cos \theta \text{ and } \sigma_3 = -p + \frac{2}{3}q \cos \left(\theta + \frac{2}{3}\pi\right).$$

Inserting the upper expressions for the principal stresses into [3] one obtains the Hoek/Brown strength criterion in terms of the stress invariants

$$\left[\frac{2}{\sqrt{3}} \frac{q}{\sigma_{ci}} \sin \left(\theta + \frac{\pi}{3}\right)\right]^2 + m \left[\frac{2}{3} \frac{q}{\sigma_{ci}} \cos \theta - \frac{p}{\sigma_{ci}}\right] - s = 0. \quad \text{A.1-4}$$

Setting  $e = 0.5$  results in an exact match between the both criteria at the extension and compression meridians. For  $\theta = 0$  and  $\theta = \pi/3$  both expressions are reduced respectively to

$$\left[\frac{q}{\sigma_{ci}}\right]^2 + m \left[\frac{2}{3} \frac{q}{\sigma_{ci}} - \frac{p}{\sigma_{ci}}\right] - s = 0 \quad \text{A.1-5}$$

$$\left[\frac{q}{\sigma_{ci}}\right]^2 + m \left[\frac{1}{3} \frac{q}{\sigma_{ci}} - \frac{p}{\sigma_{ci}}\right] - s = 0. \quad \text{A.1-6}$$

Thus, for  $e = 0.5$  the Menetrey/Willam criterion can be considered as a circumscribed approximation of the Hoek/Brown function (Fig.A.2-2).

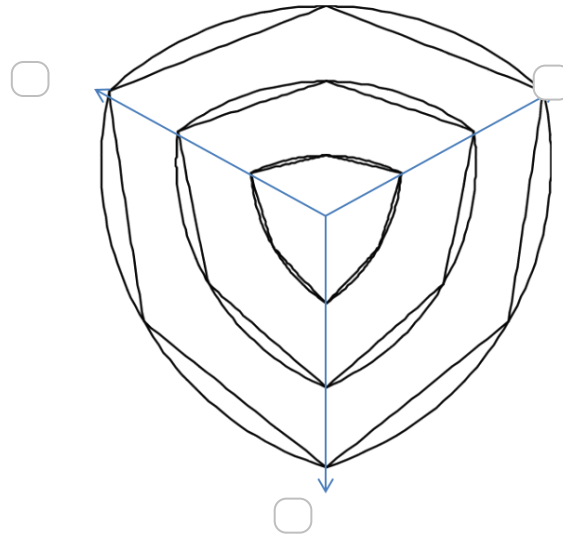


**Figure A.1-2: Comparison between the Deviatoric traces of the Menetrey/Willam failure model (smooth curves) and the 1980 Hoek-Brown criteria at three levels of confinement in the principal stress space**

In contrast to the Hoek/Brown model that doesn't account for the intermediate principal stress, the dependence on  $\sigma_2$  in the case of the Menetrey/Willam criterion [1] is governed by the eccentricity parameter  $e$ . Increasing eccentricity values cause a higher dependence on  $\sigma_2$  with the deviatoric trace of the Menetrey/Willam model approaching a circle (Fig A.2-3).

Thus, the Menetrey/Willam model possesses a material parameter that can be adjusted to match the true triaxial failure data if this is required.

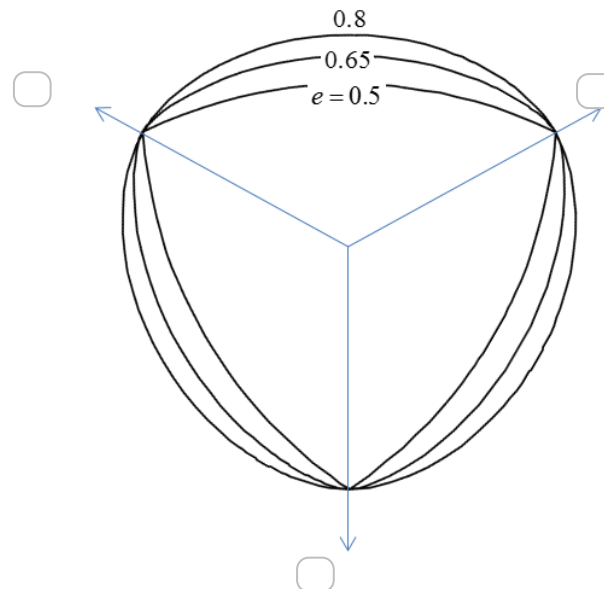


**Figure A.1-3: Deviatoric traces of the Menetrey/Willam failure function for three different eccentricity values.**

In 1992 the original Hoek/Brown criterion was extended (3) by an additional parameter  $a$  to the following form

$$\left(\frac{\sigma_1 - \sigma_3}{\sigma_{ci}}\right)^{\frac{1}{a}} + m \frac{\sigma_3}{\sigma_{ci}} - s = 0, \tag{A.1-7}$$

that allows to change the curvature of the failure envelope, particularly in the very low normal stress range to account for very low or zero tensile strength in heavily jointed or very poor rock masses. A corresponding extension of the Menetrey/Willam model takes the form



$$\left[\frac{q}{\sigma_{ci}}\right]^{\frac{1}{a}} + m \left[\frac{1}{3} \frac{q}{\sigma_{ci}} R(\theta, e) - \frac{p}{\sigma_{ci}}\right] - s = 0, \quad \text{A.1-8}$$

which is the failure criterion in the framework of the LR2 model.

Accordingly, the above failure function [7] can be considered as a circumscribed approximation of the 1992 Hoek/Brown (3) criterion.

The plastic strain potential is given by the relation

$$\mathbf{D}_p = \dot{\lambda} \frac{\partial G}{\partial \boldsymbol{\sigma}}, \quad \text{A.1-9}$$

where  $\dot{\lambda}$  is the magnitude of the plastic strain increment and  $G$  is the flow potential

$$G = \sigma_{ci} \left[\frac{q}{\sigma_{ci}}\right]^{\frac{1}{a}} + \frac{1}{3} m q R(\theta, e) - d_g p. \quad \text{A.1-10}$$

Here,  $d_g$  is the dilation parameter in the bulk. If the flow potential differs from the yield function the flow rule is non-associative which is the case for most geotechnical materials.

The model is implemented in such a way that all the strength parameters as well as the dilation and the Elastic modulus can be prescribed as piecewise linear functions of the equivalent plastic strain which is the accumulated deviatoric plastic strain

$$p_{eeq}^{dev} = \int_0^t \left( \dot{\lambda} \left\| \left( \frac{\partial G}{\partial \boldsymbol{\sigma}} \right)^{dev} \right\| \right) dt \quad \text{A.1-11}$$

to account for the stress-strain behaviour of the rock type, i.e.  $s$ ,  $m_b$ ,  $d_g$  and the Young's modulus are piecewise linear functions of  $p_{eeq}^{dev}$ .  $\|\mathbf{A}\|$  is the norm of a tensor  $\mathbf{A}$  and  $(\mathbf{A})^{dev}$  the deviatoric part of a tensor  $\mathbf{A}$ .

### A.1.3. Representation of explicit structure

The behaviour of explicit discontinuities is approximated using cohesive elements (formulation COH3D6 in ABAQUS). These elements are used because they can capture the mechanical response of thin structures at large strains, which normal tetrahedral finite elements cannot achieve effectively. Cohesive elements allow simulation of the discrete behaviour associated with structures and can be used to construct a rockmass model compromising continuum regions separated by discontinuities. The structures are free to dislocate, dilate and degrade. The constitutive behaviour of the cohesive elements can be defined using the LR2 continuum-based constitutive model, or a constitutive model specified directly in terms of traction versus separation with Coulomb yield criterion with cohesion.

The first approach is typically used to model layers of finite thickness, while the second approach is useful in applications for discontinuities of zero thickness such as fractures. Both models have the LR2 feature of elastic-plastic material behaviour in such a way that all the strength parameters as well as the dilation and the Elastic modulus can be prescribed as piecewise linear functions of accumulated plastic strain or the accumulated fault slip.

Discontinuities modelled with continuum LR2 material behaviour have the same set of material properties as LR2 bulk materials (s. chapter A.1.2 Constitutive model for the continuum parts).

The main feature of the traction-separation fault behavior is the onset of the fault slip is described by the following cohesive-frictional criterion

$$\tau - p_n \tan \beta - c = 0 \quad \text{A.1-12}$$

with  $c$  and  $\beta$  being the fault cohesion and friction angle, respectively. Further,  $\tau$  is the magnitude of the shear stress resolved onto the fault plane and  $p_n$  the normal stress acting across the fault. The kinematic of the fault slip deformation is described by the plastic strain rate

$$D_p = \dot{\gamma}[\text{sym}(\mathbf{s} \otimes \mathbf{n}) + \tan \psi \mathbf{n} \otimes \mathbf{n}] \tag{A.1-13}$$

with  $\dot{\gamma}$  being the fault slip rate and  $\psi$  the fault dilation angle. Further,  $\mathbf{n}$  is the unit normal vector of the fault plane (i.e. the orientation of the finite element) and  $\mathbf{s}$  the unit vector into the direction of the resolved shear stress. The constitutive fault parameters  $c$ ,  $\beta$  and  $\psi$  are prescribed as piecewise linear functions of the accumulated fault slip  $\gamma$ . The required parameter to define the mechanical behaviour of a traction-separation cohesive section are:

D	Constitutive thickness	These parameters are a function of the accumulated fault slip.
$\rho$ [kg/m <sup>3</sup> ]	Density	
E [GPa]	Elastic modulus	
$\nu$	Poisson's ratio	
d	Dilation	
s	Fault cohesion	
a	Fault friction angle	

**Table A.1-1 Material properties for traction-separation cohesive sections**

**A.1.4. Extension for the case of transversal isotropy**

The isotropic LR2 framework is extended for the case of transversal isotropy using the theory of liner stress transformation. The main assumption in this theory is that the anisotropic yield function of the actual stress  $\sigma$  is equivalent to an isotropic yield function of the linear transformed stress  $\sigma^*$

$$f_{aniso}(\sigma) = f_{iso}(\sigma^*) \tag{A.1-14}$$

With this approach the usage of an arbitrary isotropic yield function is possible.

The linear stress transformation:

$$\sigma^* = \mathbf{L}\sigma \tag{A.1-15}$$

is performed via a fully symmetric 4<sup>th</sup> order tensor  $\mathbf{L}$  that has to satisfy the material symmetry conditions (similar to the elastic stiffness tensor). It is also called the stress weighting tensor. Depending on the material anisotropy type it has different number of independent material constants.

Rock with a population of parallel weakness planes or cracks can be considered as transverse isotropic. With  $x_3$  axis being the symmetry axis and written in the material symmetry frame (Fig A.1-4),

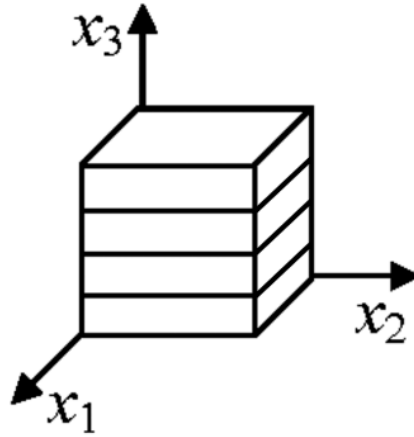


Figure A.1-4: Material symmetry frame of a transverse isotropic material.

$L$  has the following form:

$$L = \begin{pmatrix} n & 0 & 0 & 0 & 0 & 0 \\ 0 & n & 0 & 0 & 0 & 0 \\ 0 & 0 & 1 & 0 & 0 & 0 \\ 0 & 0 & 0 & n & 0 & 0 \\ 0 & 0 & 0 & 0 & s & 0 \\ 0 & 0 & 0 & 0 & 0 & s \end{pmatrix} \quad \text{A.1-16}$$

with only two independent material constants  $n$  and  $s$ .

To extend the LR2 framework for the case of transverse isotropy, the actual stress in the equation [8] is replaced by the stress transformed via [16]

$$\sigma^* = L\sigma = \begin{pmatrix} \sigma_{11}n \\ \sigma_{22}n \\ \sigma_{33} \\ \sigma_{12}n \\ \sigma_{23}s \\ \sigma_{13}s \end{pmatrix} \quad \text{A.1-17}$$

The meaning of the anisotropy constants  $s$  and  $n$  becomes clear if the yield function is analysed for the case of pure shear loading parallel to the cracks and of uniaxial compressive loading parallel to the cracks, respectively.

In the case of pure shear loading parallel to the cracks the yield condition reads:

$$f_{iso}(L\sigma) = f_{iso}(\sigma_{13}s) = 0$$

and  $\sigma_{13}s = CS_{iso}$  follows. Accordingly, parameter  $s$  represents the reduction factor of the cohesive strength with respect to the isotropic case if shear loading is applied parallel to the cracks.

For the case of uniaxial compressive loading parallel to the cracks (loading direction  $x_1$  or  $x_2$ ) the yield criterion reads

$$f_{iso}(L\sigma) = f_{iso}(\sigma_{11}n) = 0$$

and  $\sigma_{11}n = UCS_{iso}$  follows. Accordingly, parameter  $n$  represents the reduction factor of the uniaxial compressive strength with respect to the isotropic case if the uniaxial compressive load is applied parallel to the cracks. If compressive load is applied in  $x_3$  direction  $\sigma_{33} = UCS_{iso}$  follows which means that the uniaxial compressive strength perpendicular to the cracks is not influenced by them.

For an arbitrary direction of the uniaxial compressive load with respect to the material symmetry frame the stress weighting tensor  $L$  has to be transformed into the loading coordinate system. As a result, the simple diagonal shape is lost and the components of the transformed stress tensor  $\sigma^* = L\sigma$  attains shear components that depends also on constant  $s$ . Accordingly, the uniaxial compressive strength for such a transverse isotropic material depends on both anisotropy constants.

The pictures below show the dependence of UCS from the rotation angle of the load axis relative to  $x_3$  axis for load direction varying from  $0^\circ$  (perpendicular to the cracks) to  $90^\circ$  (parallel to the cracks) for different combinations of  $s$  and  $n$  values.

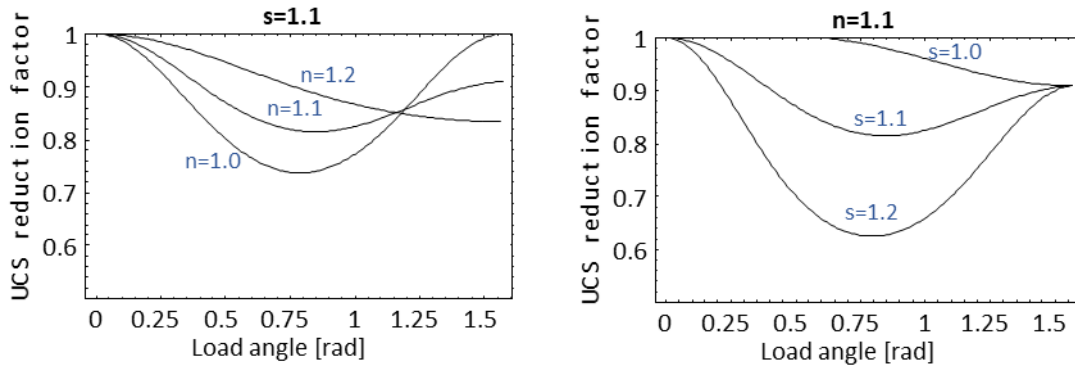


**Figure A.1-5: Influence of the loading direction on UCS for different combinations of  $n$  and  $s$  values**

**A.1.5. Model parameter to determine rock strength**

The application of the constitutive model for a particular rock type or the mechanical behaviour of a discontinuity requires the determination of a set of model parameters. One common approach is to determine the model parameter with help of the GSI (geological strength index) system (see (3) and (4) for the application) and the value  $m_i$  (frictional strength of the intact rock mass): This allows an initial determination of elastic properties  $E$  and  $\nu$ , the frictional strength of the broken rock  $m_b$  and the cohesive strength  $s$  as well as the dilation.

UCS [MPa]	Uniaxial Compressive Strength	
GSI	Geological Strength Index	
$m_i$	Frictional strength of intact rock	
D	Damage parameter (Hoek-Brown)	
$\rho$ [kg/m <sup>3</sup> ]	Plastic strain	
$m_b$	HB parameter for frictional strength of broken rock	These parameters are a piecewise linear function of the accumulated plastic strain.
E [GPa]	Elastic modulus	
$\nu$	Poisson's ration	
d	Dilation	
s	cohesive strength parameter	
a	strength parameter	

**Table A.1-2 Material properties for continuum LR2 material**

A set of these parameters describes the onset of yielding for a rock type. To describe the post-yield behaviour of stress-strain relation of the rock the implementation of the constitutive model allows an arbitrary number of characteristic points to describe the stress-strain curve of the material. An example for the documentation of material properties is provided in the next figure:

Material property set: M12		UCS (MPa)	Density (kg/m <sup>3</sup> )	k (m/s)	Peak							Transitional					Residual						
Material	Code				mb	s	a	e	d	Eb (GPa)	v	PS_start	mb	s	d	Eb (GPa)	v	PS_start	mb	s	d	Eb (GPa)	v
Quartz andesite	QAND	90	2,700	1E-09	1.27	1.23E-03	0.503	0.6	0.079	8.71	0.25	0.5%	1.27	1.23E-03	0.079	8.71	0.25	1.5%	0.59	1.50E-04	0.018	1.67	0.25
Younger andesite	YAND	24	2,700	1E-08	0.55	1.25E-04	0.521	0.6	0.034	1.37	0.25	0.5%	0.55	1.25E-04	0.034	1.37	0.25	1.5%	0.37	4.16E-05	0.011	0.29	0.25
Undifferentiated ignimbrite	UDIG	60	2,700	1E-04	3.09	2.22E-03	0.505	0.6	0.193	5.81	0.25	0.5%	3.09	2.22E-03	0.193	5.81	0.25	1.5%	1.52	2.46E-04	0.048	1.86	0.25
Welded ignimbrite	WEIG	90	2,700	1E-08	4.19	3.87E-03	0.505	0.6	0.262	9.49	0.25	0.5%	4.19	3.87E-03	0.262	9.49	0.25	1.5%	1.91	3.35E-04	0.060	2.67	0.25
Unwelded sandy ignimbrite	UWIG	24	2,700	1E-04	4.07	1.17E-02	0.502	0.6	0.255	8.71	0.25	0.5%	4.07	1.17E-02	0.255	8.71	0.25	1.5%	1.45	4.68E-04	0.045	1.64	0.25
Lake sediments	LSED	2.4	1,900	1E-04	0.21	2.40E-04	0.530	0.6	0.013	0.37	0.25	0.5%	0.21	2.40E-04	0.013	0.37	0.25	1.5%	0.17	1.38E-04	0.005	0.28	0.25
Surface sediments	SSED	2.4	1,900	1E-04	0.21	2.40E-04	0.530	0.6	0.013	0.37	0.25	0.5%	0.21	2.40E-04	0.013	0.37	0.25	1.5%	0.17	1.38E-04	0.005	0.28	0.25
Alluvium	ALLU	12	1,700	1E-04	2.01	3.87E-03	0.505	0.6	0.126	3.46	0.25	0.5%	2.01	3.87E-03	0.126	3.46	0.25	1.5%	0.82	2.40E-04	0.026	0.82	0.25
Tuff	TUFF	12	1,700	1E-04	2.18	3.87E-03	0.505	0.6	0.136	3.46	0.25	0.5%	2.18	3.87E-03	0.136	3.46	0.25	1.5%	0.89	2.40E-04	0.028	0.82	0.25
Blue Shear	BLUE	2.4	2,100	1E-08	2.45	7.30E-04	0.515	0.6	0.153	0.65	0.25	0.5%	2.45	7.30E-04	0.153	0.65	0.25	1.5%	1.44	1.38E-04	0.045	0.28	0.25
Mineralised structures	QTVN	60	2,700	1E-04	0.65	1.97E-04	0.516	0.6	0.040	2.20	0.25	0.5%	0.65	1.97E-04	0.040	2.20	0.25	1.5%	0.31	3.04E-05	0.010	0.15	0.25
Other cohesive elements	COH1	2.4	2,700	Note 1	1.20	1.38E-04	1.000	0.6	0.075	0.50	0.25	0.5%	1.20	1.38E-04	0.075	0.50	0.25	1.5%	0.87	1.38E-04	0.027	0.50	0.25
Quartz andesite 2	QAND2	78	2,700	1E-09	1.11	8.55E-04	0.505	0.6	0.069	6.92	0.25	0.5%	1.11	8.55E-04	0.069	6.92	0.25	1.5%	0.51	1.50E-04	0.016	1.67	0.25
Quartz andesite 3	QAND3	66	2,700	1E-09	0.65	1.97E-04	0.515	0.6	0.040	2.20	0.25	0.5%	0.55	1.25E-04	0.034	1.37	0.25	1.5%	0.39	5.00E-05	0.012	0.40	0.25
Milking Cow	Elastic	Note 2	Note 3							0.05	0.25												
Backfill	Elastic	2,160	1E-04							0.05	0.25												
Underground voids	Elastic									1E-04	0.25												

Notes  
 1: Different k for cohesive elements not applied in this simulation.  
 2: Density within the Milking Cow assumed to be the same as original rock.  
 3: k within the Milking Cow assumed to be 1E-3 of k in original rock.

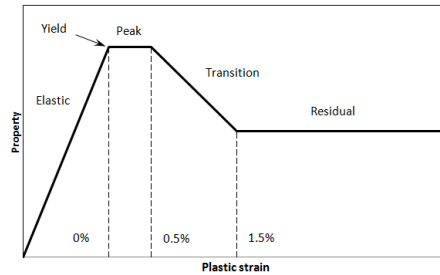


Figure A.1-6: Example for documentation of material properties of the LR2 framework.

### A.1.6. Modelling softening behaviour

The image below shows frequently used idealizations for the softening behaviour of the rock materials. (P) denotes the peak strength material, (T) indicates the onset of softening and (R) examples for the residual strength level.

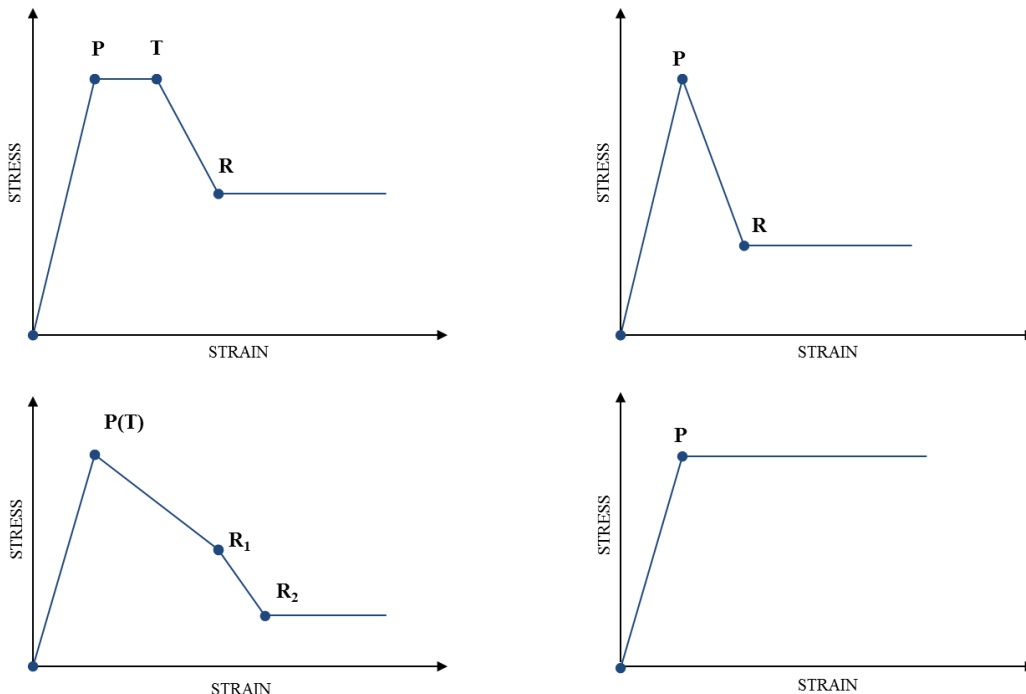


Figure A.1-7: Idealizations for the softening behaviour of the rock materials. (P) denotes the peak strength material, (T) indicates the onset of softening and (R) examples for the residual strength level.

In the LR2 framework the softening behaviour is introduced in such a way that all the strength parameters as well as the dilation and the Elastic modulus can be prescribed as piecewise linear functions of accumulated plastic strain to account for the stress-strain behaviour of the rock type, i.e.  $d_g$ ,  $s$  and  $m_b$  and the Young's

modulus can evolve independently according to the available laboratory data or available description of the deformation and damage behaviour rock mass.

**A.1.7. The common damage scale**

As a purely phenomenological model the constitutive equations do not incorporate a damage variable that allows the direct quantification of the damage state of the rock.

For non-linear elastic-plastic models as used in the LR2 framework the rock mass damage is related to the amount of accumulated equivalent plastic strain, which is the amount of permanent (irreversible) rockmass deformation after yield. The table below shows a possible correlation of plastic strain values with the damage state of the rock. The specific correlation of plastic strain levels with damage states is often referred to as the “common damage scale (CSD)”, which can vary depending of the softening behaviour of the investigated rock.

Plastic strain	Damage state	Observed behaviour
>5%	Very significant	Gross distortion and comminution.
~3%	Significant	Extensive fracturing of intact rock.
~1.5%	Moderate	Constant load leads to increasing deformation.
~0.7%	Minor	No significant decrease in strength or stiffness.
<0.35%	None to very minor	Undisturbed in situ conditions.

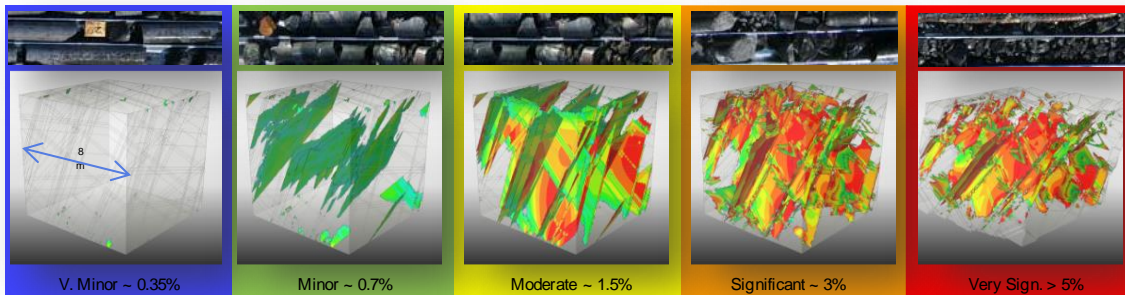


**Table A.1-8 Correlation of plastic strain values with the damage state of the rock**

**A.1.8. Assessing seismic potential with RER**

The mining of excavations in rock re-distributes stress and causes damage to the rock mass and discontinuities. The resulting reduction in strength and degradation in stiffness of the damaged rock and structures leads to further deformation and release of stored elastic strain energy.

One portion of this released energy is consumed by the damage process - frictional sliding and the creation of new surfaces. This energy cannot be retrieved, so is counted as ‘dissipated’. If the value of the released elastic energy is higher than the energy dissipated by the irreversible damage, the surplus is emitted into the surrounding rock. These release events are seismic events.

The magnitude (and/or the rate) of the released energy during these events can be measured in a mine using a seismic monitoring system or calculated using a model. The instantaneous, peak (i.e. maximum) rate of energy release from a volume of rock (i.e. the energy that is not dissipated) is the Rate of Energy Release (RER).

The calculated rate of energy release (RER) is used to represent seismic potential in the model. Levkovitch et al. (2013) describe RER in some detail. RER is calculated as follows:

Each model frame comprises many numerical time steps as part of the explicit FE solution procedure. For each time step, the instantaneous rate of energy release is calculated for each finite element. This is the change in elastic strain energy less the dissipated plastic energy, and represents the energy radiated from

the element out into the surrounding environment. The dissipated plastic energy represents irreversible work done on the rockmass through processes such as friction on joint surfaces and creation of new fractures, and is calculated from the plastic strain condition of the element.

The RER is the maximum value of the instantaneous rate of energy release calculated all the time steps during a model frame.

RER is recorded for every tetrahedral element and every cohesive element in the FE simulation at every frame. This allows RER to be calculated for the homogenised rockmass (represented with tetrahedral elements), and for the explicit structures (represented with cohesive elements). Both are important: The largest events are expected on structures, but many lower magnitude events are expected in the homogenised rockmass.

### **A.1.9. Mechanical response in the presence of pore-water pressure**

In the LR2 framework the governing rock or soil is regarded as a deformable porous medium, consisting of a solid skeleton and a pore space. A fluid (e.g., water) may partially or fully saturate this pore space and is allowed to flow through connected pores, i.e. to permeate through the rockmass. Within the conceptual modelling approach both the skeleton and the voids are considered to be homogeneously smeared within the Representative Volume Element (RVE), where the proportion of pore volume space to the bulk volume is denoted as porosity.

At any material point in the model, the fluid is subjected to a fluid pressure. The spatial distribution of the fluid pressure does vary and results from the respective hydro-geological setting. This pressure is obtained as a result of a separate hydrological analysis.

The fluid interacts with the solid rock skeleton. In case of a single-phase water flow the respective fluid pressure acting on the solid skeleton is referred to as pore-water-pressure  $p_w$ , or, in case of a multi-phase flow, as wetting phase pressure.

The stresses of the entire RVE, denoted as total stresses, can be decomposed in two parts. One part is represented by the effective stresses of the solid skeleton, and the other part by the fluid pressure acting onto the solid skeleton. This is referred to as effective stress concept of Terzaghi (1936):

$$\boldsymbol{\sigma}_{tot} = \boldsymbol{\sigma}_{eff} + \alpha_B p_w \mathbf{1}. \quad (\text{A.1-18})$$

The sign convention is such that  $p_w$  being positive in compression, and of  $\boldsymbol{\sigma}$  negative in compression, i.e.,  $p = -1/3 \text{tr}(\boldsymbol{\sigma})$ . Further,  $\alpha_B$  denotes the Biot coefficient which is a material parameter depending on the rock type that is generally bound between  $0 < \alpha_B \leq 1$ . Typical values for the Biot coefficient are summarized in the literature for a range of materials. Total stresses are always used to fulfil the linear momentum (equilibrium). The constitutive response of the porous material, however, is always updated using the effective stresses. Hence, the presence of pore-water pressure reduces the skeleton stresses such that the effective confinement pressure is reduced and the material may be subject to earlier yielding. As a special case, a pore-water pressure exceeding the total confining pressure, i.e.,  $p_w > -1/3 \text{tr}(\boldsymbol{\sigma}_{tot})$ , results in a plastic apex-mode deformation, also referred to as tensile cracking. This situation may arise in cases where a large  $p_w$  is present in a de-stressed material region, such as near a free surface.

### **A.1.10. References**

- (1) Terzaghi, K. (1936) "The shear resistance of saturated soils." Proceedings for the 1st. Intl. Conf. on Soil Mechanics and Foundation Engineering (Cambridge, MA), 1, 54-56.
- (2) Menetrey P. & Willam K.: "Triaxial failure criterion for concrete and its generalization", *ACI Structural Journal*. 92(3): 311-317, 1995.

- (3) Hoek, E. & Brown E.T.: "Empirical strength criterion for rock masses", Journal of the Geotechnical Engineering Division. 106(9): 1013-1035, 1980.
- (4) Hoek, E., Wood, D. and Shah, S.: "A modified Hoek-Brown criterion for jointed rock masses", Proc. rock characterization, symp. Int. Soc. Rock Mech.: Eurock '92, (J.Hudson ed.). 209-213, 1992
- (5) M. Cai et al. / International Journal of Rock Mechanics & Mining Sciences 44 (2007) 247–265
- (6) Reusch, F., Levkovitch, V. & Beck, D. : "Multi-scale, non-linear numerical analysis of mining induced deformation in complex environments" in "Rock Mechanics in Civil and Environmental Engineering" , Jian Zhao (Editor), Vincent Labiouse (Editor), Jean-Paul Dudt (Editor), Jean-Francois Mathier (Editor), CRC Press, 2010, 697-700.
- (7) Levkovitch, V., Reusch, F. & Beck, D. : "Application of a non-linear confinement sensitive constitutive model to mine scale simulations subject to varying levels of confining stress" in "Rock Mechanics in Civil and Environmental Engineering" , Jian Zhao (Editor), Vincent Labiouse (Editor), Jean-Paul Dudt (Editor), Jean-Francois Mathier (Editor), CRC Press, 161-164, 2010.